THE CRYSTAL STRUCTURES OF

π-CYCLOPENTADIENYL(TRIETHYLPHOSPHINE)COPPER(I), π-$C_5H_5CuP(C_2H_5)_3$

AND

$Fe_3As_2(CO)_9$

by

L. T. J. DELBAERE

A Thesis Submitted to

The Faculty of Graduate Studies and Research

University of Manitoba

In Partial Fulfilment

of the Requirements for the Degree

Doctor of Philosophy

1969

ABSTRACT

Cyclopentadienyl(triethylphosphine)copper(I), $C_5H_5CuP(C_2H_5)_3$, has the cell dimensions $a_o = 8.60 \pm .02$ Å, $b_o = 11.04 \pm .01$ Å, $c_o = 7.67 \pm .01$ Å and $\beta = 115.3 \pm .5°$. The space group of the crystal is $P2_1/m$ (No. 11) and Z = 2. The structure was solved, using the intensities obtained from equi-inclination Weissenberg photographs, by three dimensional Patterson, Fourier and least-squares methods to a final R index of 0.145 when a set of hydrogen atoms was included at chemically expected positions. The analysis revealed the presence of two enantiomers distributed apparently equally and randomly throughout the crystal. The C_5H_5 ring is π-bonded to the copper atom with average bond lengths of 2.24 Å for Cu-C and 1.38 Å for C-C. The presence of a π-bonded ring is in accord with the thermal stability of the compound. π-$C_5H_5CuP(C_2H_5)_3$ is monomeric and obeys the inert gas rule.

$Fe_3As_2(CO)_9$ has the cell dimensions $a_o = 10.82 \pm .01$ Å, $b_o = 10.96 \pm .02$ Å and $c_o = 13.29 \pm .02$ Å. The space group of the crystal is Bmmb (equivalent to No. 63) and Z = 4. The intensities were estimated from equi-inclination Weissenberg photographs. The structure was solved by three dimensional Patterson, Fourier and least squares methods to a final R index of 0.107. The analysis revealed a disordered structure consisting of one molecule randomly distributed in two orientations which were related by a crystallographic two-fold rotation axis. The idealized molecular symmetry is $3/m(C_{3h})$. There is an equilateral triangle of iron atoms with the average Fe-Fe bond distance

of 2.62 ± .01 Å. The two arsenic atoms in the molecule lie above and below the triangle of iron atoms and are related by the mirror plane containing the iron atoms. The arsenic atoms are bonded equally to the iron atoms with an average As-Fe bond of 2.35 Å. The other average bond lengths are 1.80 Å for Fe-C and 1.125 Å for C-O.

ACKNOWLEDGEMENTS

This work was accomplished under the supervision of Dr. D.W. McBride of the Department of Chemistry at the University of Manitoba with the aid of a University of Manitoba teaching assistantship (1965-1966), University of Manitoba Fellowships (1966-1968) and a National Research Council Bursary (1968-1969). The author wishes to thank Dr. D.W. McBride for his encouragement and guidance during the course of this work.

The author is very grateful to Dr. R.B. Ferguson of the Department of Geology of the University of Manitoba for his help and for the use of his X-ray laboratory facilities. Dr. F.R. Ahmed of the National Research Council is thanked for providing the X-ray crystallographic programs used in this research.

Grateful acknowledgement is made to Mr. L. Kruczynski for his valuable suggestions, for providing the crystals of $Fe_3As_2(CO)_9$ and for a portion of the photographic work. The author also wishes to thank Mr. R. Pryhitko for the remainder of this photographic work, Dr. C. Reichert for recording and interpreting the mass spectrum and Mr. Bob Jones for typing this manuscript.

To Carol

TABLE OF CONTENTS

PART I - THE CRYSTAL STRUCTURE OF π-CYCLOPENTADIENYL-(TRIETHYLPHOSPHINE)COPPER(I), π-$C_5H_5CuP(C_2H_5)_3$

PAGE

LIST OF TABLES

LIST OF FIGURES

PART I

THE CRYSTAL STRUCTURE OF π-CYCLOPENTADIENYL(TRIETHYLPHOSPHINE)-COPPER(I), π-$C_5H_5CuP(C_2H_5)_3$

CHAPTER I

INTRODUCTION

Cyclopentadienyl(triethylphosphine)copper(I), $C_5H_5CuP(C_2H_5)_3$, was first prepared by Wilkinson and Piper (1956). The compound was sublimed at 60°C and 10^{-5} mm. Hg vacuum to form aggregates of small white needle-like crystals. The compound's properties, thermal stability above room temperature and no extensive polymerization, make it unique among the organometallic compounds of copper. Three possible types of bonds by which the cyclopentadienyl group can be bonded to the copper atom in $C_5H_5CuP(C_2H_5)_3$ are a π-bond (Fig. 1 (a) as in ferrocene (Dunitz, Orgel and Rich (1956)), a σ-bond (localized metal-carbon bond) (Fig. 1 (b)) as the σ-C_5H_5 ring in $(\pi\text{-}C_5H_5)Fe(CO)_2(\sigma\text{-}C_5H_5)$ (Bennett *et al.* (1966)) and an ionic bond (Fig. 1 (c)) as in manganese cyclopentadienide $Mn(C_5H_5)_2$ (Wilkinson, Cotton and Birmingham (1956)). Limited polymerization may occur. Fig. 1 (d) is an example of such a polymeric structure.

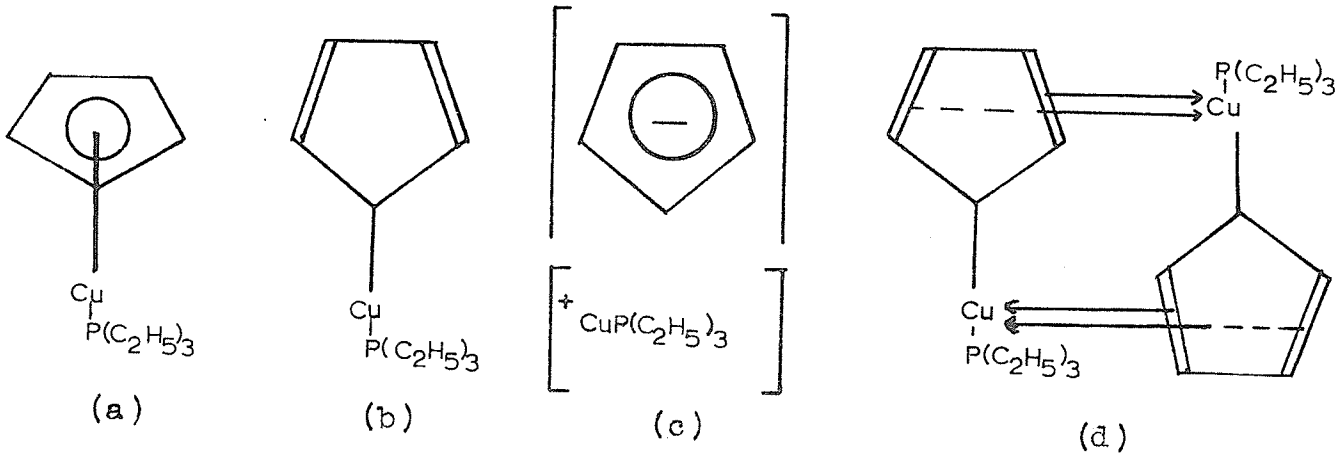

Fig. 1.

In general, a compound with an ionically-bonded cyclopentadienyl ring has the following properties: insolubility in hydrocarbon solvents, vigorous reaction with air, inflaming and smoldering in the solid state, reaction with hydrochloric acid or water to yield cyclopentadiene, reaction with carbon dioxide to yield carboxylic acid salts and reaction with ferrous chloride to quantitatively yield ferrocene. A compound with a π-bonded cyclopentadienyl ring would not be expected to have these properties. If no extensive polymerization occurs, this compound is likely to sublime in a vacuum. A compound with a σ-bonded cyclopentadienyl ring would be expected to undergo hydrolysis with hydrochloric acid but not have the remaining properties of a cyclopentadienide.

$C_5H_5CuP(C_2H_5)_3$ is very soluble in petroleum ether, decomposes in air after 3 - 4 hours, is hydrolysed by hydrochloric acid, does not react with water or carbon dioxide, and reacts with ferrous chloride in tetrahydrofuran to yield ferrocene almost quantitatively. Wilkinson and Piper (1956) stated that the chemical, physical and infrared evidence for the nature of the bonding between the cyclopentadienyl ring and the copper atom is indecisive, but they proposed a σ-bonded C_5H_5 ring for the compound as being the most consistent with the properties.

Very unstable tertiary phosphine complexes of methylcopper were reported by Costa, Pellizer and Rubessa (1964) and by House, Respess and Whitesides (1966). Methyl compounds are generally as stable or more stable than their σ-bonded

cyclopentadienyl analogues as shown by $(\pi\text{-}C_5H_5)Cr(NO)_2CH_3$ and $(\pi\text{-}C_5H_5)Cr(NO)_2(\sigma\text{-}C_5H_5)$ and also $(\pi\text{-}C_5H_5)Fe(CO)_2CH_3$ and $(\pi\text{-}C_5H_5)Fe(CO)_2(\sigma\text{-}C_5H_5)$ (Piper and Wilkinson (1956)). Thus a σ-bonded C_5H_5 ring in a tertiary phosphine complex of copper is likely to be unstable.

In the crystal structure of the phenylethynyl(trimethylphosphine)copper tetramer reported by Corfield and Shearer (1966), copper is both π-bonded and σ-bonded to ethynyl groups. This suggested that $C_5H_5CuP(C_2H_5)_3$ may also be stabilized by π-bonding.

Because of the special properties of the compound, the existence of several possible structures, and our preparation of well-formed single crystals an X-ray structure analysis was undertaken.

CHAPTER II

X-RAY DIFFRACTION THEORY

A crystal structure is a three dimensional periodic arrangement of a group of atoms in space to form the crystal. A space lattice is a representation of this repeat pattern with a lattice point representing the group of atoms. The unit cell is the smallest repeat unit of the lattice. The symmetry of the unit cell determines the crystal system.

Certain non-translational symmetry elements are found in space lattices. A consideration of these symmetry elements and all their possible combinations results in thirty-two crystal classes or point groups. A crystal form is an assemblage of equivalent faces of a crystal (e.g. a prism or a cube). Any crystal form belongs to one of these point groups. The symmetry elements in a point group must pass through a single point. However, in a crystal structure all symmetry elements need not pass through one point. This is due to the presence of translational symmetry elements i.e. screw axes and glide planes. A screw axis involves repetition of atomic positions by rotation about a line plus translation parallel to the line. A glide plane involves repetition of an atomic position by reflection across the plane and translation parallel to the plane. All possible combinations of the crystallographically permissible symmetry elements, both translational and non-translational, yields two hundred and thirty space groups. Every crystal structure must belong to one of these space groups.

When a monochromatic X-ray beam strikes a crystal, the electrons of the atoms periodically absorb energy from the beam and re-emit it as X-radiation of the same frequency as the incident beam. These scattered waves interfere with each other both constructively and destructively (diffraction). The directions of constructive interference, so-called "reflections" depend only on the size and shape of the unit cell. Certain "reflections" are systematically extinguished by lattice centering and by the presence of screw axes and glide planes. A study of the occurrence of these systematic absences determines the possible space groups of the crystal. The intensities of the reflections depend on the type of atoms present and their arrangement in the crystal structure.

The atoms present in a unit cell are determined from the unit cell dimensions, the chemical analysis and the density of the crystal.

In 1913, W.L. Bragg formulated the equation $n\lambda=2d_{hk\ell}\sin\theta$ for the constructive interference of an X-ray beam striking parallel neighbouring planes of a crystal lattice, where n is an integer, λ is the wavelength ($\mathring{A}$) of the X-ray beam, $d_{hk\ell}$ is the interplanar spacing ($\mathring{A}$) and θ is the angle (degrees) between the incident X-ray beam and the lattice planes.

The Bragg equation may also be expressed in the form, $\lambda=2d_{nh\ nk\ n\ell}\sin\theta$, where $d_{nh\ nk\ n\ell}=\frac{d_{hk\ell}}{n}$. The wavelength order n is incorporated into the interplanar spacing. Both notations are used by the author.

Two techniques employed in the X-ray diffraction of crystals

are powder methods which are applied primarily for indentification purposes and single crystal methods which are mainly used for crystal structure determinations. In these crystal structure elucidations, oscillation, precession and Weissenberg single crystal moving film methods were employed.

In 1921 P.P. Ewald introduced the concept of a "reciprocal lattice" in connection with the direct or space lattice in order to readily interpret single crystal photographs. The reciprocal lattice does not exist whereas the direct lattice does have physical reality. One point of the reciprocal lattice represents a whole set of equally-spaced parallel direct lattice planes; it is this representation which makes the reciprocal lattice similar to single crystal photographs. The relation between the direct and the reciprocal lattice is shown in Fig 2. This monoclinic primitive lattice is shown projected along the y-axis (2-fold axis), with the direct lattice represented by solid lines and the reciprocal lattice by dashed lines. The reciprocal lattice represents each set of parallel lattice planes of the direct lattice by a point (solid circle) normal to the planes at a distance inversely proportional to the interplanar spacing i.e. $\propto \frac{k}{d_{h0l}}$ where k is the constant of proportionality. For all X-ray work k may be taken as equal to λ. A reciprocal lattice spacing is inversely proportional to a direct lattice repeat period and a direct lattice spacing is inversely proportional to a reciprocal lattice period. The principal

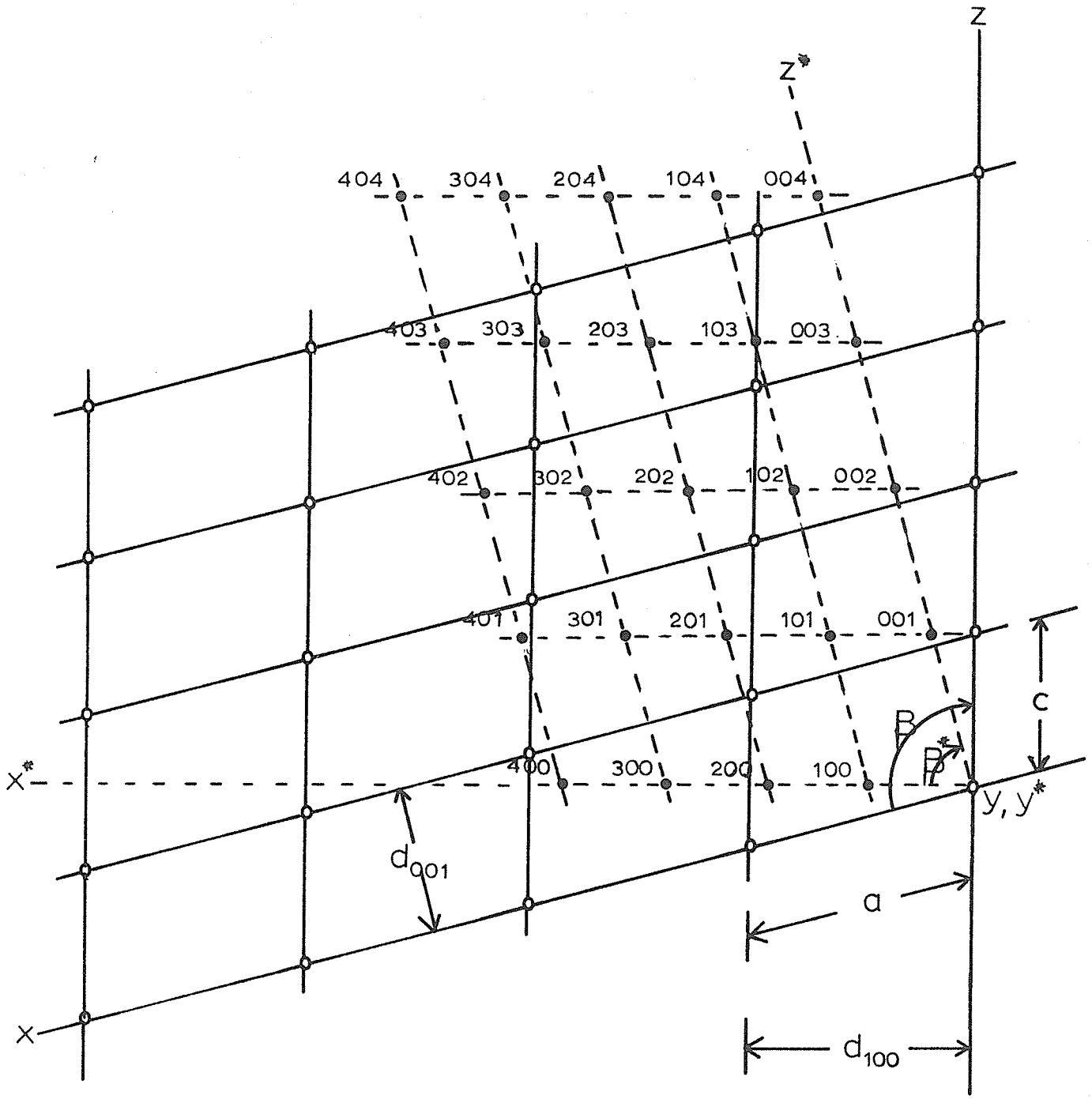

Fig 2: A monoclinic primitive lattice projected along the y axis. The direct lattice is represented by solid lines. The reciprocal lattice is represented by dashed lines.

axes of the reciprocal lattice, x^*, y^* and z^* are the normals from the origin to the three principal planes of the unit cell, (100), (010) and (001) respectively. Asterisks are added to the symbols of direct lattice elements to denote those elements of the reciprocal lattice.

The Bragg equation for reflection by the real lattice has its exact geometrical equivalent in terms of the reciprocal lattice. This leads to the concept of the "sphere of reflection" shown in Fig.3 (a). The set of direct lattice planes XX' in the reflecting position have the interplanar spacing d. The incident monochromatic X-ray beam strikes XX' at Y with the angle θ. YQ is constructed normal to these planes such that $YQ = \frac{\lambda}{d}$. AQ is constructed normal to YQ and hence parallel to the reflecting planes. Then angle $YAQ = \theta$ and $YA = \frac{YQ}{\sin\theta} = \frac{\lambda}{d \sin\theta}$. The Bragg condition for reflection is $\lambda = 2d_{nh\ nk\ n\ell} \sin\theta$. Then, $\frac{\lambda}{d \sin\theta} = 2 = YA$ for all reflecting positions. Also angle AQY is always a right angle for reflecting conditions. Thus, the locus of all points Q in one plane will be a circle and in three dimensions will be a sphere with diameter YA. Since $YA = 2$, the radius of the sphere is unity. Thus, when a set of planes is reflecting an X-ray beam, its reciprocal point is on this sphere called the sphere of reflection.

The centre of the sphere is O. OQ connects the centre of the sphere with a reciprocal lattice point on its surface and makes an angle 2θ with the undeviated X-ray beam and it

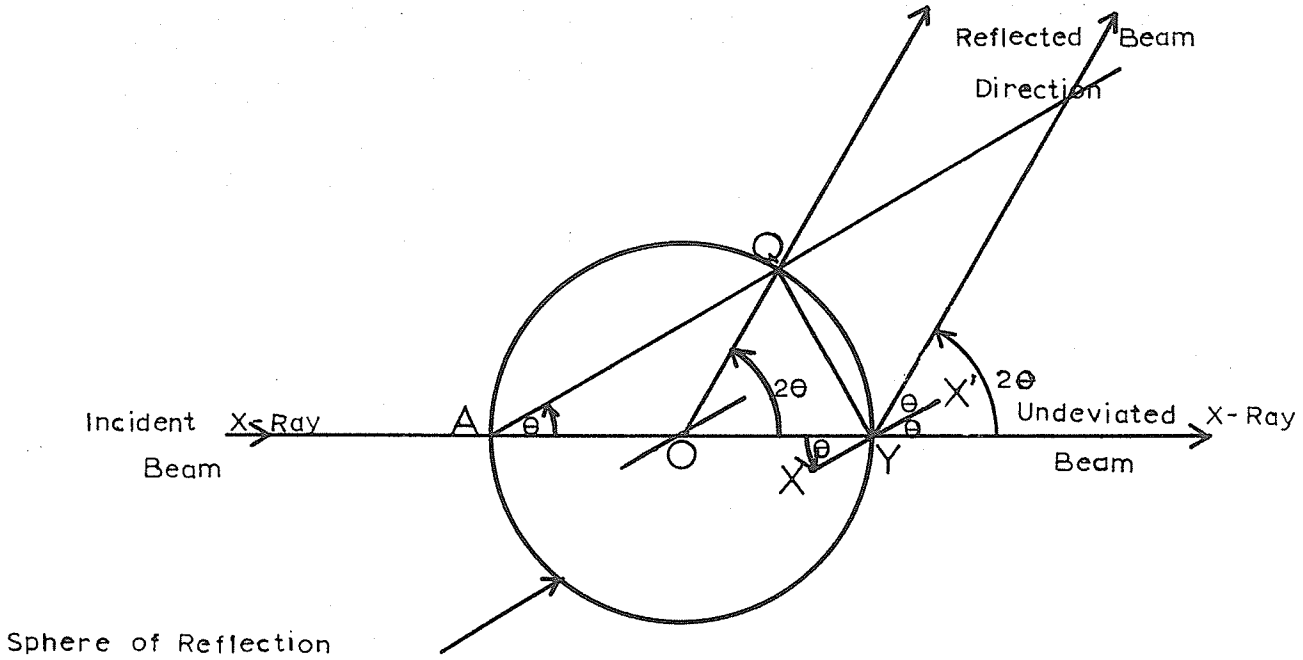

Fig. 3 (a) Sphere of reflection derivation.

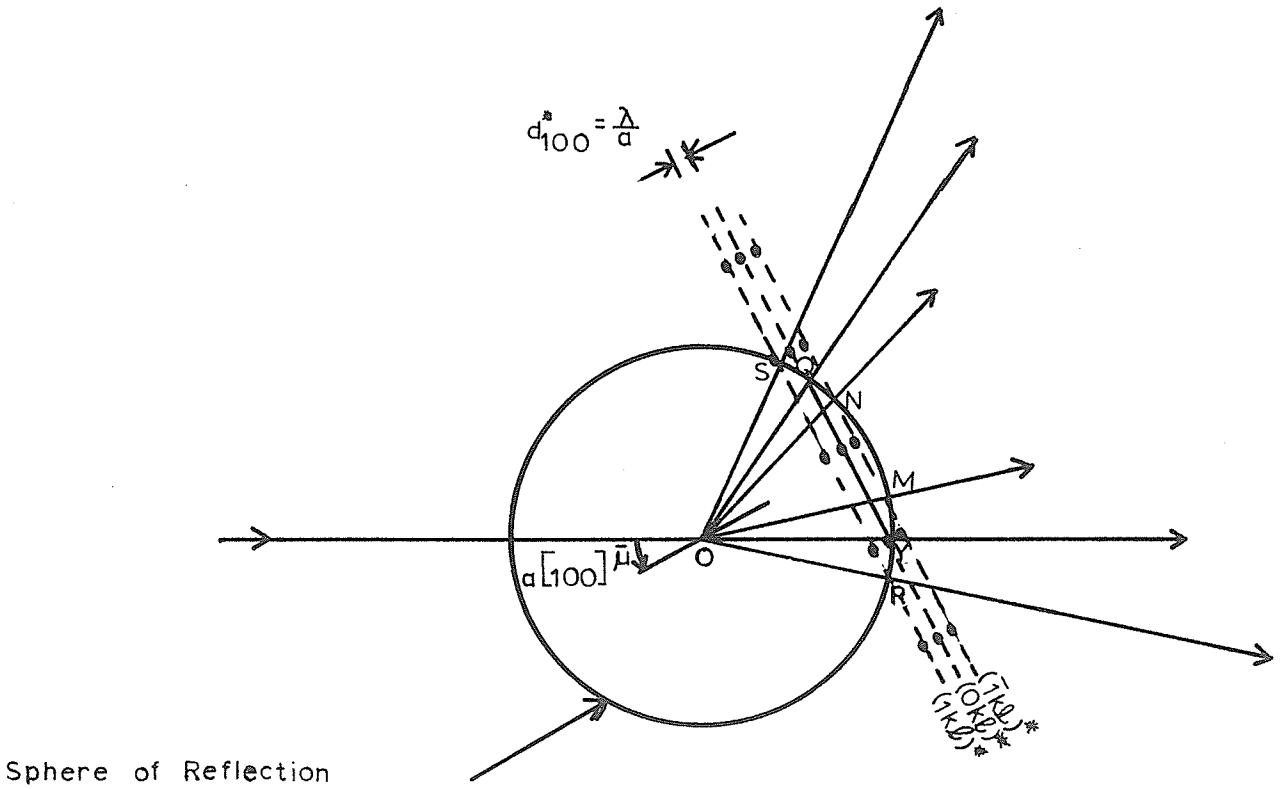

Fig. 3 (b) A crystal with its a [100] axis oriented at an angle $\bar{\mu}$ to the X-ray beam. Origin of the direct lattice is at O; origin of the reciprocal lattice is at Y.

therefore gives the direction of the reflected beam. Thus, we could place the crystal at O, the centre of the sphere. In terms of the reciprocal lattice, reflection could then be looked upon as constructing a sphere of unit radius with the crystal (or direct lattice) at its centre O, the primary beam along one diameter and the origin of the reciprocal lattice at the point where the primary beam emerges from the sphere (Y). Whenever a reciprocal lattice point, at a distance $\frac{\lambda}{d}$ from the origin, just touches the surface of the sphere, a reflected beam moves out, the incident beam being reflected by the direct lattice plane corresponding to the reciprocal lattice point.

In Fig. 3 (b) consider a crystal with its direct axis $\underline{a}$ [100] oriented at an angle $\overline{\mu}$ to the X-ray beam. Normal to this direct axis, there will be a set of reciprocal lattice planes. These reciprocal lattice planes, $(0k\ell)^*$, $(\bar{1}k\ell)^*$, $(1k\ell)^*$, etc., intersect the sphere of reflection in circles with diameters YQ, MN, RS, etc. In order to satisfy the Bragg relationship a reciprocal lattice point from any reciprocal plane must lie on the surface of the sphere - more specifically, the reciprocal lattice point must lie on the circumference of the circle formed by the intersection of the reciprocal plane and the sphere. Since the reflections are emitted from O and pass through these points, the reflections lie on the surfaces of cones which are coaxial with the $\underline{a}$ [100] axis. In single crystal methods, diffraction

cones are generated; motion of the crystal causes reciprocal planes to pass through the sphere of reflection usually with one reciprocal plane at a time being recorded on film in the photographic technique.

CHAPTER III

THE PRECESSION METHOD

A. THEORY

The precession method was developed by Buerger (1964). In this technique a single crystal is mounted for simultaneous rotation around a reciprocal axis and precession of a direct axis about the incident X-ray beam. A flat photographic film and a reciprocal lattice plane perform the same motion with respect to the incident X-ray beam direction; the reciprocal plane is recorded on the film in an undistorted form.

The arrangement for the precession method is shown in Fig. 4. The crystal is mounted for rotation around the reciprocal axis $\underline{b}^*$ (perpendicular to the plane of the paper) and precession of the direct axis $\underline{a}$ $[100]$ at an angle $\bar{\mu}$ with respect to the incident X-ray beam. The screen which is located between the crystal and film permits the reflections from only one reciprocal plane to reach the film. Because reflections from these reciprocal planes lie on the surfaces of cones which are coaxial with $\underline{a}$ $[100]$, the screen has an annular opening whose axis coincides with the precession axis.

B. PRACTICAL APPLICATION TO SINGLE CRYSTALS OF $C_5H_5CuP(C_2H_5)_3$

(i) Orientation of the crystal

In order to obtain a precession photograph of a reciprocal lattice plane, the crystal must be properly oriented. Single crystals of $C_5H_5CuP(C_2H_5)_3$, "appeared" to outline the forms $\{100\}$, $\{010\}$ and $\{001\}$ of a monoclinic crystal. In the monoclinic system, the direct axis $\underline{b}$ $[010]$ coincides with the

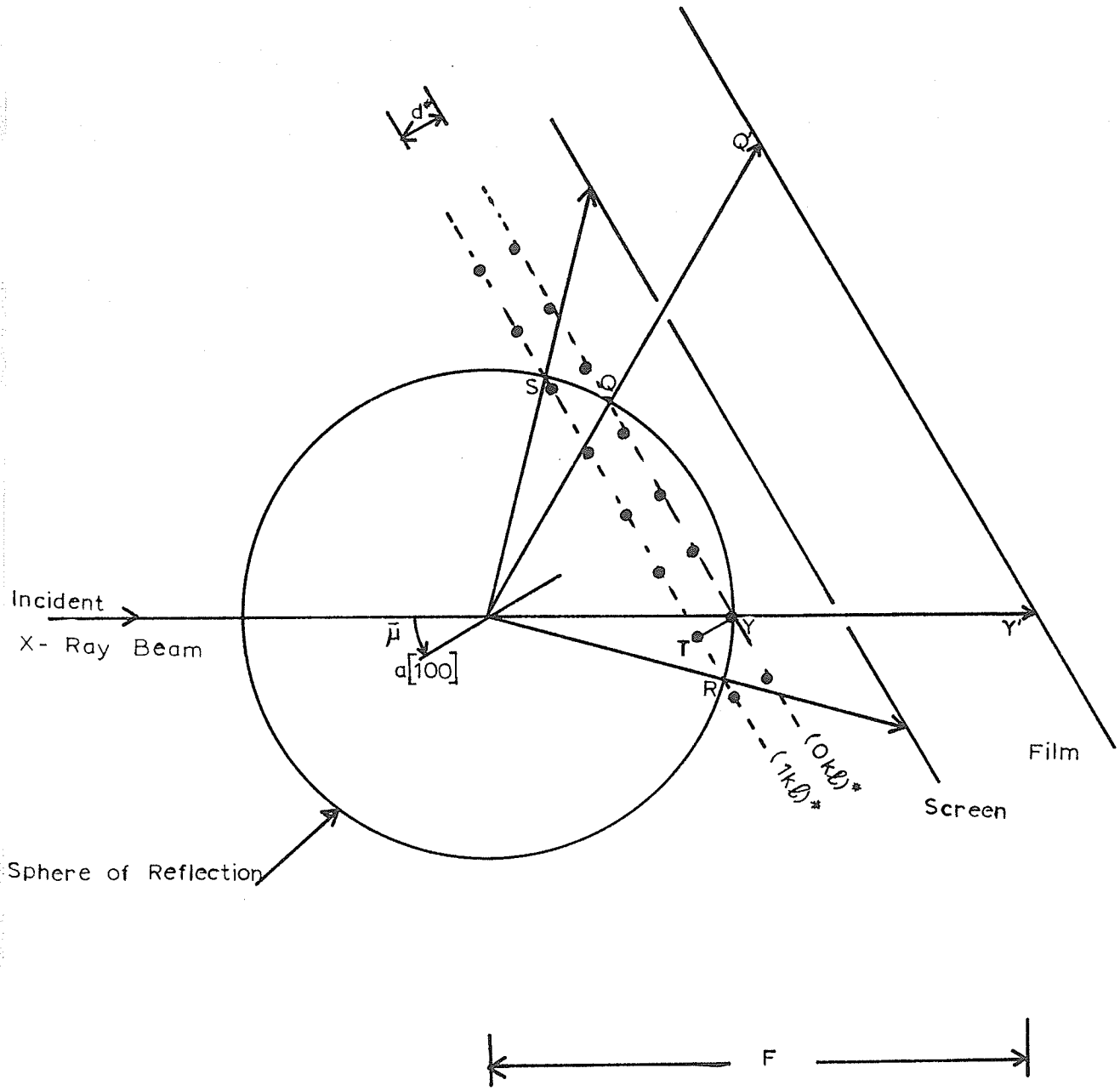

Fig. 4 Experimental arrangement for the precession method.

reciprocal axis $\underline{b}^*$. Since this "apparent" monoclinic crystal had well-developed faces, it was mounted for rotation around the "assumed" $\underline{b}\,[010]$ (also $\underline{b}^*$) axis by the use of a reflecting goniometer. The goniometer head was transferred to the precession instrument and the crystal was centered in the collimator. The dial axis was then turned until one rocker arm was perpendicular to the incident X-ray beam. A precession photograph, Fig. 5 (a), was obtained using unfiltered molybdenum radiation; the precession angle was ten degrees with the crystal to film distance being 60 mm. No screen was employed.

Fig. 5 (a) and subsequent photographs were viewed in the direction of the incident X-ray beam, i.e. from the X-ray tube to the film.

This photograph shows the strong predominance of the zero level reflections over those of the upper levels, a characteristic of orientation photographs. With $\underline{a}\,[100]$ as the precession axis, the $0k\ell$ reflections are the zero level reflections. The line connecting the two fiducial spots, which are at the extremes of the picture width, forms the axis of rotation. In Fig. 5 (a), a reciprocal lattice row is almost parallel to the fiducial spots. The angle ϕ between this reciprocal row and the axis of rotation is the adjustment to be made to the vertical rocker. In this case the vertical correction was 2.2°.

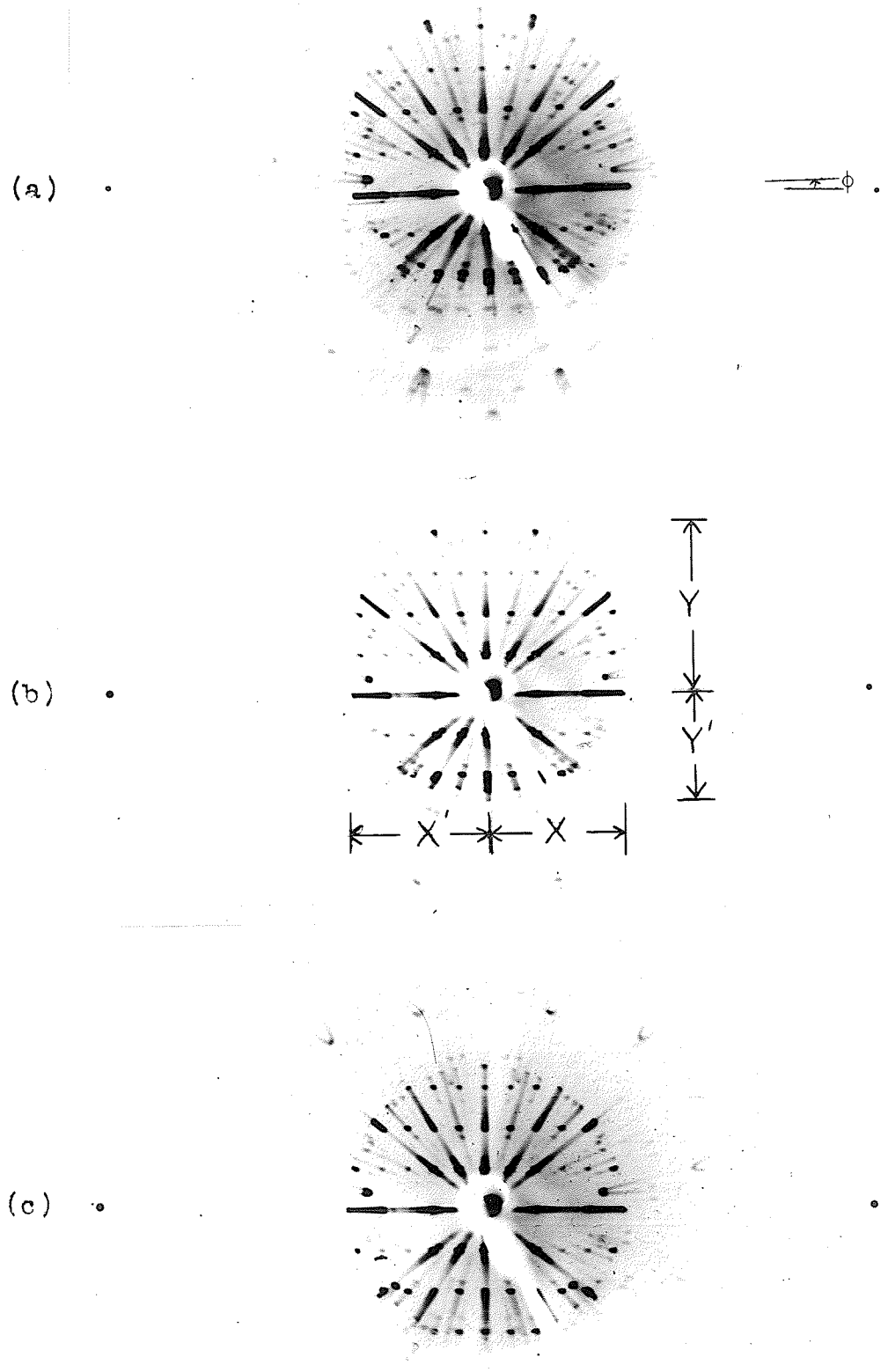

Fig. 5. Precession orientation photographs (contact prints) of $C_5H_5CuP(C_2H_5)_3$, Mo/- radiation, $\bar{\mu}$ = 10°, F= 60 mm. Details of corrections given in text.

After this adjustment was made, another photograph was taken as shown in Fig. 5 (b).

The offset of the zero level circle of reflections in a horizontal direction is due to an orientation error in the horizontal rocker. $X - X'$ is proportional to the orientation error in the horizontal plane. Using the graph given by E.W. Nuffield, (1966, Fig. 9-20) the conversion of this reading in mm on the photograph to degrees error on the horizontal rocker arm was obtained. To eliminate this error, the crystal was moved 0.4° away from the X-ray beam in the horizontal direction. The crystal is now mounted for rotation around the $\underline{b}^*$ axis. The orientation error $Y - Y'$ was used so that a direct axis of the crystal would precess about the incident X-ray beam. The conversion of this mm reading on the photograph to an angular correction in degrees in the setting of the dial axis was obtained from the same graph previously used in the $X - X'$ correction. The crystal was tilted 2.6° away from the X-ray beam for this adjustment. The photograph taken following these corrections is given in Fig. 5 (c). This photograph shows that the crystal is properly oriented for rotation around a reciprocal axis and precession of a direct axis about the X-ray beam.

(ii) Zero level photographs

For a zero level photograph, only the cone of reflections due to the zero level is permitted to pass through the screen. The crystal to film distance, F, is maintained at 60 mm for

all zero level photographs. This value is also the magnification factor of the zero level reciprocal lattice plane in dimensionless reciprocal lattice units (r. l. u.) shown by Fig. 4: $\frac{Y'C_c'}{YQ} = \frac{OY'}{OY} = \frac{F}{I} = F$.

Fig 6 (a) is a zero level precession photograph of $C_5H_5CuP(C_2H_5)_3$ with the crystal oriented for rotation around the $\underline{b}^*$ axis and precession of the $\underline{a}$ [100] axis about the X-ray beam. Molybdenum radiation with a zirconium filter was used.

(iii) Upper level photographs

In order to record higher level reciprocal lattice planes, a knowledge of d^*, the reciprocal spacing along the precession axis of the crystal is required. A cone axis photograph was used to obtain d^*.

In a cone axis photograph, the film is placed in the screen holder with the precession angle usually set at 10°. A cone axis photograph consists of reflections forming a series of concentric circles with the zero level usually being the smallest and the most intense. The circles of larger radii result from the higher order reflection cones with the first level cone corresponding to the smallest of these. The reciprocal lattice spacing, d^*, for any level is found by measuring the radius of the corresponding cone on the cone axis picture and solving the equation, $d^* = \cos \bar{\mu} - \cos \tan^{-1} \frac{R}{f}$ where $\bar{\mu}$ is the precession angle, R is the radius of the circle of reflections, and f is the crystal to film distance. Having calculated d^* and having

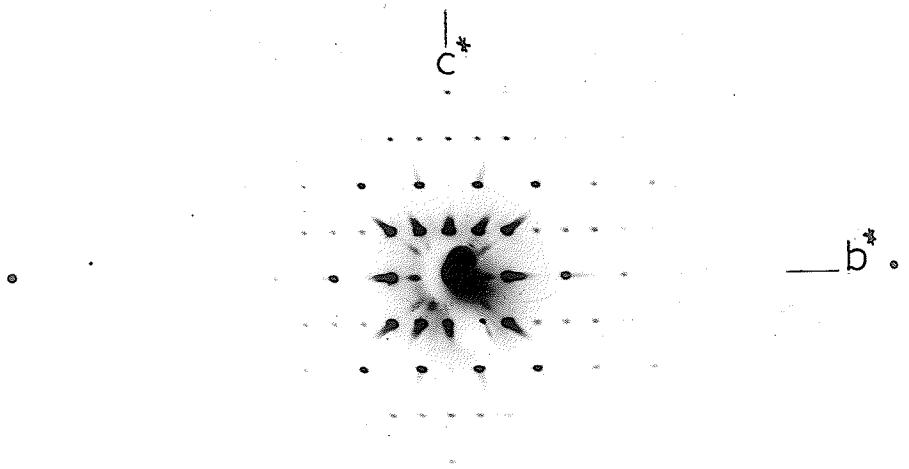

(a) 0kl precession photograph.

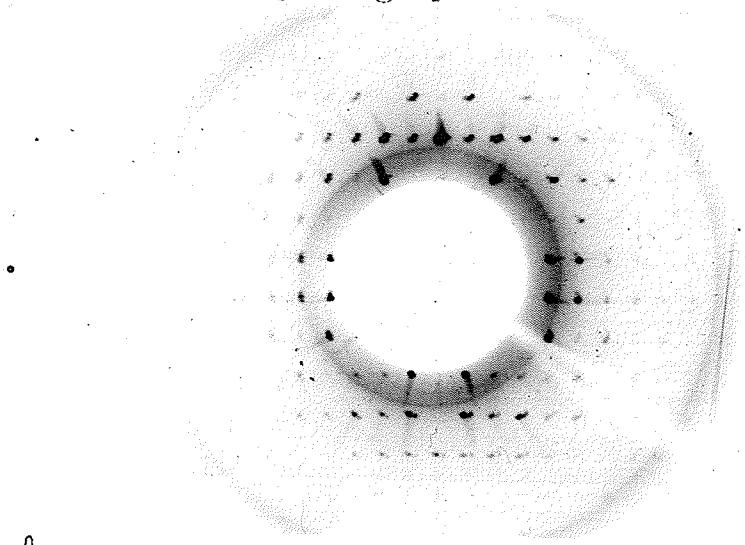

(b) 1kl precession photograph.

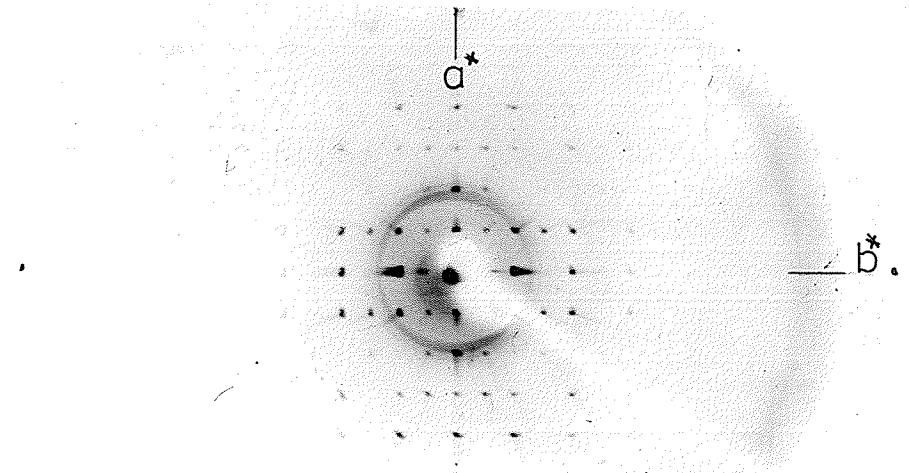

(c) hk0 precession photograph.

Fig. 6. Contact prints of precession photographs of $C_5H_5CuP(C_2H_5)_3$, Mo K_α radiation, $\bar{\mu} = 25$.

chosen a suitable screen radius, a precession angle and a crystal to screen distance, the upper level photograph may be taken. These variables are related by the equation $d^* = \cos \bar{\mu} - \cos \tan^{-1} \frac{r_s}{s}$ where r_s is the screen radius and s is the crystal to screen distance. The flat photographic film is placed in the holder used for the zero level photograph, with the holder advanced toward the crystal a distance Fd^* from the position used for the zero level photograph. This upper level photograph will have the same magnification factor as the zero level.

A first level precession photograph taken of $C_5H_5CuP(C_2H_5)_3$ with the crystal mounted for rotation around $\underline{b}^*$ with the precession axis $\underline{a}$ [100] is shown is Fig. 6 (b). This is a photograph of the $(1\ k\ \ell)^*$ reciprocal lattice plane. The blank central portion of the first level photograph results from some reciprocal lattice points remaining inside the sphere of reflection throughout the entire motion of the crystal. From Fig. 4, the small central portion of the first level reciprocal plane, $(1\ k\ \ell)^*$, of radius TR remains inside the sphere during the crystal's movement. Thus the direct lattice planes corresponding to the reciprocal lattice points in this area never reflect.

Fig. 6 (c) is a zero level precession photograph of the crystal mounted for rotation around the $\underline{b}^*$ axis with the $\underline{c}$ [001] axis as the precession axis. The dial was turned through an angle of more than 115° from the position of the $\underline{a}$ [100] axis precession in order to obtain precession of the

$\underline{c}$[001] axis about the X-ray beam. The choice of the $\underline{a}$ and $\underline{c}$ axes agreed with the morphology of the crystal i.e. both were along faces of the crystal. The value of $c^* > a^*$ preserves the convention in direct space of $c_o < a_o$. As indicated by the $(0k\ell)^*$ and $(hk0)^*$ reciprocal plane photographs, Figs. 6 (a) and (c) respectively, both the $\underline{c}^*$ and $\underline{a}^*$ axes are perpendicular to $\underline{b}^*$. The fact that both α and γ are right angles, whereas the angle β is about 115°, establishes the crystal system as monoclinic.

From the zero and first level photographs, Figs. 6 (a), (b) and (c), the only occurring systematic absence is, 0k0 present only with k even. An examination of Nuffield (1966, Table A3-2) for only this systematic absence gives the possible space groups as $P2_1$ and $P2_1/m$.

(iv) Unit cell dimensions of $C_5H_5CuP(C_2H_5)_3$ from zero level precession photographs

Precession photographs are usually measured with the use of a device shown in Fig. 7. The photograph is mounted on the glass plate. The disk is rotated to place rows of reciprocal lattice points parallel to the hairline. The translation period between rows on either side of the central row separated by n translation intervals is measured.

From Fig. 6 (a), the angle γ is a right angle. Thus the translation periods measured correspond to the magnification of the reciprocal lattice periods c^* and b^*. A calculation of the cell spacings obtained from Fig. 6 (a) is given in Table 1.

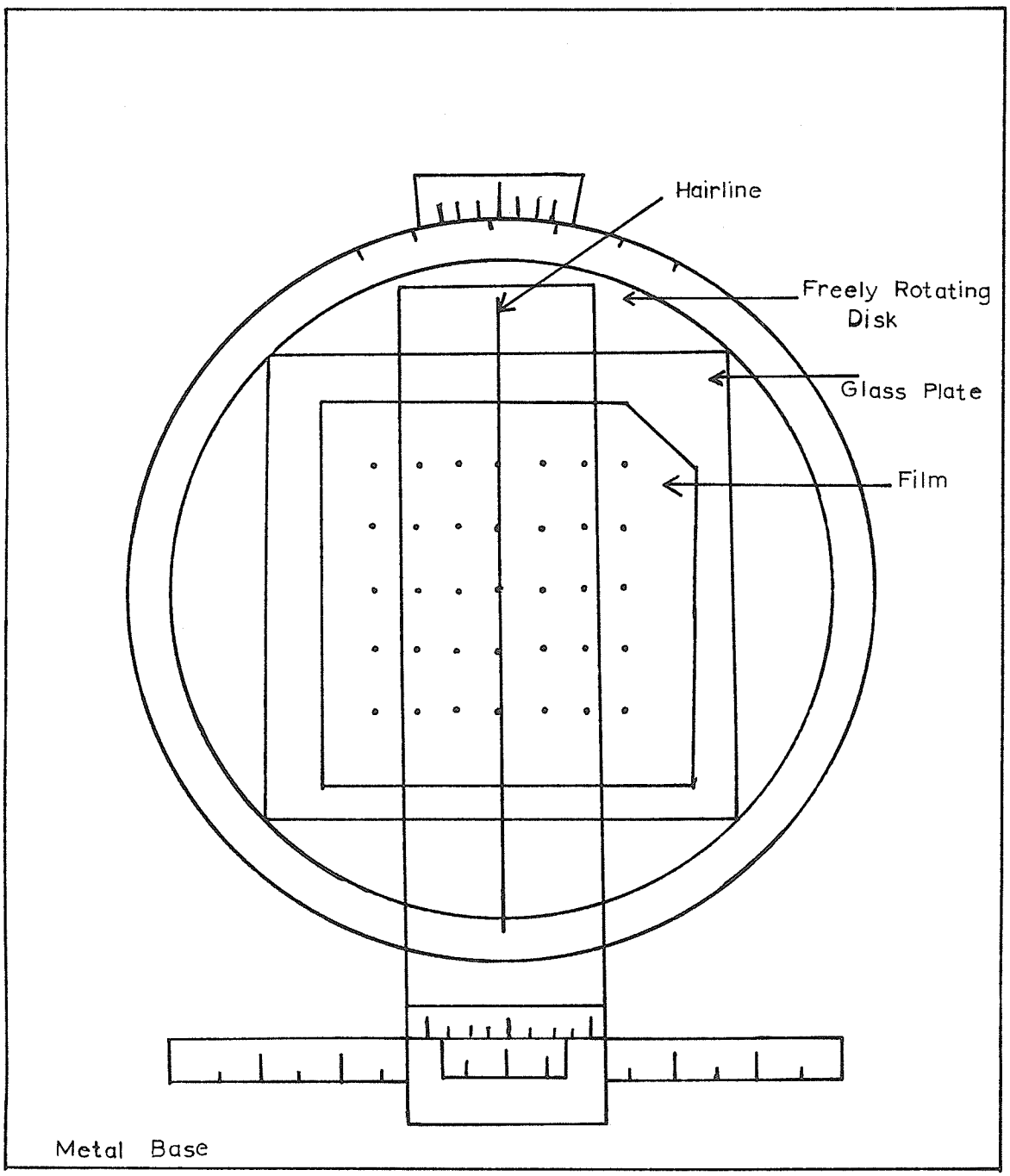

Fig. 7 Measuring device for X-ray photographs.

TABLE 1. Unit cell dimensions of a single crystal of $C_5H_5CuP(C_2H_5)_3$ from a zero level precession photograph.

The data refer to Fig. 6 (a).

λ Mo K_α = 0.7107 Å

b_o

k	Right (mm.)	Left (mm.)	2y (mm.)	y (mm.)	p* (r.l.u.)	d_{010} (Å)
1	84.90	77.20	7.70	3.85	0.0642	11.07
2	88.85	73.30	15.55	7.77	0.1296	10.97
3	92.70	69.55	23.15	11.57	0.1927	11.05
4	96.45	65.65	30.80	15.40	0.2567	11.07
5	100.30	61.80	38.50	19.25	0.3208	11.08
6	104.20	57.90	46.30	23.15	0.3858	11.05
7	108.10	54.10	54.00	27.00	0.4500	11.05
8	112.00	50.20	61.80	30.90	0.5150	11.04
9	115.80	46.20	69.60	34.80	0.5800	11.03
10	119.70	42.50	77.20	38.60	0.6433	11.05

The average of the last four readings d_{010} = 11.04 ± .01 Å

Since the y and y* axes of the crystal coincide,

$$b_o = d_{010} = 11.04 \pm .01 \text{ Å}$$

TABLE 1. (continued)

$\frac{d_{001}}{\ell}$	R (mm.)	L (mm.)	2y (mm.)	y (mm.)	p* (r.l.u.)	d_{001} (Å)
1	87.40	75.15	12.25	6.12	0.1021	6.96
2	93.10	69.00	24.10	12.05	0.2008	7.08
3	99.75	62.85	36.90	18.45	0.3075	6.93
4	105.90	56.70	49.20	24.60	0.4100	6.93
5	112.05	50.55	61.50	30.75	0.5125	6.93
6	118.25	44.55	73.70	36.85	0.6142	6.94

The average of the last four readings is $d_{001} = 6.93 \pm .01$ Å.

From a similar measurement of Fig. 6 (c),

$$d_{100} = 7.78 \pm .01 \text{ Å}.$$

CHAPTER IV

THE OSCILLATION AND ROTATION METHOD

A. THEORY

In the rotation method, a crystal is mounted about a direct axis and is oscillated around this axis through an angle of at least 180°. A fixed cylindrical film surrounding the crystal records the diffraction pattern. Oscillation photographs are produced as above except that the oscillation of the crystal is restricted to an angle less than 180°. Such photographs are used to orient a single crystal for rotation around a direct axis and to determine the repeat period along this axis.

A single row of lattice points, the points separated by the repeat period p, is along a direct axis of a crystal in Fig. 8 (a). The crystal is rotating about this axis. An X-ray beam strikes this row at right angles. At every lattice point a diffracted wave is sent out, which is the resultant scattered wave from the group of atoms which the lattice point represents. For constructive interference to occur between the diffracted rays from these lattice points, the path difference between the waves must be zero or a whole number of wave lengths i.e. $p \cos\phi = n\lambda$, where λ is the wavelength of the X-ray beam, ϕ is the angle between the axis and the diffracted ray and $n = 0, 1, 2\cdots$. For a given axis of a crystal and a given X-radiation, p and λ are constant. Then $\cos\phi$ is a constant for a given value of n. Thus, the diffracted rays lie on the surfaces of cones coaxial

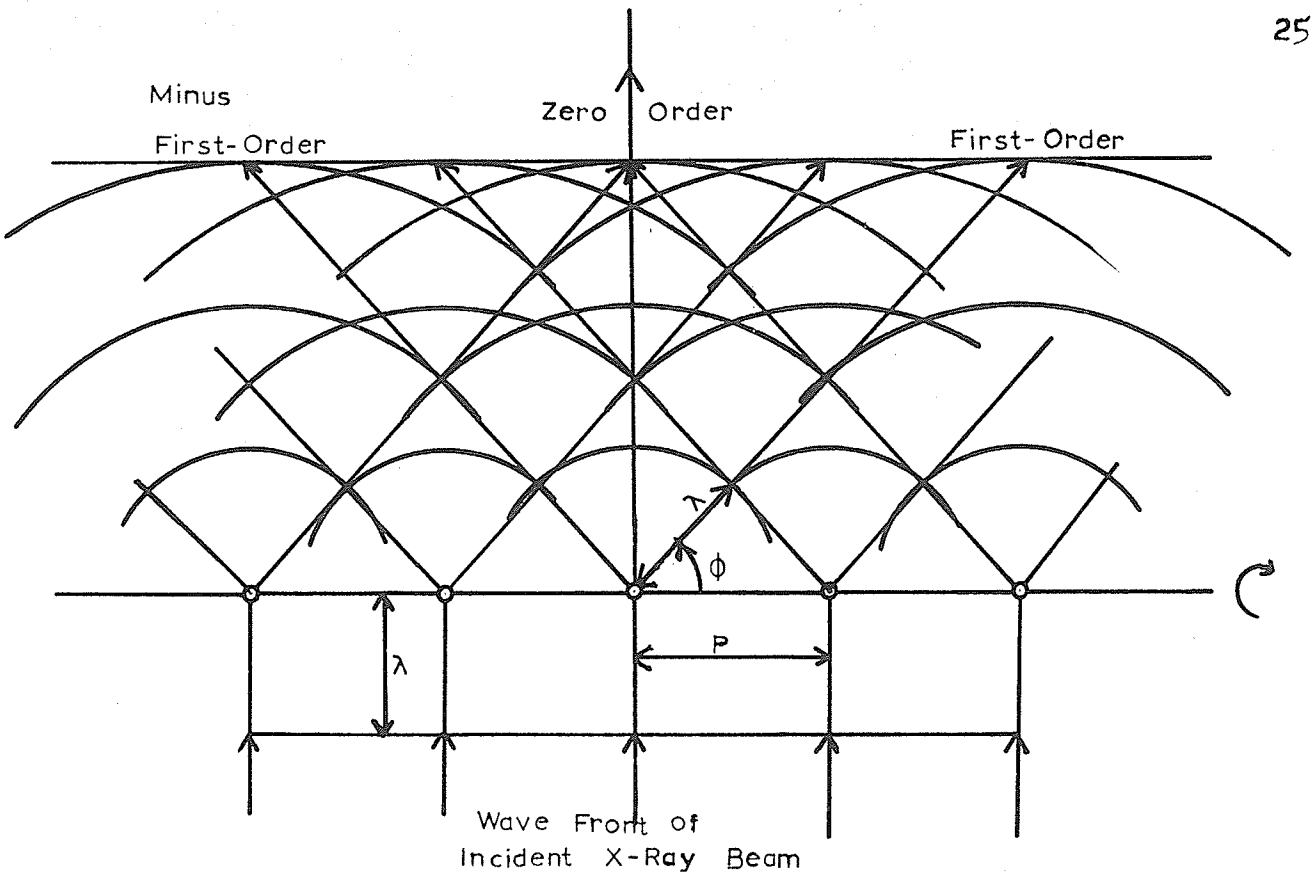

Fig. 8 (a) X-ray diffraction by a single row of lattice points separated by the repeat period p.

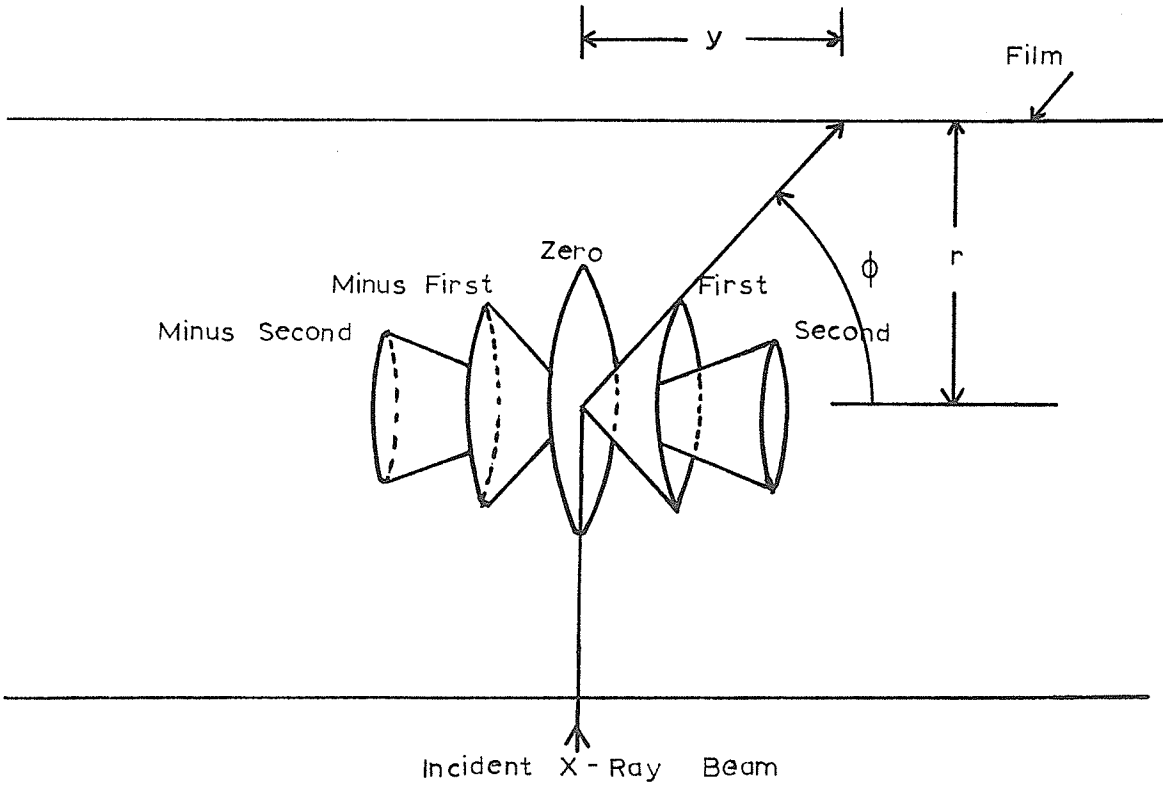

Fig. 8 (b) Diffraction cones.

with the rotation axis of the crystal where ϕ is the half-apex angle of the cone as shown in Fig. 8 (b).

This concept is indentical to Fig. 3 (b) where $\bar{\mu} = 90^{\circ}$. The zero order cone corresponds to the $(0k\ell)^*$ reciprocal lattice plane. The $(1\ k\ell)^*$ and $(\bar{1}k\ell)^*$ reciprocal planes correspond to the first order and minus first order diffraction cones. This same correlation follows for the higher order diffraction cones. When the crystal is rotated around the a [100] axis, the reflections corresponding to these reciprocal planes are recorded in straight lines on a cylindrical film. The axis of the cylindrical film is coincident with the lattice row. Because the crystal may be considered as composed of identical parallel lattice rows in three dimensions, diffracted beams are produced only in specific directions along the cones, the directions which satisfy the Bragg equation. Thus, reflection spots lying on straight lines are recorded on the cylindrical film. These lines of spots are called layer lines, each of which corresponds to a reciprocal lattice plane.

By means of our precession photographs, crystals of $C_5H_5CuP(C_2H_5)_3$ have been shown to belong to the monoclinic system. The reciprocal axis b^* and the direct axis b therefore coincide. The crystal was oriented for rotation around b^* (also b) by the techniques described in the precession method.

An oscillation photograph of a single crystal of $C_5H_5CuP(C_2H_5)_3$ with b [010] as the rotation axis using unfiltered copper radiation is given in Fig. 9.

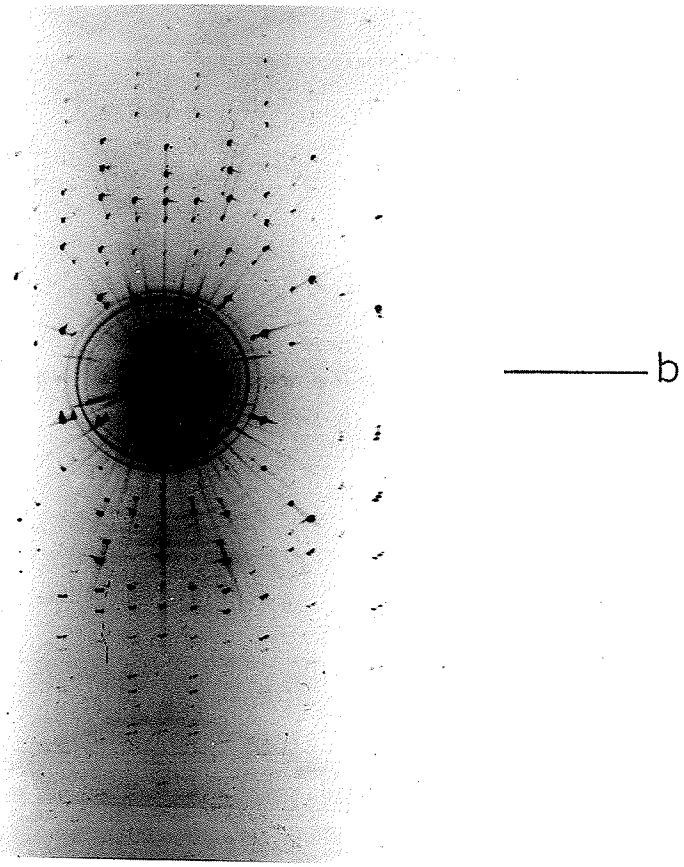

Fig. 9. Oscillation photograph (contact print) of $C_5H_5CuP(C_2H_5)_3$ rotating about the b [010] axis through an angle of 15° in a random position; the direct beam trap was not in place; multiple spots are due to the poor quality of the crystal; powder rings are due to scattering by the collimator. Cu/- radiation was used.

B. PRACTICAL APPLICATION TO A SINGLE CRYSTAL OF $C_5H_5CuP(C_2H_5)_3$

(i) Determination of the rotation period

Fig. 8 (b) shows the diffraction cones and a trace of the cylindrical film. From this diagram $\tan \phi = \frac{r}{y}$ where r is the camera radius and y is the separation of any layer line from the zero layer line. Using this equation, the relationship $p \cos \phi = n\lambda$, and measuring the oscillation photograph in Fig. 9 with the same device used for measuring the precession photographs (Fig. 7), the repeat period along the b axis was obtained. These calculations are given in Table 2. The value of $b_o = 11.14$ Å given in Table 2 is acknowledged to be inaccurate due to the poor quality of the crystal used in obtaining the photograph in Fig. 9. The value of b_o obtained from the precession method was then taken as this cell dimension.

TABLE 2. Determination of the rotation period from an oscillation photograph.

Rotation about the b [010] axis. (Unfiltered copper radiation was used).

$\lambda CuK_\alpha = 1.5418$ Å
$\lambda CuK_\beta = 1.3922$ Å

n	1		2		3		4	
	β	α	β	α	β	α	β	α
$R_{(mm.)}$	86.40	86.80	90.10	90.90	94.30	95.80	99.30	101.80
$L_{(mm.)}$	79.10	78.75	75.35	74.50	71.25	69.55	66.25	63.80
$2y_{(mm.)}$	7.30	8.05	14.75	16.40	23.05	26.25	33.05	38.00
$y_{(mm.)}$	3.65	4.03	7.40	8.20	11.53	13.15	16.53	19.00
$r/y = \tan\phi$	7.83	7.10	3.87	3.49	2.485	2.179	1.733	1.508
$\cos\phi$	0.127	0.139	0.250	0.275	0.3733	0.4171	0.4997	0.5527
$n\lambda$	1.39	1.54	2.78	3.08	4.177	4.625	5.569	6.167
$p = \frac{n\lambda}{\cos\phi} = b_o$	10.93	11.08	11.12	11.19	11.19	11.09	11.14	11.16

The average of the last four readings is $11.14 \pm .03$ Å

* The variation in the readings shows that results obtained from this method are not as precise as those given by the Precession Method.

CHAPTER V

THE EQUI-INCLINATION WEISSENBERG METHOD

A. THEORY

The Weissenberg method makes use of essentially the same experimental arrangement as that employed in the oscillation method. A crystal is rotated about a direct axis and a moving cylindrical film records the reflections of a chosen layer line. A cylindrical screen, with an equatorial slit, is inserted between the crystal and the film so as to allow only reflections of one reciprocal plane to reach the film. Horizontal translation of the cylindrical film occurs simultaneously with crystal oscillation. For Weissenberg photographs, the angle of crystal oscillation is greater than 180°. The Weissenberg instrument is designed to translate the film 1 mm for every 2° of crystal rotation. The reflections occurring on one layer line on the oscillation photograph, are recorded on the Weissenberg film in a two dimensional pattern. As a result, each reflection now has two coordinates on the film, one parallel to the axis (horizontal) and the other along the circumference of the film (vertical). The radius of the film is $\frac{360}{4\pi}$ mm. Thus a vertical coordinate of 1 mm is equivalent to an angular reading of 2°.

B. PRACTICAL APPLICATION TO SINGLE CRYSTALS OF $C_5H_5CuP(C_2H_5)_3$

(i) Zero level Weissenberg photographs

A crystal of $C_5H_5CuP(C_2H_5)_3$ was rotated about the $\underline{b}$ [010] axis (normal to the nickel-filtered copper X-ray beam) and

only the central or equatorial layer line i.e., the h 0 ℓ reflections, was allowed to pass through the Weissenberg screen; a Weissenberg photograph of the (h 0 ℓ)* reciprocal lattice plane was obtained (Fig. 10 (a)). This is a distorted picture of the reciprocal lattice. Due to the geometry of the instrument, reflections from a reciprocal lattice row which passes through the origin, fall along a straight line making an angle of 63° $26'$ with the horizontal. Reflections corresponding to reciprocal lattice rows that are parallel to rows that pass through the origin are arranged on a series of curves (festoons). The $\underline{c}^*$ and $\underline{a}^*$ axes were located on this Weissenberg photograph by a comparison with the intensties of the reflections on the $\underline{c}^*$ and $\underline{a}^*$ axes on the precession photographs (Figs. 6 (a) and 6 (c)). A Weissenberg chart was constructed through all the reflections, Fig. 10 (b). Each of the h 0 ℓ reflections on the Weissenberg photograph may then be labelled with its h and ℓ Miller indices.

(ii) Upper level Weissenberg photographs

In the equi-inclination Weissenberg method, upper level photographs are taken with the arrangement shown in Fig. 11. The rotation axis of the crystal is inclined at an angle to the X-ray beam such that the rotation axis of the reciprocal lattice intersects the level under investigation on the surface of the sphere of reflection (P). Both the diffracted beam and the undeviated X-ray beam are inclined at the same angle μ to the reciprocal levels (equi-inclination).

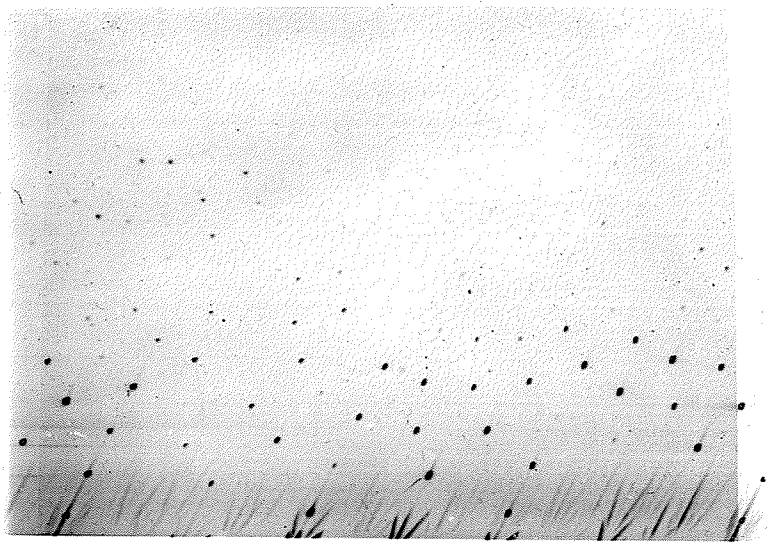

Fig. 10 (a). $h0l$ Weissenberg photograph of $C_5H_5CuP(C_2H_5)_3$, Cu K_α radiation, no direct beam line on photograph, only half (bottom) of the photograph is shown.

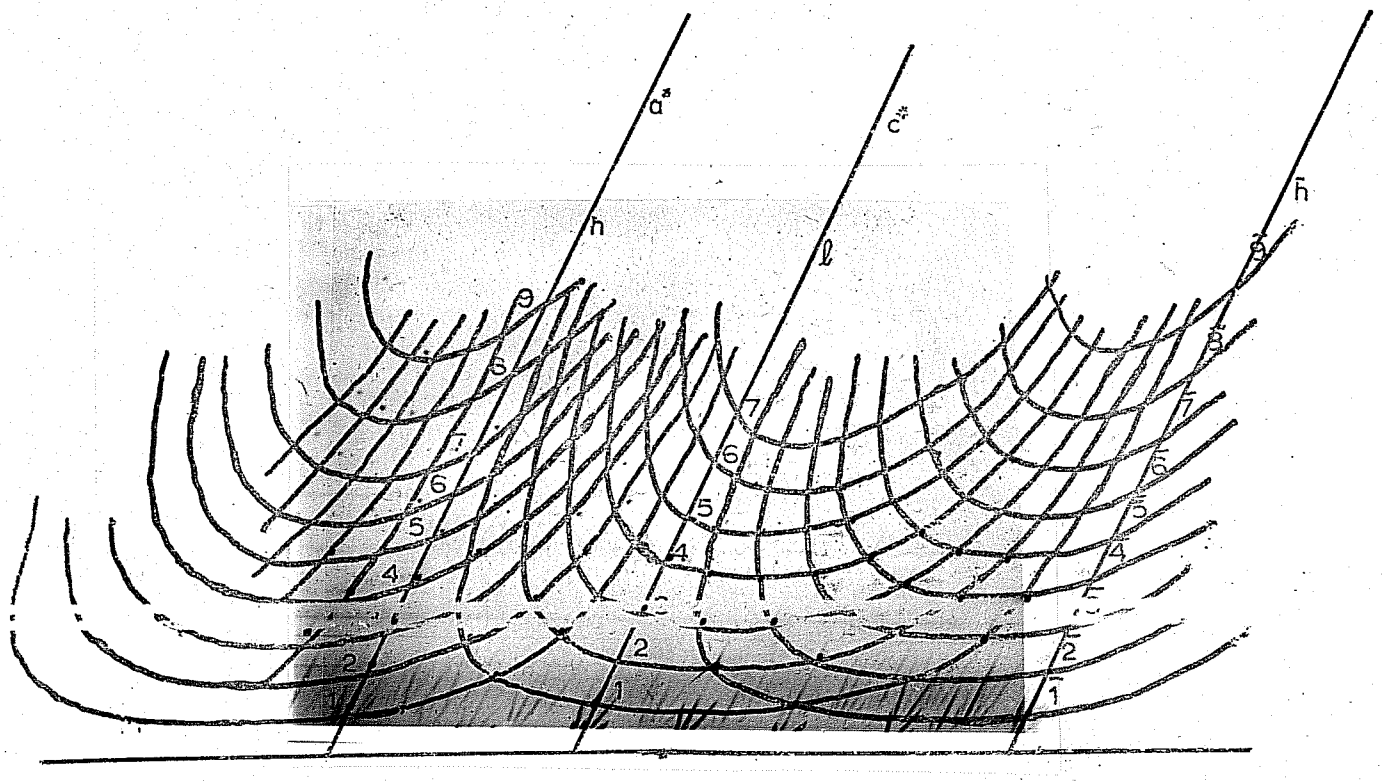

Fig. 10 (a). $h0l$ Weissenberg photograph of $C_5H_5CuP(C_2H_5)_3$, Cu K_α radiation, no direct beam line on photograph, only half (bottom) of the photograph is shown.

Fig.10 (b). Weissenberg chart for the Weissenberg photograph shown in Fig. 10 (a).

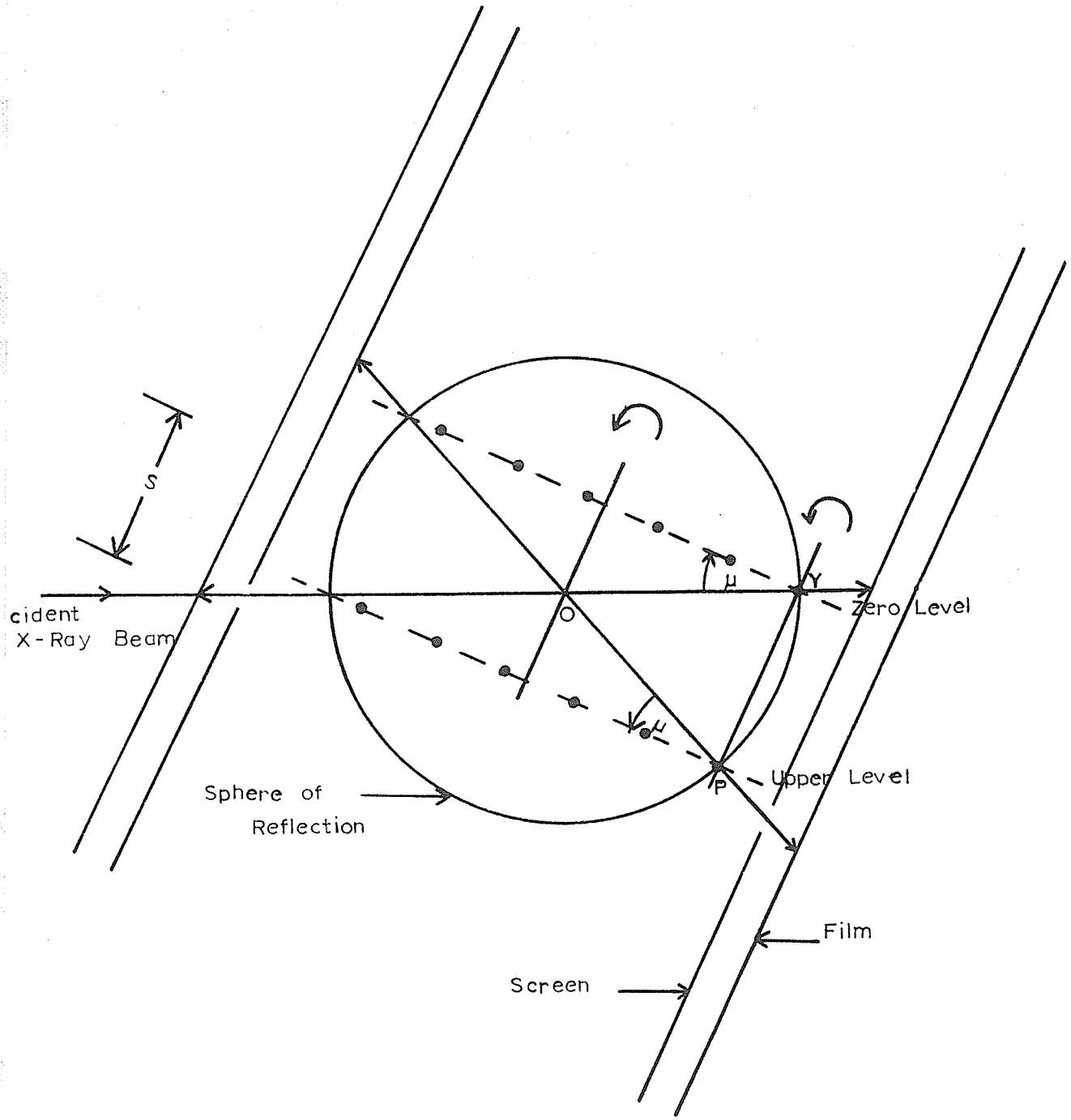

Fig. 11 Experimental arrangement for the equi-inclination Weissenberg method.

The angle μ is related to s^1 (obtained from the precession method) and y^2 (obtained from the oscillation method) by the graph illustrated in Buerger (1942, Fig. 155). The offset of the screen setting S from that for the zero level photograph is also obtained from Buerger (1942, Fig. 156)

The intensities of all the reflections for the structure elucidation of $C_5H_5CuP(C_2H_5)_3$ were obtained from Weissenberg photographs of the $h0\ell$ - $h9\ell$ levels of a crystal rotating about the b [010] axis using zirconium-filtered molybdenum radiation.

(iii) Determination of the cell dimensions from zero level Weissenberg photographs

The vertical position on either side of the film centre of Fig. 10 (a) was measured for the h 00 and 00ℓ reflections with the device shown in Fig. 7. The calculation of the cell spacings from these measurements is given in Table 3.

$1\ s$ (r.l.u.) $= d^*_{0k0} = \frac{k\lambda}{b_o} = \frac{k\lambda}{d_{010}}$ since b and b^* coincide in the monoclinic system.

$2\ y$ (mm) is the distance from the zero layer line to the upper layer line on the oscillation photograph (Fig. 9).

TABLE 3. A. Determination of the unit cell dimensions of a single crystal of $C_5H_5CuP(C_2H_5)_3$ from a zero level Weissenberg photograph (Fig. 10 (a)).

Nickel-filtered copper radiation was used. $\lambda CuK_{\bar{\alpha}} = 1.5418$ Å.

d_{100}

Index	R (mm.)	L (mm.)	2θ (°)	θ (°)	sinθ	2 sinθ	nλ (Å)	d_{100} (Å)
100	87.35	76.00	11.35	5.67	0.0989	0.1978	1.542	7.79
200	93.20	70.25	22.95	11.47	0.1989	0.3978	3.084	7.75
300	99.05	64.30	34.75	17.37	0.2986	0.5972	4.625	7.75
400	105.10	58.30	46.80	23.40	0.3971	0.7942	6.167	7.77
500	111.60	51.80	59.80	29.90	0.4985	0.9970	7.709	7.73
700	125.65	37.80	87.85	43.92	0.6937	1.3874	10.793	7.78
800	133.90	29.25	104.65	52.33	0.7915	1.5832	12.334	7.79

The average of the last four readings is $d_{100} = 7.77 \pm .02$ Å

d_{001}

Index	R (mm.)	L (mm.)	2θ (°)	θ (°)	sinθ	2 sinθ	nλ (Å)	d_{100} (Å)
001	88.20	75.45	12.75	6.37	0.1110	0.2220	1.542	6.95
002	94.40	68.65	25.75	12.87	0.2228	0.4456	3.084	6.92
003	101.10	62.15	38.95	19.47	0.3334	0.6668	4.625	6.94
004	107.90	55.25	52.65	26.32	0.4435	0.8870	6.167	6.95

The average of all the readings is $d_{001} = 6.94 \pm .01$ Å

The calculation of β^*: $\beta^*/180^\circ = 28.75/80.00$

$\beta^* = 64.69^\circ$

$\therefore \beta = 115.31^\circ$

and $\sin\beta = 0.9040$

TABLE 3. (continued)

B. Unit cell dimensions of a single crystal of $C_5H_5CuP(C_2H_5)_3$

From the precession (Table 1) and Weissenberg methods the average $d_{100} = 7.775$ A and $d_{001} = 6.935$ Å.

$$a_o = \frac{d_{100}}{\sin\beta} = \frac{7.775}{0.904} = 8.60 \pm .02 \text{ Å}$$

From the precession method (Table 1)

$$b_o = 11.04 \pm .01 \text{ Å}$$

$$c_o = \frac{d_{001}}{\sin\beta} = \frac{6.935}{0.904} = 7.67 \pm .01 \text{ Å}.$$

The volume V of the unit cell is 658.3 Å^3

C. Density and cell content (Z).

The density ρ of a single crystal of $C_5H_5CuP(C_2H_5)_3$ was 1.25 gm/cc, obtained by flotation in an aqueous sodium bromide solution.

The number of molecules/unit cell $Z = \frac{V\rho N}{M}$

where N is the Avogadro number 6.023×10^{23} and M is the molecular weight 246.8.

$$Z = \frac{658.3\times10^{-24} \times 1.25 \times 6.023\times10^{23}}{246.8} = 2.00$$

There are two molecules/unit cell in $C_5H_5CuP(C_2H_5)_3$.

D. Size of crystal, linear absorption coefficient (μ) and μR.

The crystal used for the intensity collection was approximately 0..4x.4x.4 mm.

The linear absorption coefficient $\mu = 18 \text{ cm}^{-1}$ and $\mu R = 0.4$. Therefore the absorption is negligible.

CHAPTER VI

EXPERIMENTAL

Infrared spectra were recorded using a Perkin-Elmer Model 337 Grating Infrared Spectrophotometer. Proton magnetic resonance spectra were obtained using a Varian Model A-56/60A NMR spectrometer equipped with a low temperature probe. Mass spectra were recorded by means of a Hitachi Perkin-Elmer Model RMU-6D mass spectrometer. The X-ray photographs were taken with the use of a Phillips X-ray generator in conjection with an Otto Von Der Heyde precession instrument and a Nonius Weissenberg camera using Kodak Medical X-ray film (NO SCREEN).

Microanalysis was performed by Geller Laboratories.

Cyclopentadienyl(triethylphosphine)copper(I), $C_5H_5CuP(C_2H_5)_3$ was prepared essentially by the method of Wilkinson and Piper (1956).

The preparations of Cu_2O, C_5H_5 and $P(C_2H_5)_3$

Cuprous oxide was prepared by hydrazine reduction of cupric acetate (Brauer (1954)).

Cyclopentadiene was made by the pyrolysis of dicyclopentadiene.

During the course of each of the following preparations, the reaction mixture was maintained under a nitrogen atmosphere and was stirred constantly.

Triethylphosphine was prepared by the following Grignard reaction. One liter of dry ether was added to 48.6 gms (2 moles) of magnesium turnings in a three-necked 2-liter round bottom

flask. Ethyl chloride was slowly dissolved into the solution until the supply of magnesium was exhausted. Phosphorus trichloride 46.6 mls (0.53 moles) was added dropwise to the Grignard solution by means of a pressure-equalized dropping funnel. The reaction mixture was refluxed overnight. The ether was removed by distillation. Further distillation gave 45 mls (57% yield) of triethylphosphine.

The preparation of cyclopentadienyl(triethylphosphine)-copper(I)

In a three-necked 500 ml round bottom flask 3.3 gms (23 mmoles) of the cuprous oxide was added with stirring to 150 mls of petroleum ether and 7 mls (85 mmoles) of freshly distilled cyclopentadiene. Triethylphosphine (7 mls) mixed with 10 mls of petroleum ether, was added dropwise using a pressure - equalized dropping funnel. The mixture was refluxed for three hours. The solvent was removed by distillation, the residue was placed in the vacuum sublimer shown in Fig. 12 and left overnight at 40°C and 10^{-3} mm Hg pressure. The triethylphosphine oxide (m.p. 55-56°C) present was removed and the temperature raised to 55°C. After 24 hours 3 gms (50% yield) of pure colourless crystals of π-$C_5H_5CuP(C_2H_5)_3$ were obtained (m.p. 122-124°C in vacuo, lit. 127-128°C). The compound's infrared spectrum agreed with that of Wilkinson and Piper (1956).

Analysis: Calc. for $C_{11}H_{20}CuP$: C, 53.5; H, 8.2; Cu, 25.8; P, 12.6. Found: C, 53.8; H, 8.0; Cu, 25.4; P, 12.0.

The density of $C_5H_5CuP(C_2H_5)_3$ determined by flotation of a crystal in an aqueous sodium bromide solution was 1.25 gm/cc.

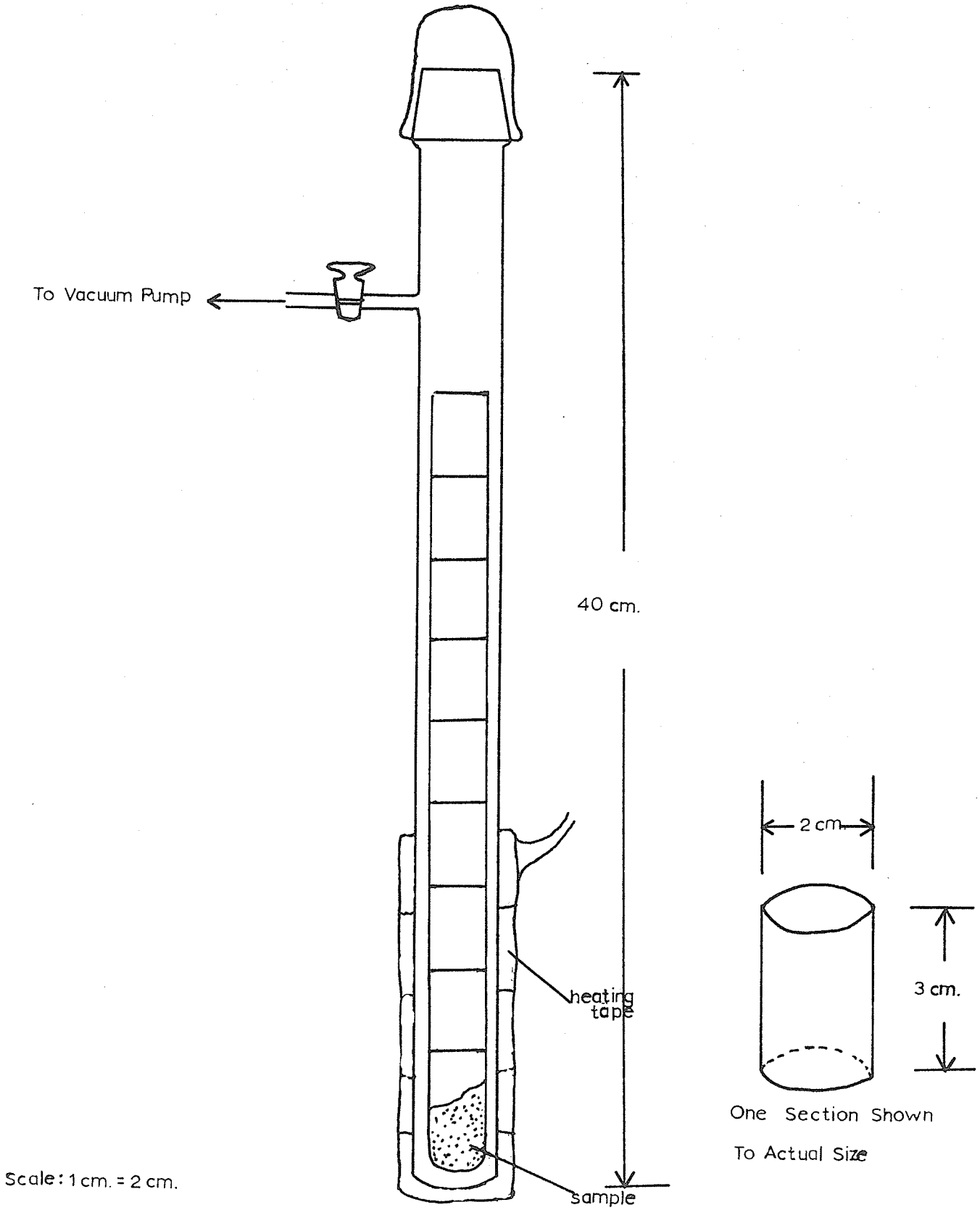

Fig 12. Sublimation Apparatus.

Crystals of the compound are stable in air for 3 - 4 hours. Subsequent oxidation causes the colourless crystals to turn green. To prevent this decomposition in air so that X-ray photographs could be taken, different coatings were applied to different crystals until a suitable material was obtained. The best coating was a thin film of a commercial aerosol hair spray (Breck regular hold) which has a water and/or alcohol base. Plastic coatings with organic solvents as a base were found to be unsatisfactory. No difference was seen in short exposure oscillation photographs taken of a crystal before and after coating. The hair spray maintained an air-tight "seal" for several days; it was reapplied after about a week to ensure that the seal was maintained.

The Preparation of Hexafluoro-2-Butyne

The method used to prepare $CF_3C \equiv CCF_3$ was mainly that of Henne and Finnegan (1949). Zinc dust (11.8 gms, 0.18 moles), 2,2,3,3-tetrachlorohexafluorobutane (21.0 gms, 0.09 moles) and zinc chloride (0.5 gms) as the catalyst were placed in a 300 cc. stainless steel bomb. Acetonitrile (100 mls) was transferred into the bomb on the vacuum rack. The mixture was maintained at 70° C for three days. Hexafluoro-2-butyne (0.023 moles) was obtained (25% yield). The infrared spectrum of the gaseous product agreed with the spectrum of $CF_3C \equiv CCF_3$ given by Smith et al. (1952).

Attempted Diels-Alder reaction of $C_5H_5CuP(C_2H_5)_3$ with hexafluoro-2-butyne

Crystals (0.15 gms, 0.0006 moles) of cyclopentadienyl-

(triethylphosphine)copper(I) were placed in a 1 liter glass vessel. Petroleum ether (50 mls) and the dienophile, $CF_3C \equiv CCF_3$ (0.001 moles) were successively transferred, by means of the vacuum rack, into this glass vessel. The mixture was maintained at 40° C for five days. The petroleum ether and the remaining $CF_3C \equiv CCF_3$ were then removed. The residue was extracted with methylene chloride. Only starting material was isolated and identified by its infrared spectrum.

CHAPTER VII

THE STRUCTURE FACTOR

A. DERIVATION

The electrons of the atoms in a crystal scatter the incident X-ray beam. The scattering of the electrons associated with each atom is combined into an atomic scattering factor, f, of the atom. In the incident X-ray beam direction, the waves scattered by all the electrons in an atom have the same path length and are therefore in phase. However, waves scattered in other directions partially interfere with one another. Accordingly, when the Bragg angle θ is zero degrees, the atomic scattering factor, f, is equal to the atomic number, Z, and as θ increases, f decreases. Atomic scattering factors are tabulated as a function of $\frac{\sin\theta}{\lambda}$ in the **International Tables for X-ray Crystallography** (1962, Vol. III).

The scattering from a unit cell depends upon the kinds and positions of the atoms present in the unit cell. The contribution from each atom in the unit cell to the wave scattered from an (hkl) plane may be represented by a vector with the amplitude f and the phase angle α. This representation is illustrated in Fig. 13 (a) for the case of a crystal structure consisting of three atoms, R, S and T. These atoms are reflecting in the first order from a set of (hkl) planes of spacing d_{hkl}. The resultant of these atomic scattering factors is the structure factor, F_{hkl}, which has the phase angle, α_{hkl}.

The values of both the structure amplitude, $|F_{hkl}|$, and the phase angle, α_{hkl}, of the structure factor depend upon the

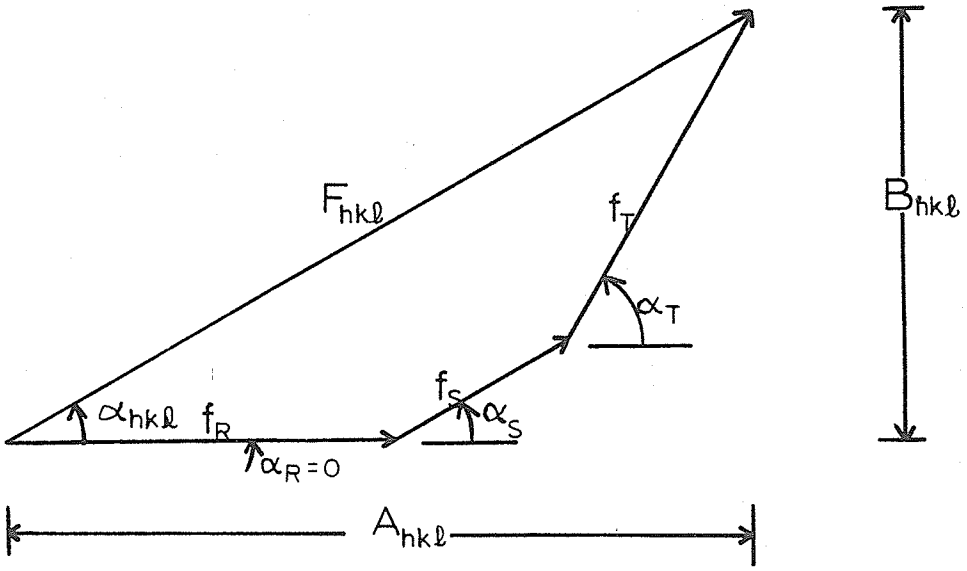

Fig. 13 (a) Structure factor from addition of atomic scattering factors.

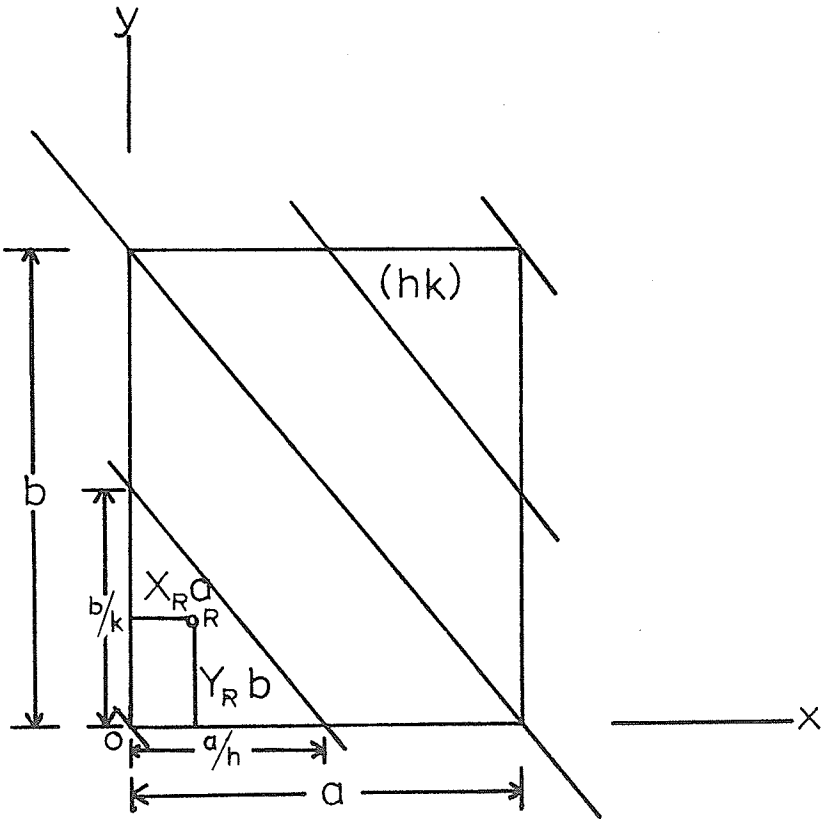

Fig. 13 (b) A two dimensional structure with only an atom R of the structure illustrated.

kind and arrangement of the atoms in the crystal structure. The structure amplitude, $|F_{hk\ell}|$, is defined as the ratio of the amplitude of the X-ray wave scattered from each ($hk\ell$) plane by the atoms in one unit cell to that scattered by one electron under the same conditions. For a particular arrangement of atoms in a unit cell, there is a particular set of diffraction waves, $F_{hk\ell}$.

The phase angle α for an atom is determined by the position of that atom in the unit cell. Consider the two dimensional structure shown in Fig. 13 (b). The set of (hk) planes is reflecting in the first order. The closest (hk) plane to the origin has intercepts $\frac{a}{h}$ and $\frac{b}{k}$ on the cell edges. These distances are equivalent to a 2π radian phase change in both the x and y directions, respectively. The position of atom R in terms of fractional coordinates (fractions of the cell edges) is (X_R, Y_R). The R atom is displaced from the origin O by the distance $X_R a$ along the x direction $Y_R b$ along the y direction. The displacements $X_R a$ and $Y_R b$ are equivalent to phase changes of $2\pi\left(\frac{X_R a}{a/h}\right) = 2\pi h X_R$ radians along the x direction and $2\pi\left(\frac{Y_R b}{b/k}\right) = 2\pi k Y_R$ radians along the y direction. The phase angle α_R is the sum of the two phase angle components, $\alpha_R = 2\pi(hX_R + kY_R)$ radians. Extending this concept to a three dimensional structure, the phase angle for an atom is $\alpha_R = 2\pi(hX_R + kY_R + \ell Z_R)$ radians, where ℓZ_R is the phase angle

component along the z direction.

From Fig. 13 (a),

$A_{hk\ell} = \sum_R f_R \cos\alpha_R = \sum_R f_R \cos 2\pi(hX_R + kY_R + \ell Z_R)$ and

$B_{hk\ell} = \sum_R f_R \sin\alpha_R = \sum_R f_R \sin 2\pi(hX_R + kY_R + \ell Z_R)$ also

$F^2_{hk\ell} = A^2_{hk\ell} + B^2_{hk\ell}$

$$= \left[\sum_R f_R \cos 2\pi(hX_R + kY_R + \ell Z_R)\right]^2 + \left[\sum_R f_R \sin 2\pi(hX_R + kY_R + \ell Z_R)\right]^2$$

and also from Fig. 13 (a),

$$\alpha_{hk\ell} = \tan^{-1}\frac{B_{hk\ell}}{A_{hk\ell}}$$

$$= \tan^{-1}\left\{\frac{\left[\sum_R f_R \sin 2\pi(hX_R + kY_R + \ell Z_R)\right]}{\left[\sum_R f_R \cos 2\pi(hX_R + kY_R + \ell Z_R)\right]}\right\}$$

In the above derivation, the structure factor was represented as a vector. The representation of the structure factor as a complex number also conveys the same information. In this latter representation, $F_{hk\ell} = A_{hk\ell} + iB_{hk\ell}$, where $i = \sqrt{-1}$ and $A_{hk\ell}$ and $B_{hk\ell}$ have the same meaning as given previously.

Since $\cos(-\phi) = \cos\phi$ and $\sin(-\phi) = -\sin\phi$,

$A_{hk\ell} = A_{\bar{h}\bar{k}\bar{\ell}}$ and $B_{hk\ell} = -B_{\bar{h}\bar{k}\bar{\ell}}$. Thus $F^2_{hk\ell} = A^2_{hk\ell} + B^2_{hk\ell} = F^2_{\bar{h}\bar{k}\bar{\ell}}$

$\therefore |F_{hk\ell}| = |F_{\bar{h}\bar{k}\bar{\ell}}|$ Friedel's law.

For the monoclinic system (b axis unique), $|F_{hk\ell}| = |F_{\bar{h}\bar{k}\bar{\ell}}| = |F_{\bar{h}k\bar{\ell}}| = |F_{\bar{h}k\ell}| \mp |F_{\bar{h}k\ell}|$ and $|F_{\bar{h}k\ell}| = |F_{hk\bar{\ell}}| = |F_{\bar{h}k\bar{\ell}}| = |F_{\bar{h}\bar{k}\ell}|$

satisfies Friedel's law and the system's symmetry. Thus, only the $hk\ell$ and $\bar{h}k\ell$ reflections are included in the structure amplitude table.

B. THE TEMPERATURE FACTOR

Atomic scattering factors are calculated for stationary atoms. However, the atoms in a crystal have thermal vibrations. At any instant these atoms are displaced from their mean positions. Consequently, waves which are reflected at the Bragg angle by successive planes are not exactly in phase (i.e. atoms in neighbouring unit cells which should scatter in phase, will scatter slightly out of phase). Thus, the atomic scattering factor is reduced by an amount which increases with increasing angle θ.

For isotropic vibration, the atomic scattering factor may be represented as $f = f_o \exp\left(-B\left(\frac{\sin\theta}{\lambda}\right)^2\right)$, where f_o is the scattering factor for the atom at rest and B is a constant relating the mean square amplitude of vibration, U ($\mathring{A}^2$), to the mean position of the atom ($8\pi^2 U$).

For anisotropic vibration, the atomic scattering factor referred to the reciprocal axes of the crystal may be represented as $f=f_o \exp -(B_{11}h^2 + B_{22}k^2 + B_{33}\ell^2 + B_{23}k\ell + B_{13}h\ell + B_{12}hk)$. These B_{ij}'s are constants and are refined in the structure determination. This anisotropic vibration equation may also

be expressed in the form $f=f_o \exp -\left[2\pi^2(U_{11}(ha^*)^2 + U_{22}(kb^*)^2 + U_{33}(\ell c^*)^2 + 2U_{23}\, k\ell b^*c^* + 2U_{13}\, h\ell\, a^*c^* + 2U_{12}\, hk\, a^*b^*)\right]$.

These U_{ij}'s are the elements of a symmetric tensor and form the matrix $\begin{pmatrix} U_{11} & U_{12} & U_{13} \\ U_{12} & U_{22} & U_{23} \\ U_{13} & U_{23} & U_{33} \end{pmatrix}$. If the crystallographic axes are not orthogonal, this U matrix may be converted by the method given in Lipson and Cochran (1966) into a matrix referred to an orthogonal set of coordinates. The eigenvalues of this converted matrix are the mean square amplitudes of vibration of the atom and form the three axes of the ellipsoid of thermal vibration.

The eigenvectors of this converted matrix are the direction cosines of these axes with respect to the orthogonal set of axes.

For the atoms in $C_5H_5CuP(C_2H_5)_3$, the orthogonal system was chosen along the x^*, y^* and z^* axes. The statements, added to the NRC-12 Bond Scan program, which are required for the calculation of the U_{ij}'s, the mean square amplitudes of vibration, and the direction cosines of these amplitudes are given in Appendix I.

C. STRUCTURE FACTOR (F_c) CALCULATION FROM A PROPOSED STRUCTURE

The parameters of only the non-equivalent atoms are required for the calculation of the structure factors in the NRC-10 Structure Factor Least Squares (S.F.L.S.) program.

The remaining atomic positions in the unit cell are generated by the addition of the equivalent positions obtained from the **International Tables for X-ray Crystallography (1962, Vol. I)**

Two simplifications are generally employed in the structure factor calculation. The first of these simplifications is used in the case of a **centrosymmetric space group. When there** is an atom at (X,Y,Z) in a centrosymmetric space group (which has the origin at a centre of symmetry) , another atom occurs at $(\bar{X},\bar{Y},\bar{Z})$. The $A_{hk\ell}$ term for this pair of atoms becomes $f_1 \cos 2\pi(hX + kY + \ell Z) + f_1 \cos 2\pi(h\bar{X} + k\bar{Y} + \ell \bar{Z}) =$ $2f_1 \cos 2\pi(hX + kY + \ell Z)$, since $\cos(-\phi) = \cos\phi$. The $B_{hk\ell}$ term for this pair of atoms becomes $f_1 \sin 2\pi(hX + kY + \ell Z) + f_1 \sin 2\pi(h\bar{X} + k\bar{Y} + \ell \bar{Z}) = 0$, since $\sin(-\phi) = -\sin\phi$. Thus, when two atoms are centrosymmetrically related, their combined effect is to double the cosine term, $A_{hk\ell}$, and to eliminate the sine term , $B_{hk\ell}$, in the structure factor expression. In general, only one half of the atoms need be included in the calculation of the structure factors of such a space group, i.e. those atoms which are not centrosymmetrically related to one another. The $B_{hk\ell}$ term is set equal to zero and the $A_{hk\ell}$ term is doubled to take the other half of the atoms into account.

The second simplification to the structure factor expression occurs with **lattice-centered space groups. The centering** of a lattice systematically reduces the number of reflections and multiplies the remaining reflections by the number of

lattice points per unit cell. Thus, it is only necessary to use the atoms in the primitive unit for the structure factor calculation (or half of these if the space group is centrosymmetric) and multiply this result by the number of lattice points per unit cell.

The NRC-10 Structure Factor Least Squares (S.F.L.S.) program takes both the centrosymmetric and lattice-centered simplifications into account. Therefore, only the equivalent positions not implied by a centre of symmetry or lattice-centering are used in the program.

The necessary equivalent positions, obtained from the **International Tables for X-ray Crystallography (1962, Vol. I)** for the non-centrosymmetric space group P_{2_1} (unique axis b) are (X,Y,Z) and $(\bar{X}, \frac{1}{2} + Y, \bar{Z})$. Similarly, the necessary equivalent positions for the centrosymmetric space group $P_{2_1/m}$ (unique axis b) are also (X,Y,Z) and $(\bar{X}, \frac{1}{2} + Y, \bar{Z})$.

Figs. 14 (a) and (b) show the symmetry elements present in space groups P_{2_1} and $P_{2_1/m}$, respectively (from International Tables for X-ray Crystallography (1962, Vol. I). Atoms may occur at general or special positions in the unit cell. Special positions lie on symmetry elements of the space group whereas general positions do not. The presence of a centre of symmetry in space group $P_{2_1/m}$ generates two additional equivalent positions from the two mentioned above, producing $(\bar{X}, \bar{Y}, \bar{Z})$ and $(X, \frac{1}{2} - Y, Z)$. This results in four general

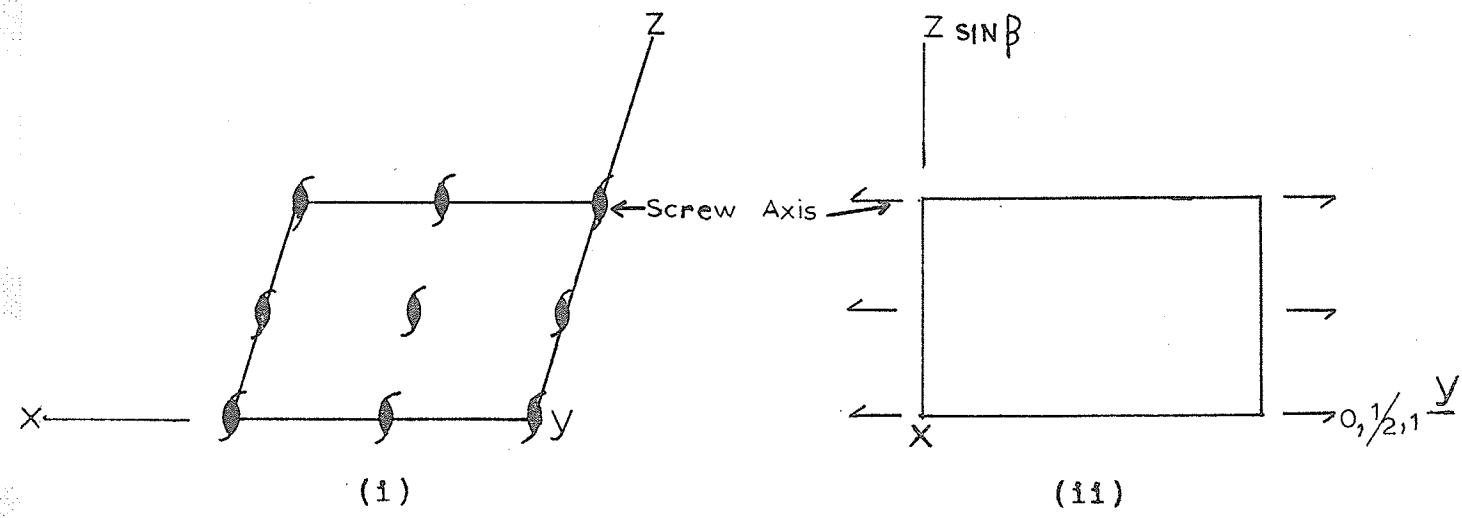

Fig. 14 (a) Space group P_{2_1} (No. 4) with projection of the unit cell (i) along the y axis and (ii) along the x axis.

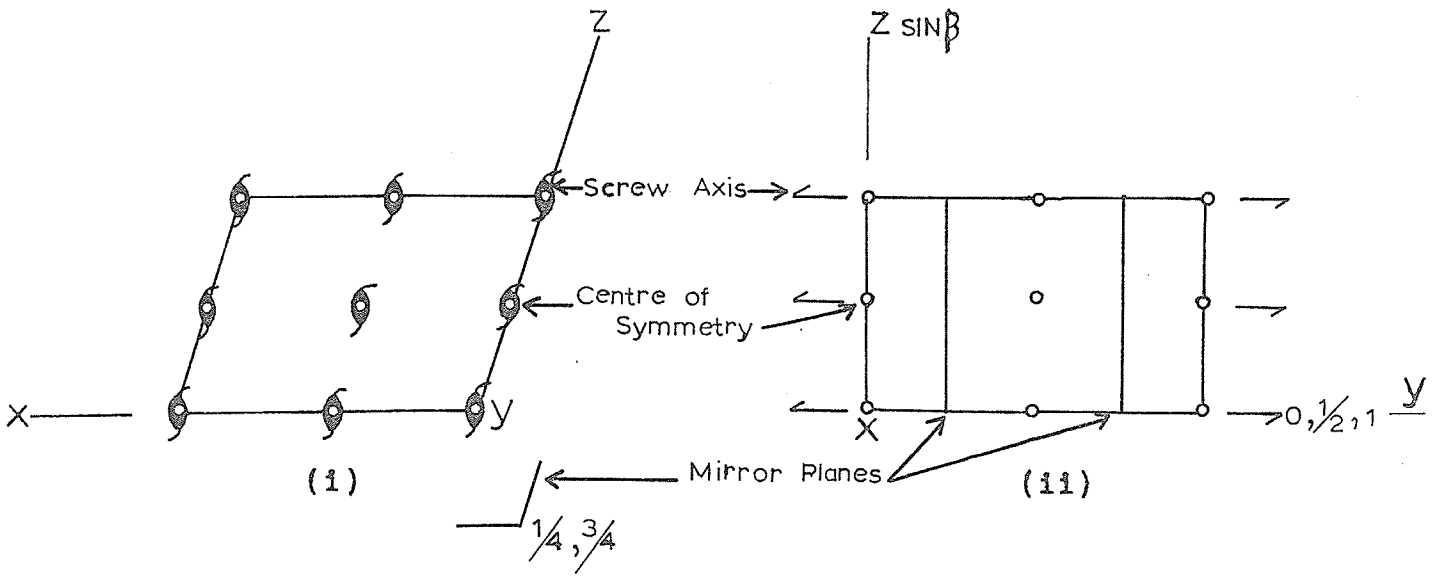

Fig. 14 (b) Space group $P_{2_1/m}$ (No. 11) with projection of the unit cell (i) along the y axis and (ii) along the x axis.

(Redrawn from the International Tables for X-ray Crystallography (1962, Vol. I)).

positions for space group $P_{2_1/m}$. Thus, if an atom lies in a general position in the space group $P_{2_1/m}$, it occurs four times in the unit cell. However, if an atom lies in a special position in the space group $P_{2_1/m}$, such as (X, $\frac{1}{4}$, Z), i.e. on the mirror plane, the centre of symmetry or the 2_1 screw axis generate only one more position from this one, ($\bar{X}$, 3/4, $\bar{Z}$). Thus, this latter atom would only occur in two positions in the unit cell. There are two molecules of $C_5H_5CuP(C_2H_5)_3$ per unit cell (from Table 3). Therefore, for the molecule to conform to space group $P_{2_1/m}$, there must be a mirror plane in the molecule itself.

This is in contrast to the space group P_{2_1} where there are no such requirements placed on the molecule since there is no centre of symmetry in the space group and the equivalent positions are all general and two-fold.

D. MEASUREMENT OF THE INTENSITIES

The Weissenberg photographs of the h0ℓ to h9ℓ levels of a single crystal of $C_5H_5CuP(C_2H_5)_3$ were recorded by the triple film pack technique using zirconium-filtered molybdenum radiation. Levels higher than h9ℓ were not photographed for the intensity collection since very few reflections were recorded for these levels on an oscillation photograph of the crystal. Three sheets of film were placed in the camera. A thin sheet of brass foil (0.001 inches thick) separated the first (A) from the second film sheet (B) and another brass foil sheet separated the second (B)

from the third (C) sheet.

The intensities of the reflections on the bottom half of the Weissenberg photographs were measured by visual comparison with the intensity scale shown in Fig. 15. Six hundred and fifteen structurally different reflections were recorded.

The intensity scale was prepared by using several timed exposures of one reflection. The Weissenberg camera and screen were used to oscillate a single crystal of cyclopentadienyl(triethylphosphine)copper(I) around the b [010] axis through an angle of 2^{o} and to record only the desired reflection. The triple film pack technique and molybdenum radiation with a zirconium filter were also used in producing the intensity scale. Thus each film of the Weissenberg pack had its own intensity scale.

E. CALCULATION OF THE STRUCTURE AMPLITUDE ($|F_o|$) FROM THE INTENSITIES

The structure amplitude is related to the intensity of a reflection by the equation; $|F_{hk\ell}|^2 = \frac{KI}{LP}$, where K is a proportionality constant, $|F_{hk\ell}|$ is the amplitude of the structure factor, L is the Lorentz factor and P is the polarization factor.

The process of diffraction partially polarizes the scattered X-ray beam; the degree of polarization depends on the angle of scattering, the Bragg angle θ. This polarization factor is independent of the method employed in recording the reflections and is given by $P = \frac{1 + \cos^2 2\theta}{2}$.

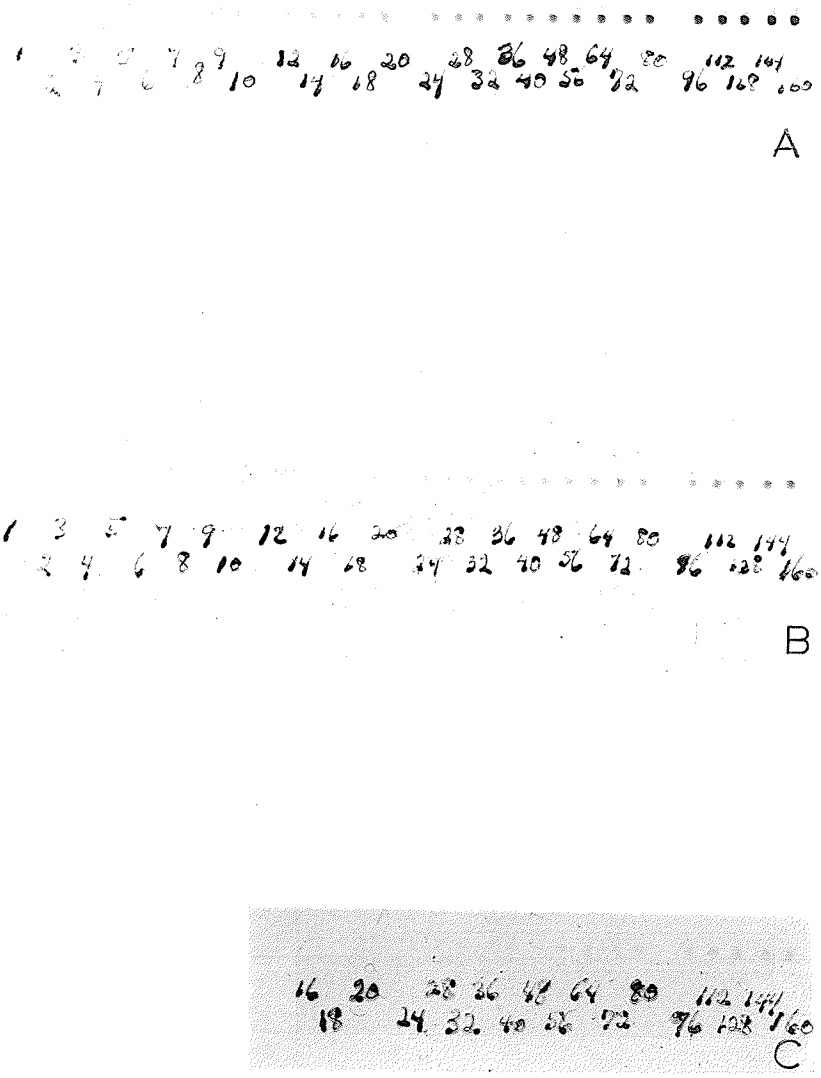

Fig. 15. Intensity scales A, B and C.

The rate at which the (hkℓ) planes of a crystal pass through the reflecting position also varies with the Bragg angle θ. The Lorentz factor corrects each intensity measurement for the time that the corresponding plane spends in passing through the reflecting position. The Lorentz factor varies with the method of recording the reflections. For the equi-inclination Weissenberg method, this factor is given by,

$$L = \frac{\sin \theta}{\sin 2\theta \sqrt{\sin^2\theta - \sin^2 \mu}},$$

where μ is the equi-inclination setting angle.

After having applied both of these corrections to the observed intensities, and having taken the square root of the result, the observed structure amplitude, $|F_o|$, was obtained.

Weissenberg photographs were taken of the 0kℓ and 1kℓ levels with a different crystal of $C_5H_5CuP(C_2H_5)_3$ mounted around the a axis. A correlation of the intensities of the h0ℓ to h9ℓ levels with each of these cross-axis photographs was attempted but proved to be unsatisfactory because of the small number of observed reflections that each level and the cross-axis photographs had in common. Instead, the levels h0ℓ to h9ℓ were placed on the same relative scale by exposure times (about 24 hours for each). For the last cycle of refinement, a rescale factor (which proved to vary slightly from the exposure time factor) was calculated for each level by a least squares method and then applied to each level. The derivation of this least squares method and the statements (added to the NRC-10 Structure Factor Least Squares program) required for these calculations are given in Appendix II.

F. THE R INDEX, THE RESIDUAL OR RELIABILITY FACTOR

X-ray intensities are proportional to $|F_{hk\ell}|^2$. From single crystal methods, the intensities of reflections from the $(hk\ell)$ planes of a crystal are obtained. From these intensities an observed structure amplitude, $|F_o|$, is derived by the methods shown in the previous section. Experimentally, only the modulus of the structure factor, $|F_{hk\ell}|$, may be obtained; the phase angle $\alpha_{hk\ell}$ is not observed.

Structure factors may be calculated for a proposed structure of a crystal (F_c's) by the equations given in sections A and B of this chapter. The $|F_o|$'s are brought on to the same scale as the F_c's by an overall empirical scale factor. The observed and calculated structure amplitudes, the $|F_o|$'s and $|F_c|$'s, respectively are compared in the R index term; $R = \frac{\sum\big||F_o| - |F_c|\big|}{\sum|F_o|}$, where the summations are taken over all the observed reflections. The R index is known as the residual or reliability factor and it serves as a criterion for the correctness of a proposed structure. The smaller the R index, the greater is the probability that the proposed structure is actually the correct structure.

CHAPTER VIII

STRUCTURE DETERMINATION

The following steps have been taken in the determination of the crystal structure of cyclopentadienyl(triethylphosphine)-copper(I): single crystals of the compound were prepared and the possible space groups and cell dimensions were determined; the intensities of the reflections of the h0ℓ to h9ℓ levels were estimated and $|F_o|^2$ and $|F_o|$ for the reflections were calculated from these intensities. The most difficult part of the structure elucidation remains, the establishment of a set of atomic parameters that will give a set of calculated structure amplitudes, $|F_c|$'s, consistent with the observed structure amplitudes.

The difficulty in determining a crystal structure arises from the fact that only the structure amplitudes, but not the phase angles, are observed experimentally. There is no general solution for the phase angle problem. There is no guarantee that a method employed will solve a crystal structure. However, the presence in a structure of a few very heavy atoms usually aids in the structure determination. In this case the positions of the heavy atoms are located by a method in which the phase angles are not required. Then, these heavy atoms are used as a phasing model from which the remaining atomic positions may be developed.

In $C_5H_5CuP(C_2H_5)_3$ the copper and phosphorus atoms are much heavier than the carbon and hydrogen atoms. Thus, a heavy-atom method was employed in the structure determination of this compound. The possible positions of these heavy atoms

were determined from a Patterson synthesis. Most of the carbon atoms were located on an electron density map based on the phases of the heavy atoms. The determination of the remaining carbon atom positions and the refinement of the atomic parameters were carried out by a least squares method. The calculated structure amplitudes of the refined structure were in close agreement with the observed structure amplitudes.

A more detailed account of the latter steps in this structure determination is given in the following sections of this chapter.

A. THE PATTERSON FUNCTION AND ITS APPLICATION

Since a crystal is a periodic arrangement of a group of atoms, the crystal may be represented by periodic functions. Fourier series are used for this purpose. Patterson (1934, 1935) showed that the Fourier summation, $P(X,Y,Z) = \frac{1}{V} \sum_{h=0}^{\infty} \sum_{k=-\infty}^{\infty} \sum_{l=-\infty}^{\infty} |F_{hkl}|^2 \cos 2\pi(hX + kY + lZ)$, gives a vectorial representation of the interatomic distances in the crystal structure, where V is the volume of the unit cell and (X,Y,Z) is any point in the unit cell expressed in fractional coordinates. The phase angle is not required for this summation. If there are two atoms, M and N, in the unit cell, at (X,Y,Z) and at (X+u, Y+v, Z+w), there will be peaks at (u,v,w) and (-u, -v, -w) corresponding to the vectors MN and NM. Subsequently, the peak at the end of a vector in the Patterson function is called a vector peak.

The two vector peaks, from each atom to itself, i.e. MM and NN, occur at the origin. The Patterson function has vector peaks from the origin which are equal to vector distances between pairs of atoms in the unit cell. The height of each peak is proportional to the product of the scattering powers of the two atoms concerned.

For n atoms in the unit cell, there will be n^2 peaks in the Patterson function. The n vectors from each atom to itself occur at the origin. The remaining (n^2-n) vector peaks will be distributed throughout the unit cell. Thus, for a structure with a moderate number of atoms, there are a very large number (n^2-n) of Patterson peaks distributed throughout the unit cell. Because the atoms in a unit cell occupy a finite volume, each Patterson peak will also be distributed over a finite volume.

In practice, only the observed reflections are included in the summation of the Patterson function. The fact that the Fourier summation is not over an infinite number of terms, leads to a series termination error. This series termination error causes the maxima in the function to be surrounded by secondary ripples, called diffraction ripples.

For a structure with a moderate number of atoms, much overlapping of the Patterson peaks and the diffraction ripples occurs. This overlapping is due to the large number (n^2-n) and to the width of the peaks in the unit cell. In general, the Patterson map for such a structure consists mainly of a collection of broad and unresolved peaks.

The height of a vector peak between two atoms is proportional to the product of the atomic scattering powers of the atoms. Therefore, vector peaks between the heavy atoms of a structure are much higher than the remaining vector peaks. If these heavy atom vector peaks can be recognized on the Patterson map, they may be interpreted in terms of possible arrangements of these atoms.

In the Patterson function, a pair of atoms (M and N) in the unit cell gives rise to two centrosymmetric peaks at (u,v,w) and (-u,-v,-w). All Patterson functions are centrosymmetric because of the presence of all vector peaks occurring in centrosymmetric pairs. The space group for a Patterson function is obtained from the space group of the crystal by replacing all translational symmetry elements by their corresponding translation-free symmetry elements and adding a centre of symmetry if it is not already present. Thus the space groups $P2_1$ and $P2_1/m$ in direct space correspond to the space group $P2/m$ (No. 10) in Patterson space. The space group $P2/m$ (unique axis $\underline{b}$) was then used for the calculation of the Patterson function. The Patterson function for this space group, may be expressed in the form, $P(X,Y,Z) =$

$$\frac{4}{V}\sum_{h=0}^{\infty}\sum_{k=0}^{\infty}\sum_{l=0}^{\infty}\left\{\left|F_{hkl}\right|^2 \cos 2\pi(hX+lZ)+\left|F_{\bar{h}kl}\right|^2 \cos 2\pi(-hX+lZ)\right\}\cos 2\pi kY,$$

where only the non-equivalent reflections are included in the calculation (from International Tables For X-Ray Crystallography (1962, Vol. I).

The NRC-2 Data Reduction program was used in Chapter VI to apply the Lorentz and the polarization factors to the observed intensities of reflections from a single crystal of $C_5H_5CuP(C_2H_5)_3$ to produce $|F_o|^2$ and $|F_o|$ for these reflections.

Using the $|F_o|^2$ obtained from the data reduction and using the NRC-8 Fourier program, a series of Patterson sections parallel to (010) were calculated. Three very strong vectors of about the same peak height were observed. One of these vectors corresponded to the expected Cu-P distance of 2.2 Å and was nearly coincident with the a axis. The other two peaks occurred on the $y = \frac{1}{2}$ section. One peak was interpreted as the Cu-Cu vector occurring between the two molecules in the unit cell and the other peak to two superimposed Cu-P vectors also between the two molecules.

The two possible space groups for $C_5H_5CuP(C_2H_5)_3$ have been shown in Chapter III to be $P2_1$ and $P2_1/m$. With only two molecules in the unit cell, the space group $P2_1/m$ would necessitate a mirror plane in the molecule itself; this seemed unlikely. The copper and phosphorus atoms of the molecule were placed at $y = \frac{1}{4}$ (mirror plane of the space group $P2_1/m$, see Fig. 14 (b)) to conform to both space groups.

Two possible orientations of the Cu-P bond were suggested by the Patterson map. These possibilities are shown in Fig. 16 (a) and (b) with the projection along the y axis of

the unit cell. The upper copper and phosphorus atoms in both figures have a y coordinate of $\frac{1}{4}$ whereas the equivalent lower copper and phosphorus atoms have a y coordinate of $3/4$.

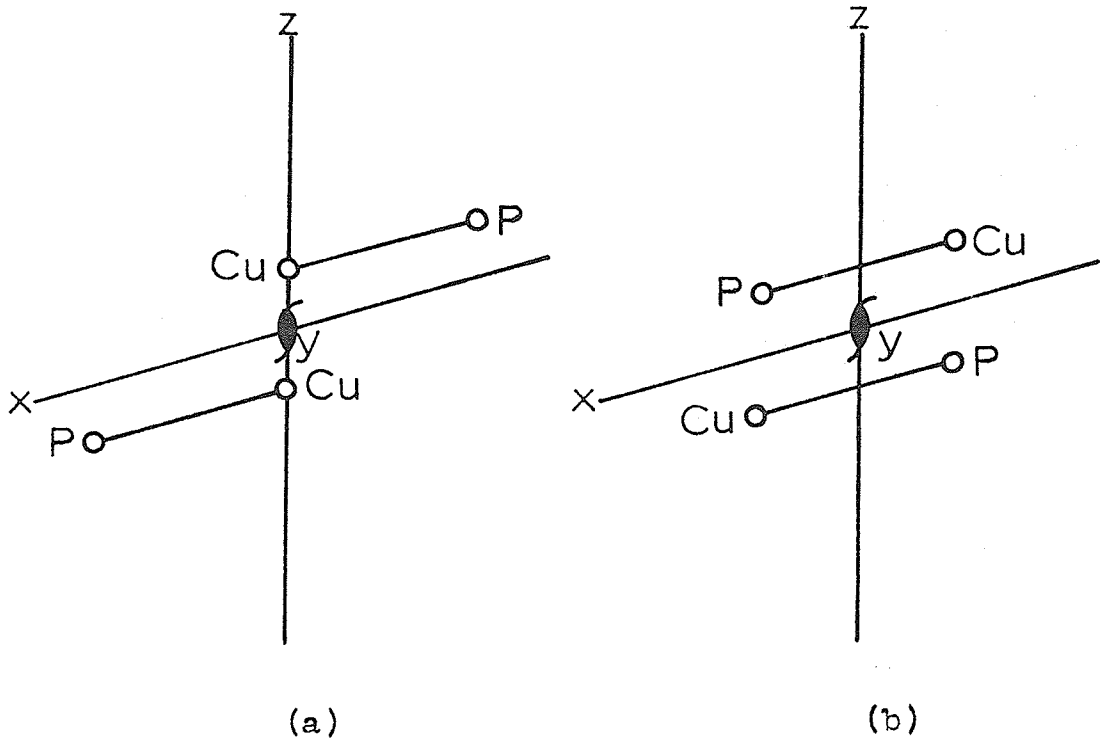

Fig. 16 **Two orientations of the Cu-P bond suggested by the Patterson map.**

B. THE ELECTRON DENSITY FUNCTION AND ITS APPLICATION

The electron density varies periodically throughout a crystal. The electron density at any point (X,Y,Z) in the unit cell may be expressed by the Fourier series,

$$\rho(X,Y,Z) = \frac{1}{V}\left[F_{000} + 2\sum_{h=0}^{\infty}\sum_{k=-\infty}^{\infty}\sum_{\ell=-\infty}^{\infty} A_{hk\ell}\cos 2\pi(hX+kY+\ell Z) + B_{hk\ell}\sin 2\pi(hX+kY+\ell Z)\right],$$

where F_{000} is the total number of electrons in the unit cell, and the conjugate terms $hk\ell$ and $\overline{hk\ell}$ have been combined.

An electron density map is obtained in the following manner. First, an approximate structure is proposed and the structure factors (F_c's) are calculated. Each of the structure factors has both an amplitude and a phase angle. The phase angles obtained for this trial structure are applied to the observed structure amplitudes, $|F_o|$'s, to produce A_o's and B_o's. These A_o's and B_o's are the A_{hkl}'s and B_{hkl}'s used in the electron density expression for the calculation of the electron density map.

If the proposed structure is reasonably correct, the resulting map will be an improved version of the trial structure. If all the atoms of the true structure were not included in the trial structure, the positions of the omitted atoms may be revealed on this map. Improved atomic parameters may be obtained from this map and used to calculate new structure factors with more accurate phase angles. If the set of improved atomic parameters is reasonably close to that of the true structure, these parameters may be refined by successive electron density maps or by a least squares method. Either of these methods should result in a satisfactory agreement of the observed and calculated structure amplitudes. However, if the trial structure is not close enough to the true structure, other models must be proposed.

An electron density map contains the symmetry elements of the proposed structure. As a result, false symmetry elements will be present in the calculated map if the trial

structure has symmetry elements in addition to those present in the true structure.

Because the electron density summation is only over the observed reflections, the electron density map also has a series termination effect similar to that of the Patterson map. Electron density peaks are surrounded by diffraction ripples as a result of this effect.

An approximate electron density map with the phase angles based only on the copper and phosphorus atoms (using $P2_1$) was computed by the NRC-8 Fourier program for the structure of $C_5H_5CuP(C_2H_5)_3$ in Fig. 16 (a) and another similar map for that in Fig. 16 (b). The positions of the copper and phosphorus atoms generate a centre of symmetry and mirror planes (at y = 1/4, 3/4), i.e. the symmetry of space group $P_{2_1/m}$, Fig. 14 (b)) in these electron density calculations.

The centrosymmetric map for the structure shown in Fig. 16 (a) gave peaks which occurred mainly on the mirror plane. These peaks could not be readily interpreted as forming a chemically possible structure. Attempts to refine proposed sets of carbon atoms along with the copper and phosphorous atoms for this structure were unsuccessful. Consequently, this structure was rejected.

The centrosymmetric map based on the phase angles determined from the positions of the copper and phosphorus atoms in Fig. 16 (b) clearly revealed the positions of the five carbon atoms of the ring. One ring carbon was found to lie on the mirror plane and the other four occurred as

two pairs reflected across the mirror plane. The positions of the methyl carbon atoms were also indicated on this map. Thus, the positions of the copper, phosphorus, ring carbon and end carbon atoms of the ethyl groups, conform to the space group $P2_1/m$. There remained two sets of chemically possible positions for the inner carbon atoms of the ethyl groups as shown in Figs. 17 (a) and (c). The electron density peak of each carbon atom in either set of methylene carbon atoms was poorly resolved and was half the height of a methyl or ring carbon atom.

C. THE METHOD OF LEAST SQUARES

(i) Theory

Initial approximate parameters for atoms may be obtained from an electron density map. More accurate parameters for the atoms may be found by refinement of these approximate parameters by the least squares method. The least squares method assumes that the best parameters for the atoms, minimize the sums of the squares of the properly weighted differences between the observed and calculated structure amplitudes. In our least squares method, the quantity minimized is $D = \sum_{hk\ell} W(|F_o| - |F_c|)^2$, where W is the weight given to the reflection considered and $|F_o|$ and $|F_c|$ are its observed and calculated structure amplitudes. $|F_o|$ and $|F_c|$ are on the same scale. The summation is over the structurally different observed reflections.

The calculated structure amplitude, $|F_c|$, is determined by the scale factor and the positional and thermal parameters

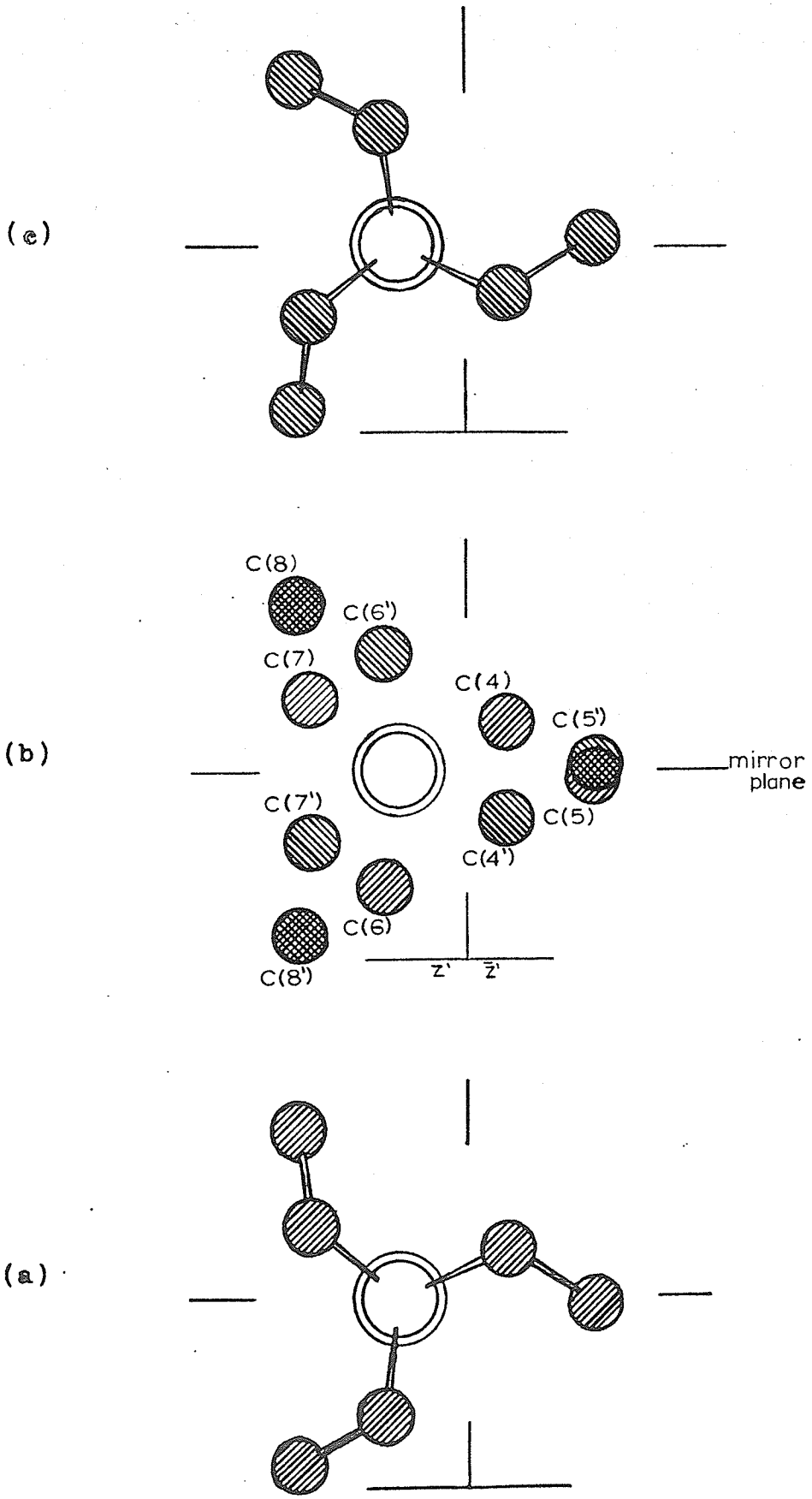

Fig. 17 Projection of the ethyl carbons along the Cu-P bond; (a) and (c) are the two enantiomers and (b) is their superposition.

of each atom. There are N such parameters p_j (j = 1,N). For minimization, the derivative of D with respect to each of these parameters is taken and set equal to zero,

$$\frac{\partial D}{\partial p_j} = \sum_{hk\ell} W(|F_o| - |F_c|) \frac{\partial |F_c|}{\partial p_j} = 0.$$

There are N such equations. These equations may be rewritten as $\sum_{hk\ell} W \Delta F \frac{\partial F_c}{\partial p_j} = 0$, j= 1,2...N The summation is over the observed reflections.

The original parameters, p_j, are assumed to be close to the parameters, $p_j + b_j$, in the refined structure, where the b_j's are the shifts relating the original parameters to the final parameters. A Taylor's expansion of ΔF as a function of $p_j + b_j$ is

$$\Delta F(p_j + b_j) = \Delta F(p_j) - b_j \sum_{i=1}^{N} \frac{\partial |F_c(p_j)|}{\partial p_i}$$ neglecting higher order terms. Substituting this value of ΔF into the previous equation gives

$$\sum_{hk\ell} W \left[\Delta F - b_j \sum_{i=1}^{N} \frac{\partial |F_c|}{\partial p_i} \right] \frac{\partial |F_c|}{\partial p_j} = 0, \quad j = 1, N$$ rearranging gives

$$\left[\sum_{hk\ell} W \sum_{i=1}^{N} \frac{\partial |F_c|}{\partial p_i} \frac{\partial |F_c|}{\partial p_j} \right] b_j = \sum_{hk\ell} W \Delta F \frac{\partial |F_c|}{\partial p_j}, \quad j = 1, N.$$

These N linear equations are called the normal equations. The ΔF and $|F_c|$'s are calculated with the assumed parameters p_j.

These normal equations may also be expressed in matrix form, AB=V , where the elements of the NxN A matrix are

$a_{ij} = \sum_{hk\ell} W \frac{\partial|F_c|}{\partial p_i} \frac{\partial|F_c|}{\partial p_j}$, those in the column matrix B are the parameter shifts b_j and those in the column matrix V are $v_j = \sum_{hk\ell} W\Delta F \frac{\partial|F_c|}{\partial p_j}$. Using matrix algebra, $A^{-1} AB = A^{-1}V$

$$B = A^{-1}V$$

where A^{-1} is the inverse matrix of A. Thus, by obtaining the inverse matrix of A and performing the multiplication on the right hand side of the equation, the matrix B, whose elements are the shifts in the parameters, is obtained. If the original parameters were sufficiently accurate approximations, these parameters plus the shifts should give better values for the parameters. Several iterations are performed, with the starting parameters for each repetition being the final parameters derived in the preceding calculation. This process is repeated until convergence is achieved, i.e. the shifts in the parameters are negligible compared to the parameters themselves.

If the original parameters were not sufficiently close to those of the true structure, the refinement may diverge (producing a very large R index) or converge to an unsatisfactory structure. A structure would be unsatisfactory if the R index were too large and/or if the bond distances and angles differ greatly from chemically similar known bond distances and angles. Some or all of the original parameters would have to be adjusted and the refinement repeated.

The NRC-10 Structure Factor Least Squares program

uses a block diagonal approximation in solving the normal equations. The interaction between the parameters of different atoms is neglected by setting the A matrix elements $a_{ij} = 0$ if i and j are parameters of different atoms. The normal equations may then be expressed in separate blocks, each block containing the parameters of one atom. For anisotropic vibration, there is a 9 x 9 matrix block for the X,Y,Z and B_{ij} parameters of each atom. The scale parameter (which places $|F_c|$ and $|F_o|$ on the same scale) and a single overall isotropic thermal parameter are included in a separate 2 x 2 block. The matrix blocks are inverted separately and the corresponding parameter shifts are obtained.

The NRC-10 S.F.L.S. program was converted into a full matrix least squares program. This rewritten program is given in Appendix III.

The full matrix program uses all the elements in the A matrix, i.e. the interactions between the atoms are considered. The parameter shifts are obtained by the Gaussian elimination method using the GELS subroutine of the Scientific Subroutine Package supplied to the IBM 360/65 computer at the University of Manitoba.

In general, the full matrix program requires a longer computational time and greater storage area than the block diagonal approximation; however, the former usually converges to the best parameters much more rapidly than the latter. Also, the block diagonal method usually has more difficulty than the full matrix method in refining the parameters from

atoms which are close together.

Both the block diagonal and full matrix programs were used in the least squares refinement of the structure of $C_5H_5CuP(C_2H_5)_3$.

(ii) The weighting scheme

A weighting scheme, which considers the probable error of measurement of a reflection, is used in the least squares method. The method used in calculating the weights is essentially that given in Stout and Jensen (1968).

Unit weights were assigned to the reflections in the intitial stages of refinement. Near the end of refinement, mean values of $|\Delta F|$ versus mean $|F_o|$'s were plotted for groups of reflections of similar magnitudes. At least fifty reflections were included in each group. From the resulting graph $|\overline{\Delta F}|$ was approximately given by $|\overline{\Delta F}| = 1.23 + 0.0540\ |\overline{F_o}|$. The weight W is taken as $W = \frac{1}{|\Delta F|^2} = \frac{1}{(1.23 + 0.0540\ |F_o|)^2}$ for a reflection.

The statements, added to the NRC-10 S.F.L.S. program, which are required for the calculation of the weighting scheme and the application of the weights are given in Appendix IV.

(iii) The estimated standard deviations from the least squares method

The estimated standard deviation (e.s.d.) of a parameter p_j from the least squares method is $\sigma_{p_j} = \sqrt{\frac{a_{jj}^{-1} \left(\sum_{hkl} W|\Delta F|^2\right)}{m-n}}$,

where the summation is taken over the observed reflections, $\Delta F = |F_o| - |F_c|$ for a reflection with W being the weight given to the reflection, a^{-1}_{jj} is the diagonal element of the parameter j in A^{-1} (the inverse of matrix A), m is the number of reflections and n is the number of variable parameters in the structure. The block diagonal program was used to calculate the estimated standard deviations (e.s.d.'s) of the parameters since the elements of A^{-1}, the inverse matrix of A, were calculated in the block diagonal program but not in the full matrix version.

D. LEAST SQUARES REFINEMENT OF THE CYCLOPENTADIENYL-(TRIETHYLPHOSPHINE)COPPER(I) STRUCTURE

In section B of this chapter, the approximate electron density map with phase angles based only on the copper and phosphorus atoms clearly revealed the positions of all the cyclopentadienyl ring carbon atoms, the end carbon atoms of the ethyl groups, the copper and the phosphorus atoms. All of these atoms conform to the requirements of space group P_{2_1}/m. However, two sets of chemically possible positions remained for the methylene carbon atoms as shown in Figs. 17 (a) and (c).

Least squares calculations based on P_{2_1} symmetry and including only one of the enantiomers (shown in Figs. 17 (a) and (c) without ring carbon atoms) in the structure led to unsatisfactory results i.e. some bond distances and angles were too far from chemically similar known bond distances (the C-C bond distances in the ring varied from 1.25 Å to 1.46 Å with each value having an e.s.d. of 0.05 Å whereas

the chemically expected value is around 1.40 Å). The R index for this structure was 0.157. Another model, in which each molecule was forced to have a mirror plane by placing C (5) on that plane and relating C (6) to C (7) by reflection, was also unacceptable since some bond distances and angles were too far from their chemically expected values (R=0.158). Thus, a single molecule conforming to either space group P_{2_1} or space group $P_{2_1/m}$ did not completely describe the crystal structure. Only a disordered model containing two enantiomers each with one-half occupancy refined to a structure consisting of chemically reasonable bond distances and angles and R = 0.151. Such a model satisfies the requirements of the space group $P_{2_1/m}$. The two enantiomers are shown without the ring carbon atoms in a projection along the Cu-P bond (almost parallel to the a axis) in Figs. 17 (a) and (c), with their superposition throughout the structure shown in Fig. 17 (b). Fig. 18, is an electron density map through the mean plane of the methylene carbon atoms using the final structure factors. A comparison of this map with Fig. 17 (b) shows the close correlation between the electron distribution and the disordered structure.

Fig. 19 is also a projection of both enantiomers along the Cu-P bond. One enantiomer is shown in closed circles and the non-identical portion of the other is given in dashed circles. Within its estimated standard deviation, C (5) is in a identical position in both enantiomers. However, best refinment was achieved with this atom slightly

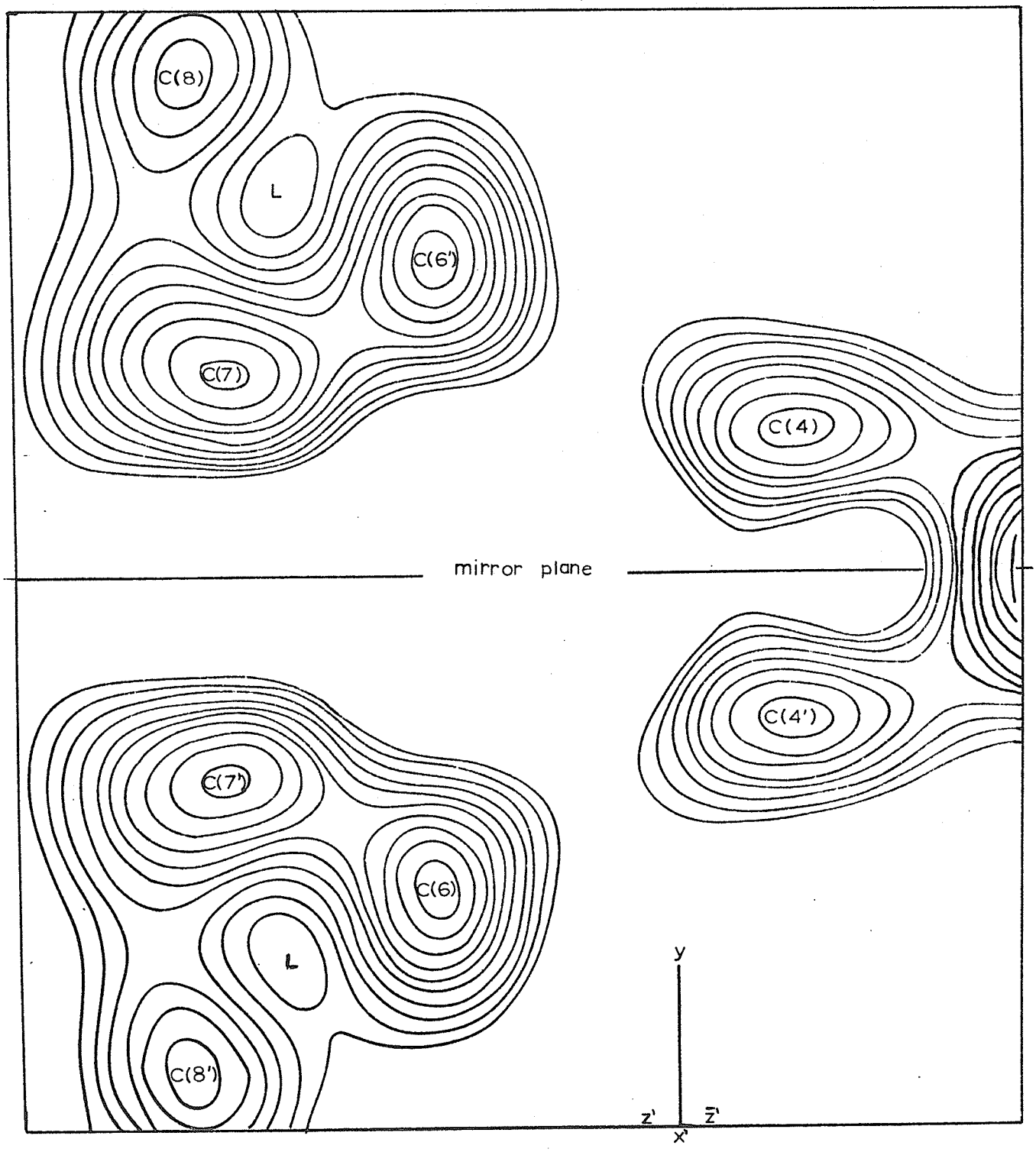

Fig. 18 Electron density map of the mean plane through the methylene carbon atoms; the lowest contour is 1 e/Å^3 with the contour interval 0.2 e/Å^3; L denotes "Low".

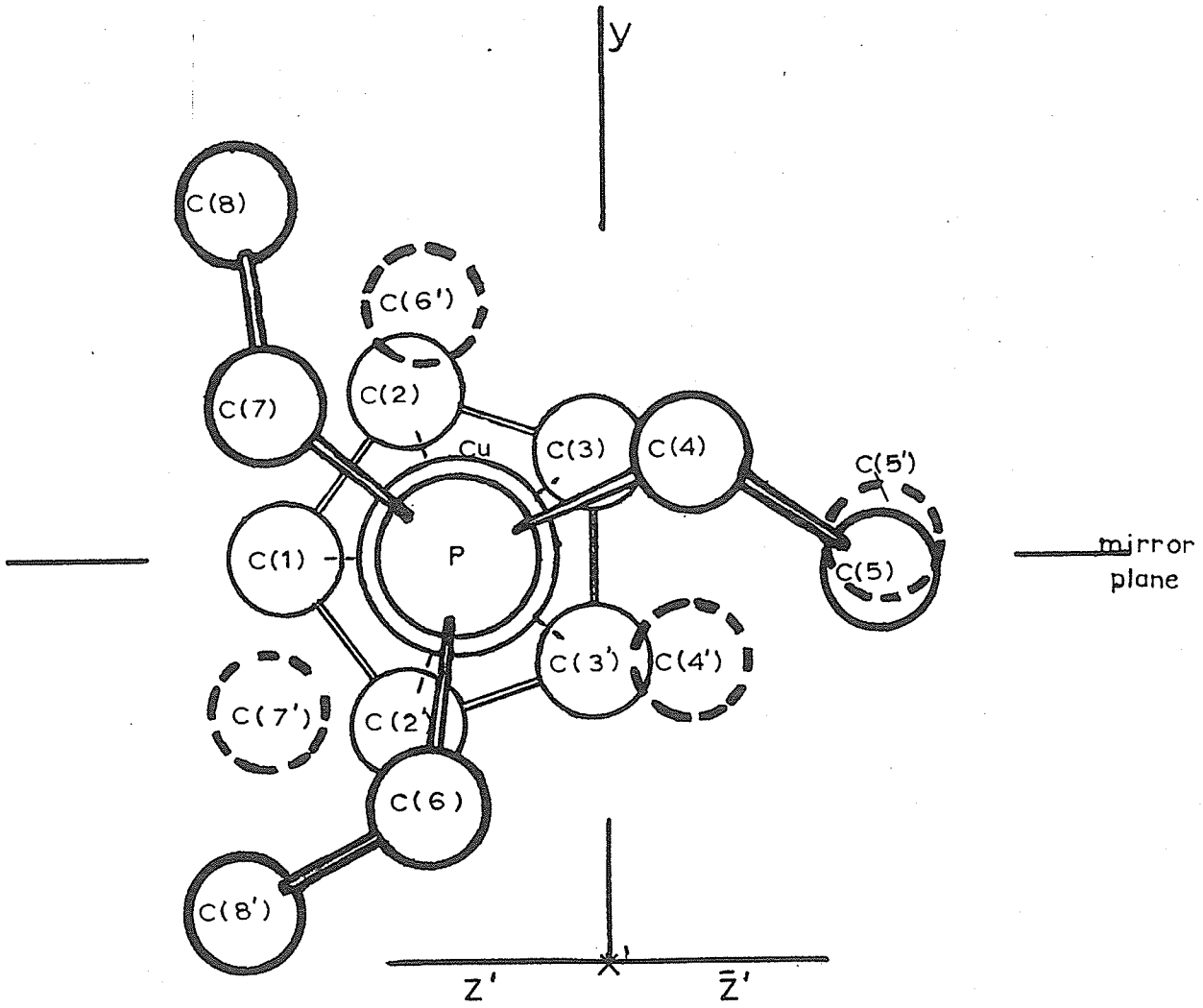

Fig. 19 Projection of the molecule along the Cu-P bond. One enantiomer is shown in closed circles and the non-identical portion of the other is given in dashed circles.

displaced from the mirror plane.

Considering the observed reflections only, refinement of the disordered structure was carried out using several cycles of least squares fitting of the positional parameters of all the non-hydrogen atoms and of the temperature factors, initially isotropic but later anisotropic. Slow convergence led to a final R index of 0.151. The R index was lowered to 0.145 with the inclusion of a set of hydrogen atoms at chemically expected positions and refinement of the parameters of all the atoms except the hydrogens. These refined parameters are within the estimated standard deviations of the refined parameters before the hydrogen atoms were included, the latter being those shown in Table 4 (a), p. 77. The hydrogen atom parameters are given in Table 4 (b).

The following statements show that convergence was achieved in the least squares calculation. In the final least squares cycle, the largest and the average absolute value of the atomic coordinate shifts (expressed in fractional coordinates) were: for the copper atom 6×10^{-5} and 5×10^{-5}, for the phosphorus atom 3×10^{-5} and 2×10^{-5} and for the carbon atoms 81×10^{-5} and 37×10^{-5}. The maximum positional parameter shift was less than one-third of the e.s.d. whereas the average positional parameter shift as a fraction of the e.s.d. was less than one-tenth.

E. THE DIFFERENCE FOURIER SYNTHESIS

A difference Fourier synthesis shows the agreement between the proposed model and the true structure. A

difference synthesis may be expressed by the Fourier series, $\rho_o(X,Y,Z)-\rho_c(X,Y,Z)=\frac{1}{V}\left[\Delta F_{000}+2\sum_{h=0}^{\infty}\sum_{k=-\infty}^{\infty}\sum_{\ell=-\infty}^{\infty}(A_o-A_c)\cos 2\pi(hX+kY+\ell Z)\right.$ $\left.+(B_o-B_c)\sin 2\pi(hX+kY+\ell Z)\right]$, where the difference between the observed (ρ_o) and calculated (ρ_c) electron density functions is taken and ΔF_{000} is the number of residual electrons in the unit cell (i.e. the number of electrons in the true structure not included in the assumed structure). A difference map is virtually free of the series termination effect since the series termination errors in both electron density functions are essentially subtracted out in the difference function.

In the last stage of refinement of the structure of $C_5H_5CuP(C_2H_5)_3$, a difference Fourier synthesis was carried out using the structure factors calculated with the hydrogens included. This difference map revealed a peak of 1.6 $e/\text{Å}^3$ between the copper and phosphorus atoms. This peak is small when compared with the copper and phosphorus peaks of 30 $e/\text{Å}^3$ and 15 $e/\text{Å}^3$ respectively occurring on the electron density map. The remainder of the difference map was between 1.0 and -1.2 $e/\text{Å}^3$ with the maxima and minima occurring on the mirror plane.

CHAPTER IX

RESULTS AND DISCUSSION

A. X-RAY ANALYSIS

The results which were obtained from the X-ray crystallographic structure determination of cyclopentadienyl-(triethylphosphine)copper(I) are tabulated as follows: the final atomic coordinates (Table 4), the observed and calculated structure factors (x10) using the refined parameters before hydrogen atoms were included (Table 5), the bond distances and interbond angles (Table 6), the thermal vibration tensor components (U_{ij}'s) of the atoms (Table 7) and the mean plane between the cyclopentadienyl ring carbon atoms (Table 8).

The X-ray analysis revealed the presence of two enantiomers distributed apparently equally and randomly throughout the crystal. A projection of the unit cell viewed along the c axis is shown in Fig. 20. The atoms of one enantiomer are illustrated in solid circles and the non-identical portion of the other is given in dashed circles. The copper, phosphorus, ring carbon and the methyl carbon atoms off the mirror plane, C (8) and C (8'), have identical positions in both enantiomers. C (5) is on the mirror plane within its estimated standard deviation; however, best refinement was achieved with this atom treated as two half-atoms (mirror images of one another) slightly displaced from this plane. Only the methylene carbon atoms do not conform to $P_{2_1/m}$ symmetry in both enantiomers.

TABLE 4. Atomic coordinates

A. Non-hydrogen atoms and their estimated standard deviations (x 10^4).

	x/a		y/b		z/c	
Cu	-0.1288	(4)	0.2500	(-)	0.1110	(6)
P	0.1348	(8)	0.2500	(-)	0.1589	(11)
C(1)	-0.3237	(31)	0.2500	(-)	0.2347	(48)
C(2)	-0.3501	(24)	0.3528	(24)	0.1159	(36)
C(3)	-0.3979	(28)	0.3151	(28)	-0.0632	(33)
C(4)*	0.1701	(62)	0.3146	(66)	-0.0488	(91)
C(5)*	0.0760	(50)	0.2408	(94)	-0.2436	(72)
C(6)*	0.2367	(46)	0.0945	(41)	0.2053	(52)
C(7)*	0.2809	(40)	0.3451	(42)	0.3632	(70)
C(8)	0.2214	(44)	0.4703	(37)	0.3750	(50)

B. Hydrogen atoms (B_{iso} = 6.0 for each)

H	-0.3308	0.2500	0.3733
H	-0.3401	0.4167	0.2282
H	-0.4128	0.3940	-0.1499
H*	0.3024	0.3060	-0.0260
H*	0.1400	0.4140	-0.0620
H*	0.3588	0.1339	0.3046
H*	0.1980	0.0340	0.0720
H*	0.3430	0.3782	0.2750
H*	0.3140	0.2990	0.5020
H*	-0.0541	0.2360	-0.3000
H*	0.1942	0.1920	-0.2540
H*	0.1017	0.2940	-0.3520
H	0.2267	0.4755	0.5117
H	0.2849	0.5435	0.3259
H	0.0814	0.4870	0.2966

These are the hydrogen atom positions adopted on chemical grounds.

* has an occupation factor of 0.5

The atomic scattering factors for H, C, P and Cu^{+1} and the correction for anomalous dispersion for P and Cu^{+1} were taken from the International Tables for X-Ray Crystallography (1962, Vol. III).

TABLE 5. The observed and calculated structure factors(x10) for $C_5H_5CuP(C_2H_5)_3$.

K= 9

H	L	FOBS	FCAL
2	0	28	26
0	1	-109	-150
2	1	46	53
0	2	-196	-141
0	3	-104	-103
-4	1	67	90
-5	1	44	77
-1	2	-102	-89
-2	2	-93	-48
-4	2	154	148
-5	2	81	80
-4	3	64	81

K= 8

H	L	FOBS	FCAL
2	0	-31	-33
3	0	-143	-122
4	0	-189	-146
5	0	-87	-92
6	0	56	33
7	0	62	62
1	1	105	129
6	1	59	19
0	2	-46	-50
0	3	-91	-118
0	4	-67	-95
-3	1	-140	-117
-4	1	-112	-116
-5	1	-48	-52
-1	2	-31	-49
-6	2	37	17
-1	4	-72	-88
-4	4	122	114
-5	4	51	80

K= 7

H	L	FOBS	FCAL
2	0	-121	-117
3	0	-30	-18
7	0	-48	-6
1	1	105	110
2	1	-138	-129
3	1	-144	-154
4	1	-140	-121
6	1	46	50
0	2	296	300
1	2	108	93
2	2	-125	-139
3	2	-147	-130
4	2	-71	-101
0	3	121	92
1	3	48	43
4	3	-63	-66
-2	1	101	107
-3	1	-72	-76
-4	1	-162	-147
-5	1	-103	-113
-8	1	51	50
-1	2	228	205
-2	2	37	46
-3	2	-175	-174
-4	2	-199	-194
-5	2	-102	-105
-7	2	64	85
-8	2	61	86
-1	3	146	121
-2	3	57	70
-3	3	-143	-139
-4	3	-155	-152
-5	3	-39	-34
-8	3	60	59
-1	4	-97	-67
-2	4	-35	-46
-3	4	-86	-12
-1	5	-122	-102
-2	5	-105	-101
-4	5	41	67
-5	5	90	86
-6	5	55	48
-8	5	-51	-44
-1	6	-64	-74
-2	6	-44	-49
-5	6	65	79
-6	6	47	46
-5	7	49	26

K= 6

H	L	FOBS	FCAL
3	0	239	266
4	0	227	202
5	0	170	124
6	0	-58	-27
7	0	-96	-92
8	0	-70	-74
1	1	-239	-250
3	1	130	127
4	1	56	73
5	1	93	93
6	1	62	23
7	1	-48	-65
0	2	74	85
2	2	-100	-109
3	2	-55	-74
5	2	42	24
0	3	249	227
2	3	-125	-135
3	3	-122	-116
0	4	110	76
2	4	-63	-46
3	4	-86	-96
3	5	-66	-58
-2	1	81	92
-3	1	229	230
-4	1	148	146
-5	1	83	105
-6	1	-40	-60
-7	1	-116	-101
-1	2	-115	-19
-2	2	119	103
-3	2	134	131
-5	2	-35	-25
-7	2	-43	-42
-1	3	260	216
-2	3	103	82
-3	3	-93	-80
-4	3	-206	-170
-5	3	-104	-99
-6	3	-48	-73
-7	3	43	21
-1	4	254	199
-2	4	109	111
-3	4	-109	-115
-4	4	-193	-195
-5	4	-118	-108
-7	4	68	48
-2	5	37	18
-4	5	-38	-44
-5	5	-40	-73
-7	5	45	52

K= 5

H	L	FOBS	FCAL
2	0	215	203
3	0	36	45
5	0	-54	-27
6	0	-110	-114
1	1	-175	-157
2	1	305	245
3	1	247	257
4	1	137	137
6	1	-89	-79
7	1	-62	-85
0	2	-327	-308
1	2	-198	-203
2	2	119	138
3	2	269	245
4	2	132	156
5	2	39	72
6	2	-60	-38
0	3	-180	-181
1	3	-141	-125
2	3	-46	-14
3	3	127	116
4	3	72	89
0	4	32	14
1	4	-34	-28
2	4	-103	-101
3	4	-39	-45
4	4	-99	-9
0	5	57	63
2	5	-57	-74
4	5	-65	-29
0	6	57	38
-2	1	-247	-229
-3	1	252	211
-4	1	245	252
-5	1	134	118
-6	1	36	39
-7	1	-40	-67
-8	1	-44	-68
-1	2	-244	-308
-2	2	-203	-167
-3	2	217	241
-4	2	341	302
-5	2	194	200
-7	2	-164	-157
-8	2	-113	-119
-1	3	-215	-208
-3	3	219	224
-4	3	133	138
-5	3	56	87
-7	3	-110	-114
-8	3	-79	-89
-9	3	-65	-26
-2	4	98	103
-3	4	78	72
-6	4	-37	-61
-7	4	-69	-56
-8	4	43	28
-1	5	189	174
-2	5	186	172
-4	5	-102	-115
-5	5	-110	-103
-6	5	-112	-87
-9	5	69	71
-1	6	114	87
-2	6	108	77
-4	6	-38	-80
-5	6	-139	-136
-6	6	-41	-80
-8	6	45	59
-1	7	43	10

K= 4

H	L	FOBS	FCAL
2	0	33	7
3	0	-409	-408
4	0	-343	-348
5	0	-144	-157
6	0	84	94
7	0	164	139
8	0	113	86
9	0	89	44
1	1	530	348
8	1	107	104
3	1	-202	-184
4	1	-103	-142
5	1	-118	-97
6	1	-36	-31
7	1	74	73
0	2	-51	-56
1	2	76	95
2	2	183	189
3	2	29	44
7	2	-42	-25
0	3	-183	-181
1	3	-104	-99
2	3	156	130
3	3	164	171
4	3	74	90
0	4	-166	-167
1	4	-97	-79
2	4	93	96
3	4	128	178
4	4	54	68
0	5	-61	-66
3	5	68	58
1	6	-54	-10
0	7	41	14
-2	1	-60	-88
-3	1	-316	-299
-4	1	-264	-281
-5	1	-150	-156
-6	1	93	85
-7	1	178	164
-8	1	93	82
-1	2	-152	-126
-2	2	-330	-295
-3	2	-95	-130
-4	2	80	104
-5	2	41	49
-6	2	72	53
-7	2	36	60
-1	3	-240	-225
-2	3	-263	-259
-3	3	70	62
-4	3	236	271
-5	3	205	216
-6	3	97	109
-7	3	-50	-61
-8	3	-141	-122
-9	3	-42	-34
-1	4	-238	-228
-2	4	-102	-101
-3	4	167	162
-4	4	184	200
-5	4	176	170
-6	4	92	98
-7	4	-88	-98
-8	4	-155	-146
-9	4	-72	-67
-1	5	-105	-122
-3	5	66	68
-4	5	75	61
-6	5	81	83
-7	5	-83	-81
-8	5	-40	-50
-9	5	-42	-27
-1	6	35	10
-2	6	49	57
-6	6	-37	-34
-8	6	58	28
-1	7	39	53
-2	7	54	72
-6	7	-49	-62

K= 3

H	L	FOBS	FCAL
2	0	-182	-154
6	0	141	85
7	0	41	56
1	1	149	151
2	1	-153	-138
3	1	-347	-347
4	1	-255	-256
5	1	-50	-67
6	1	132	133
7	1	168	139
0	2	494	471
1	2	303	302
2	2	-132	-174
3	2	-298	-377
4	2	-173	-217
5	2	-66	-77
6	2	59	67
7	2	132	115
0	3	189	203
1	3	208	208
2	3	32	26
3	3	-127	-148
4	3	-107	-98
1	4	85	78
2	4	76	89
3	4	38	53
4	4	98	24
0	5	-144	-113
2	5	56	79
3	5	140	126
0	6	-109	-93
-2	1	190	204
-3	1	-69	-79
-4	1	-313	-351
-5	1	-249	-248
-6	1	-36	-9
-7	1	73	84
-8	1	142	88
-9	1	47	59
-1	2	564	437
-2	2	136	103
-3	2	-208	-229
-4	2	-325	-384
-5	2	-228	-268
-7	2	163	144
-8	2	214	172
-9	2	72	77
-1	3	244	258
-3	3	-228	-232
-4	3	-198	-201
-5	3	-128	-149
-7	3	127	116
-8	3	150	129
-1	4	-52	-60
-2	4	-204	-212
-3	4	-102	-118
-4	4	45	63
-6	4	51	57
-7	4	39	48
-1	5	-216	-167
-2	5	-190	-170
-4	5	152	137
-5	5	170	155
-6	5	181	131
-8	5	-113	-102
-1	6	-158	-141
-2	6	-53	-50
-4	6	110	104
-5	6	142	130
-6	6	75	88
-7	6	-42	-31
-8	6	-117	-81
-6	8	-56	-35

K= 2

H	L	FOBS	FCAL
2	0	-75	-47
3	0	283	291
4	0	718	564
5	0	205	229
6	0	-96	-78
7	0	-178	-176
8	0	-140	-117
1	1	-771	-543
2	1	-98	-43
3	1	216	231
4	1	250	258
5	1	97	107
7	1	-93	-80
8	1	-41	-45
0	2	-51	-10
2	2	-163	-161
3	2	-44	-69
6	2	79	82
7	2	40	24
0	3	297	320
1	3	68	69
2	3	-215	-246
3	3	-175	-201
4	3	-95	-103
6	3	56	76
0	4	210	196
1	4	30	55
2	4	-119	-131
3	4	-147	-156
4	4	-94	-29
0	5	114	124
3	5	-38	-51
4	5	-63	-43
3	6	58	41
0	7	-39	-25
-2	1	307	278
-3	1	315	373
-4	1	442	445
-6	1	-95	-82
-7	1	-144	-128
-8	1	-140	-150
-9	1	-42	-33
-1	2	175	168
-2	2	245	250
-3	2	194	227
-4	2	68	84
-5	2	-192	-230
-6	2	-120	-115
-7	2	-34	-42
-9	2	41	49
-1	3	422	385
-2	3	350	278
-3	3	-152	-154
-4	3	-290	-327
-5	3	-312	-303
-6	3	-85	-92
-7	3	42	52
-8	3	123	119
-9	3	130	122
-1	4	241	247
-2	4	223	230
-3	4	-169	-155
-4	4	-307	-310
-5	4	-228	-263
-6	4	-82	-89
-7	4	120	135
-8	4	183	175
-9	4	124	97
-1	5	66	89
-3	5	-116	-94
-4	5	-99	-90
-5	5	-50	-78
-6	5	-34	-43
-7	5	104	95
-8	5	93	84
-1	6	-34	-32
-2	6	-58	-33
-5	6	34	50
-6	6	44	48
-7	6	37	35
-8	6	-39	-25
-1	7	-93	-95
-2	7	-59	-57
-4	7	37	18
-5	7	102	86
-6	7	66	57
-8	7	-41	-36
-9	7	-68	-53
-2	8	-41	-41

K= 1

H	L	FOBS	FCAL
2	0	-268	-194
3	0	310	328
5	0	-183	-201
6	0	-90	-63
7	0	-42	-40
1	1	117	129
2	1	185	203
3	1	290	366
4	1	253	271
5	1	52	68
6	1	-158	-132
7	1	-148	-151
8	1	-49	-68
0	2	-669	-540
1	2	-291	-242
2	2	151	139
3	2	316	375
4	2	252	275
5	2	129	114
6	2	-92	-85
7	2	-94	-119
8	2	-51	-64
0	3	-273	-263
1	3	-313	-279
3	3	114	137
4	3	46	86
5	3	61	76
6	3	-66	-7
7	3	-71	-44
0	4	98	93
1	4	-122	-100
2	4	-129	-118
3	4	-57	-82
5	4	46	34
0	5	181	168
1	5	-73	-61
2	5	-92	-92
3	5	-98	-99
0	6	117	86
1	6	-61	-30
-2	1	456	365
-3	1	-66	-54
-4	1	230	272
-5	1	387	337
-7	1	-41	-59
-8	1	-152	-114
-9	1	-91	-85
-1	2	-635	-577
-2	2	-104	-75
-3	2	119	140
-4	2	612	527
-5	2	268	275
-6	2	-81	-77
-7	2	-40	-56
-8	2	-255	-202
-9	2	-150	-132
-1	3	-237	-246
-3	3	190	195
-4	3	247	298
-5	3	142	164
-6	3	-52	-48
-7	3	-98	-73
-8	3	-160	-151
-9	3	-66	-54
-1	4	83	59
-2	4	141	148
-3	4	147	155
-5	4	-35	-41
-6	4	-38	-60
-7	4	-41	-44
-9	4	67	31
-1	5	276	246
-2	5	198	154
-4	5	-183	-202
-5	5	-156	-155
-6	5	-88	-109
-8	5	45	100
-9	5	48	60
-1	6	160	144
-2	6	92	78
-4	6	-167	-168
-5	6	-127	-137
-6	6	-42	-62
-8	6	113	95
-1	7	63	23
-3	7	61	20
-5	7	-44	-42
-8	7	48	36
-1	8	-49	-20
-6	8	68	37

K= 0

H	L	FOBS	FCAL
2	0	-676	-422
3	0	-233	-322
4	0	-571	-542
5	0	-184	-189
6	0	55	63
7	0	209	160
8	0	161	139
9	0	71	45
1	1	182	166
2	1	146	111
3	1	41	7
4	1	-277	-294
5	1	-157	-189
7	1	110	100
8	1	69	49
1	2	321	284
2	2	258	253
3	2	32	16
6	2	-67	-74
1	3	-74	-83
2	3	206	228
3	3	177	199
4	3	119	131
6	3	-74	-76
1	4	-35	-37
2	4	204	203
3	4	155	127
4	4	87	99
3	5	62	18
4	5	47	69
0	2	-81	-56
0	3	-243	-265
0	4	-313	-328
0	5	-83	-84
0	7	-46	-2
-2	1	-41	-15
-3	1	-611	-539
-4	1	-804	-726
-5	1	81	81
-6	1	149	133
-7	1	126	90
-8	1	155	173
-9	1	49	40
-1	2	-761	-641
-2	2	-207	-146
-3	2	-81	-85
-4	2	-154	-171
-5	2	243	289
-6	2	134	129
-8	2	44	44
-9	2	-48	-71
-1	3	-255	-326
-2	3	-311	-355
-4	3	271	356
-5	3	314	405
-7	3	-40	-48
-8	3	-119	-114
-9	3	-182	-166
-1	4	-273	-301
-2	4	-103	-138
-3	4	181	209
-4	4	287	324
-5	4	227	256
-6	4	75	79
-7	4	-128	-127
-8	4	-210	-179
-9	4	-179	-118
-1	5	-101	-105
-2	5	-145	-145
-3	5	124	118
-4	5	190	191
-5	5	88	93
-7	5	-126	-112
-8	5	-78	-97
-9	5	-48	-32
-1	6	120	114
-2	6	55	32
-7	6	-62	-54
-1	7	63	36
-2	7	75	74
-5	7	-120	-122
-1	8	49	42
-3	8	67	21

TABLE 6. Interatomic distances and angles and their estimated standard deviations.

		σ
Cu-P	2.136	0.009 Å
P-C(4)	1.885	0.065
P-C(6)	1.891	0.044
P-C(7)	1.858	0.047
Average P-C	1.878	0.053
C(4)-C(5)	1.587	0.095
C(7)-C(8)	1.489	0.062
C(6)-C(8')	1.540	0.052
Average ethyl C-C	1.539	0.072
Cu-C(1)	2.252	0.031
Cu-C(2)	2.229	0.024
Cu-C(3)	2.239	0.026
Average Cu-C	2.238	0.026
C(1)-C(2)	1.412	0.032
C(2)-C(3)	1.321	0.034
C(3)-C(3')	1.438	0.044
Average ring C-C	1.381	0.035
P-Cu-C(1)	148.7	0.7°
P-Cu-C(2)	148.0	0.7
P-Cu-C(3)	148.5	0.7
Average P-Cu-C	148.4	0.7
Cu-P-C(4)	113.4	2.0°
Cu-P-C(6)	113.9	1.3
Cu-P-C(7)	115.5	1.4
Average Cu-P-C	114.3	1.6
P-C(4)-C(5)	113.6	4.5
P-C(7)-C(8)	116.7	3.0
P-C(6)-C(8')	112.4	2.7
Average P-C-C	114.2	3.5
C(4)-P-C(6)	105.8	2.4
C(4)-P-C(7)	101.8	2.5
C(6)-P-C(7)	105.2	1.9
Average C-P-C	104.3	2.3
C(1)-C(2)-C(3)	108.1	2.3
C(2)-C(3)-C(3')	108.3	2.4
C(2)-C(1)-C(2')	107.0	2.2
Average ring C-C-C	107.8	2.3

TABLE 7. Thermal vibrational tensor components U_{ij} ($\AA^2$)

The largest estimated standard deviations are 0.003 for the copper atom, 0.006 for the phosphorous atom while the standard deviations range from 0.011 - 0.103 for the carbon atoms.

	U_{11}	U_{22}	U_{33}	U_{23}	U_{13}	U_{12}
Cu	0.050	0.087	0.094	0.0	0.029	0.0
P	0.043	0.068	0.071	0.0	0.021	0.0
C(1)	0.027	0.169	0.087	0.0	0.028	0.0
C(2)	0.060	0.065	0.132	0.032	0.050	0.013
C(3)	0.073	0.133	0.082	0.014	0.041	0.006
C(4)	0.081	0.183	0.161	-0.005	0.088	-0.012
C(5)	0.094	0.368	0.130	0.236	0.046	0.054
C(6)	0.059	0.060	0.058	-0.028	-0.002	0.027
C(7)	0.033	0.051	0.124	-0.035	0.014	-0.012
C(8)	0.151	0.142	0.108	-0.068	0.046	-0.031

TABLE 8. Cyclopentadienyl ring: mean plane and distances.

1. The equation of the mean plane through the C_5H_5 ring is

$$-0.9877X + 0.0002Y - 0.1564Z - 3.2382 = 0$$

where X,Y,Z refer to the orthogonal set of axes, X along a, Y along b, and Z along c^*.

2. Distances of atoms from plane ($\AA$)

C(1)	0.018
C(2)	-0.014
C(2')	-0.015
C(3)	0.006
C(3')	0.006
Cu	-1.904
P	-4.040

The difference between the copper and phosphorus distances to the mean plane through the C_5H_5 ring is equal to the Cu-P bond length. Therefore the Cu-P bond is normal to this mean plane.

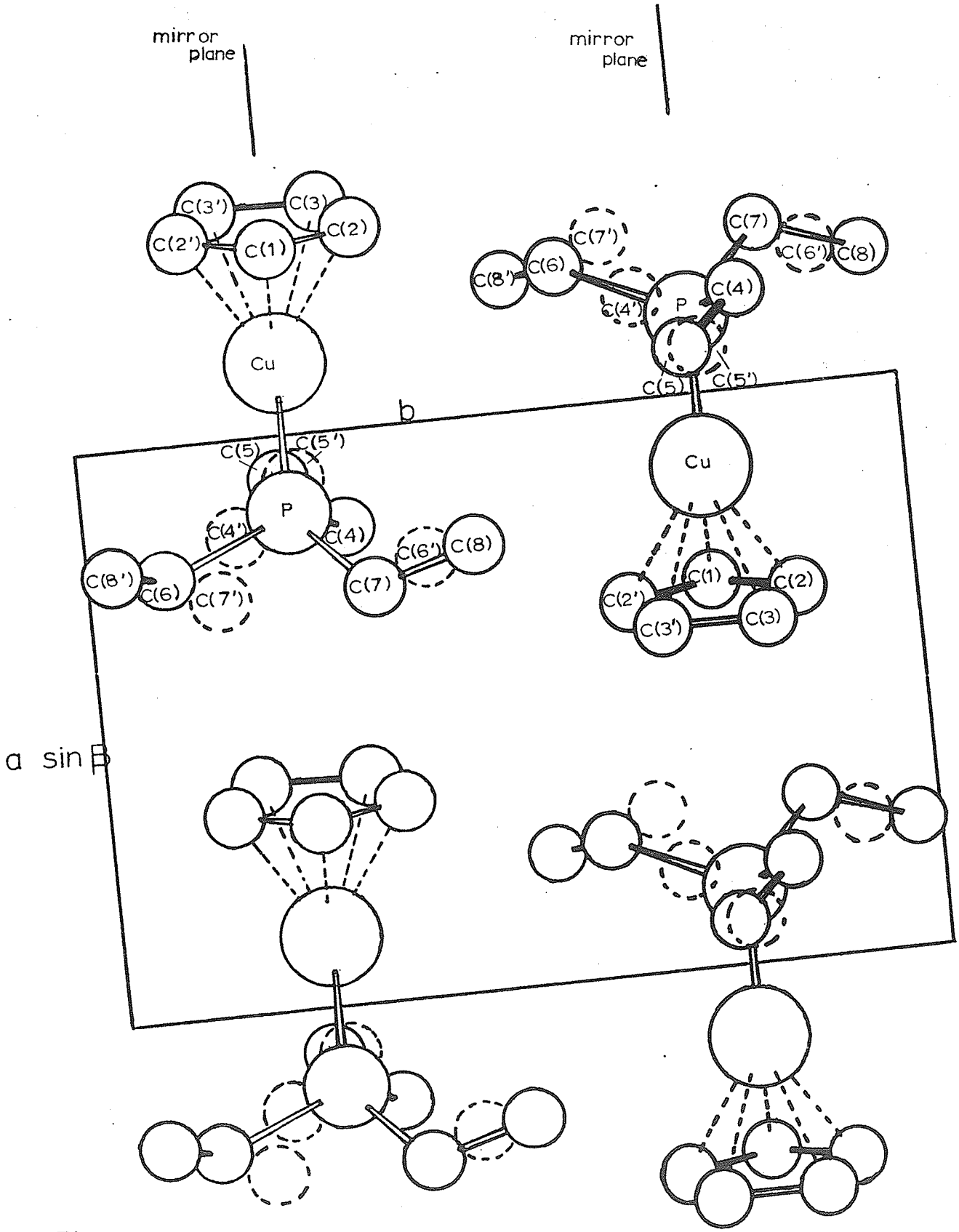

Fig. 20 Projection of the unit cell along the z axis.

The random distribution of the enantiomers can be understood from a consideration of possible intermolecular interactions. The positions of the methyl carbon atoms, which form an almost equilateral triangle as shown in Fig. 17 and in Fig. 19, are those that might be expected from packing considerations. Since C (5) lies on the mirror plane within its e.s.d., all of the atoms except the methylene carbon atoms form a set which conforms to $P_{2_1/m}$ symmetry. Because of this symmetry, this set of atoms can show no preference in its interactions with right-or left-handed molecules. Once the positions of the members of this set are fixed only intermolecular interactions between methylene groups could induce ordering of the enantiomers. However, the shortest intermolecular distance between methylene carbon atoms is 4.43 Å. If hydrogen atoms are considered, the closest intermolecular distance of approach between methylene hydrogen atoms is approximately 2.3 Å. The closest intermolecular distance between any pair of non-hydrogen atoms is 3.76 Å. Hence, any molecular interactions are relatively weak which is in accord with the high volatility of the compound.

An examination of Table 6 shows that each individual bond length (within its e.s.d.) is equal to the average bond length (within its e.s.d.) of all chemically equivalent bond distances.

The Cu-P distance is 2.14 Å. From the sum of the covalent

radii of Pauling (1967) the predicted value for a Cu-P bond length is 2.45 Å. However, this experimental value of the Cu-P distance can be compared with the experimental average value of 2.23 Å obtained by Corfield and Shearer (1966) in the structure of phenylethynyl(trimethylphosphine)-copper(I). The P-C bond distances average 1.88 Å. Summing the covalent radii of Pauling (1967) gives 1.87 Å for a P-C bond length whereas the average experimental value of 1.83 Å was obtained by Corfield and Shearer (1966).

The Cu-C ring distances, presented in Table 6, average 2.24 Å. Table 8 shows that the distance of the copper atom from the mean ring plane is 1.90 Å, and that the Cu-P bond is normal to the mean ring plane. Clearly, the cyclopentadienyl ring in $C_5H_5CuP(C_2H_5)_3$ is π-bonded to the copper atom rather than being σ-bonded as proposed by Wilkinson and Piper (1956) and also by Whitesides and Fleming (1967). Figs. 19 and 20 distinctly illustrate the π-bonding of the cyclopentadienyl ring to the copper atom. The presence of a π-bonded C_5H_5 ring is in accord with the thermal stability of the molecule. In π-$C_5H_5CuP(C_2H_5)_3$, copper achieves an inert gas configuration making the copper atom isoelectronic with the nickel atom in π-cyclopentadienyl-(nitrosyl)nickel, π-C_5H_5NiNO. A Ni-C bond distance of 2.11 Å in π-C_5H_5NiNO was found by Cox, Thomas and Sheridan (1958) using microwave spectroscopy. This distance may be compared with the average Cu-C ring distance of 2.24 Å. The average C-C bond length in the ring is 1.38 Å. This

is similar to the average C-C bond length of 1.40 Å in the π-cyclopentadienyl ring of $(\pi\text{-}C_5H_5)\,Fe(CO)_2(\sigma\text{-}C_5H_5)$ whose crystal structure was determined by Bennett et al. (1966)

B. ATTEMPTED DIELS ALDER REACTION

Wilkinson and Piper (1956) reacted the dienophile maleic anhydride with cyclopentadienyl(triethylphosphine)-copper(I). Red precipitates which could not be characterized were formed. However, triethylphosphine also reacts with maleic anhydride.

More recently, in the author's attempted reaction of the dienophile hexafluoro-2-butyne ($CF_3C{\equiv}CCF_3$) with π-cyclopentadienyl(triethylphosphine)copper(I) in petroleum ether solution, only starting material could be identified. The structure of a possible Diels-Alder adduct of $CF_3C{\equiv}CCF_3$ with $C_5H_5CuP(C_2H_5)_3$ is given in Fig. 21.

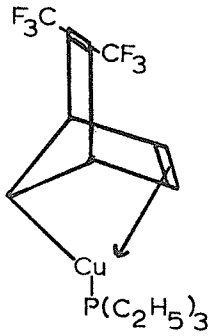

Fig. 21. A possible Diels-Alder adduct.

Hexafluoro-2-butyne is such a strong dienophile that it even forms a Diels-Alder adduct with the benzene derivative, durene (Krespan, McKusick and Cairns (1960)). At room temperature, $CF_3C{\equiv}CCF_3$ also reacts with nickelocene $Ni(\pi\text{-}C_5H_5)_2$ to form a Diels-Alder adduct (McBride, Dudek and Stone (1964)). However, with the formation of the adduct, the nickel atom achieves an inert gas configuration. If the cyclopentadienyl ring in $C_5H_5CuP(C_2H_5)_3$ were π-bonded (Fig. 1 (a)), the copper atom would already have the inert gas configuration; the subsequent formation of a Diels-Alder adduct would destroy this stable electron configuration. In this case the Diels-Alder reaction would be less likely to occur for cyclopentadienyl-(triethylphosphine)copper(I) than for nickelocene.

If the C_5H_5 ring in $C_5H_5CuP(C_2H_5)_3$ were σ-bonded (Fig. 1 (b)) to the copper atom, the compound would be expected to readily form a Diels-Alder adduct with $CF_3C{\equiv}CCF_3$; if the ring were π-bonded, the formation of the adduct would still be possible but not as probable. The fact that the author was not able to isolate a Diels-Alder adduct of hexafluoro-2-butyne with cyclopentadienyl-(triethylphosphine)copper(I), strongly suggests that the C_5H_5 ring is π-bonded to the copper atom when the compound is in petroleum ether solution.

C. LOW TEMPERATURE NUCLEAR MAGNETIC RESONANCE (NMR) STUDIES

A low temperature nuclear magnetic resonance study was performed by Bennett et al. (1966) on the compound

(π-C_5H_5)$Fe(CO)_2$(σ-C_5H_5) from 30°C to -100°C in carbon disulfide solution. At 30°C, two resonance peaks are seen in the proton magnetic resonance spectrum, one at τ 5.6 which is assigned to the π-C_5H_5 ring protons and the other at τ 4.3 which is assigned to the σ-C_5H_5 ring protons. Upon cooling to -100°C, the peak at τ 5.6 remains a single peak. The peak at τ 4.3 collapses with cooling and three new resonance peaks appear from -60°C to -100°C. Two of these peaks occur at around τ 4 and the third at τ 6.5. The three new peaks have the approximate intensity ratio of 2:2:1 respectively.

The room temperature nuclear magnetic resonance (NMR) spectrum of $C_5H_5CuP(C_2H_5)_3$, obtained by Piper and Wilkinson (1956) in toluene solution, showed a single sharp peak for the protons of the C_5H_5 ring. More recently, Whitesides and Fleming (1967) performed a low temperature study (between 0° and -70°C) of the NMR spectrum of this compound in various solvents. In sulfur dioxide solution at 0°C, these latter authors observed a single sharp peak at τ 3.7 for the protons of the C_5H_5 ring. Upon cooling to -70°C, this peak broadens and splits to form three peaks at τ values of 3.05, 3.43 and 5.54. These three peaks had relative areas of approximately 2:2:1. The same authors reported that qualitatively similar spectra were obtained for the ring protons in proprionitrile and petroleum ether solutions. However, in triethylamine and triethylphosphine solutions of the organometallic compound, only

a single peak for the cyclopentadienyl ring protons was observed upon cooling to -70°C. From these observations, Whitesides and Fleming (1967) assigned a σ-bonded C_5H_5 ring to the structure of cyclopentadienyl(triethylphosphine)-copper(I) (Fig 1 (b)). They also excluded the possibility that the compound whose spectrum was observed in sulfur dioxide solution was actually an adduct of the organometallic compound with sulfur dioxide.

The fact that the single peak for the cyclopentadienyl ring protons in $C_5H_5CuP(C_2H_5)_3$ split with cooling to -70°C, in some, but not all solvents, is evidence that there is a solvent effect involved in the splitting.

Low temperature NMR spectra of the compound $C_5H_5CuP(C_2H_5)_3$ conducted by the author are given in Fig. 22, 23 and 24. Fig. 22 shows that similar results were obtained in sulfur dioxide solution as those reported by Whitesides and Fleming (1967). The peak at τ 3.4 in the 0°C spectrum is due to a decomposition product. The solution was allowed to stand at -5°C for three days. The subsequent NMR spectrum at 0°C showed that the peak at τ 3.7 was absent and that the peak due to the decomposition product at τ 3.4 was increased in height. This decomposition peak did not split when the sample was cooled to -70°C.

Contrary to the results of Whitesides and Fleming (1967), no splitting of the single peak due to the protons in the C_5H_5 ring of cyclopentadienyl(triethylphosphine)copper(I) was observed in petroleum ether solution

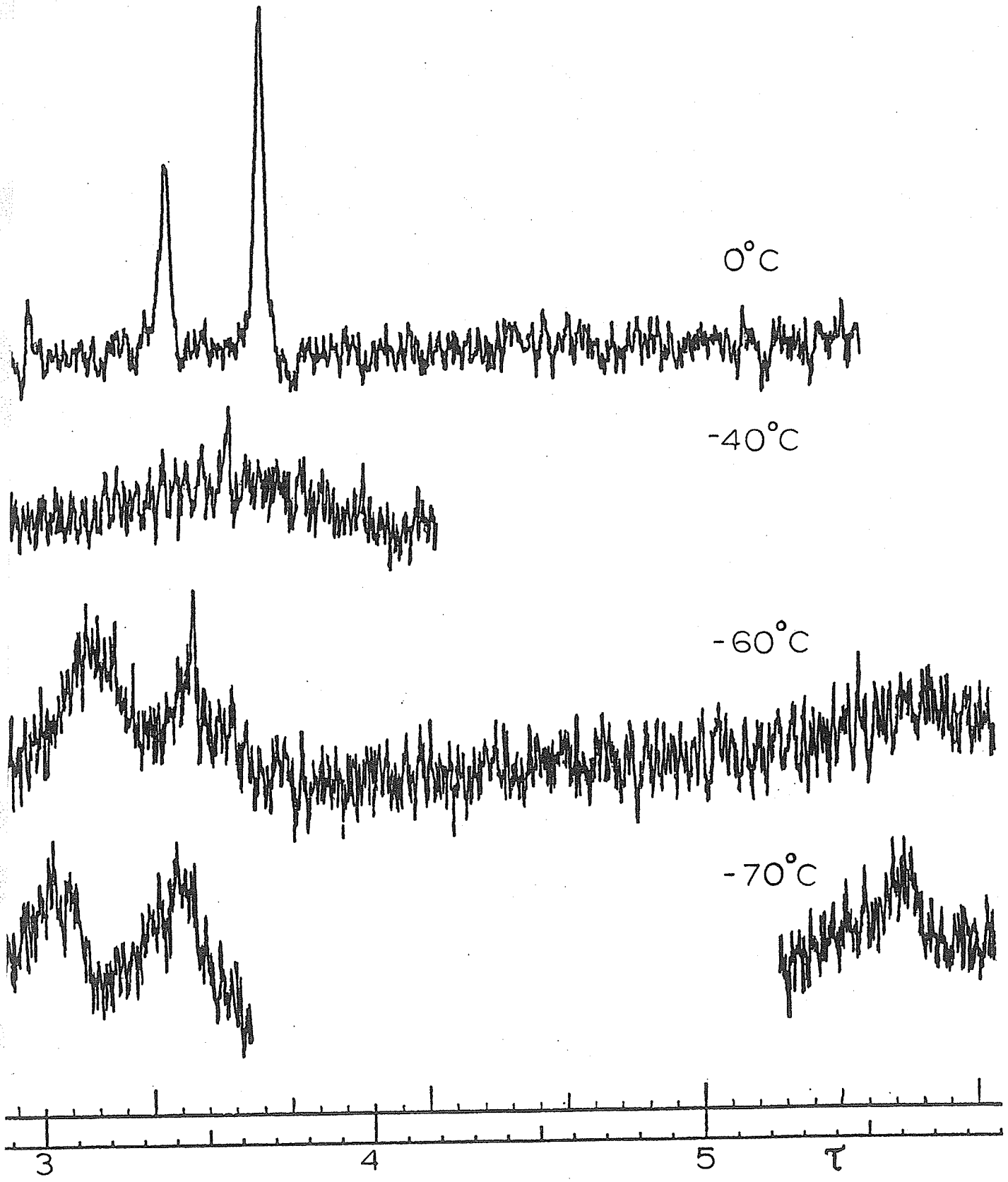

Fig. 22 Low temperature nuclear magnetic resonance spectra of $C_5H_5CuP(C_2H_5)_3$ in sulfur dioxide solution.

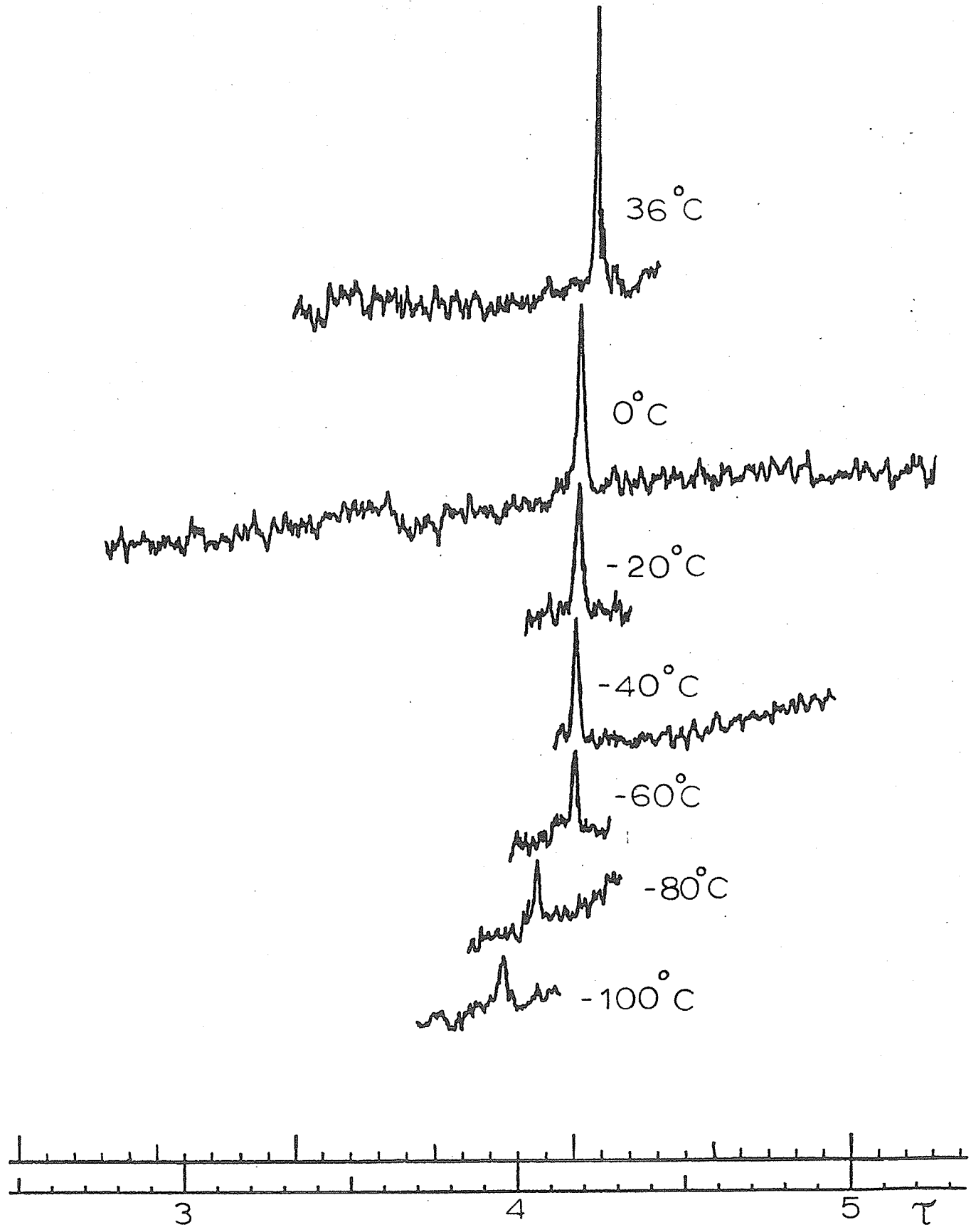

Fig. 2[3] Low temperature nuclear magnetic resonance spectra of $C_5H_5CuP(C_2H_5)_3$ in petroleum ether solution.

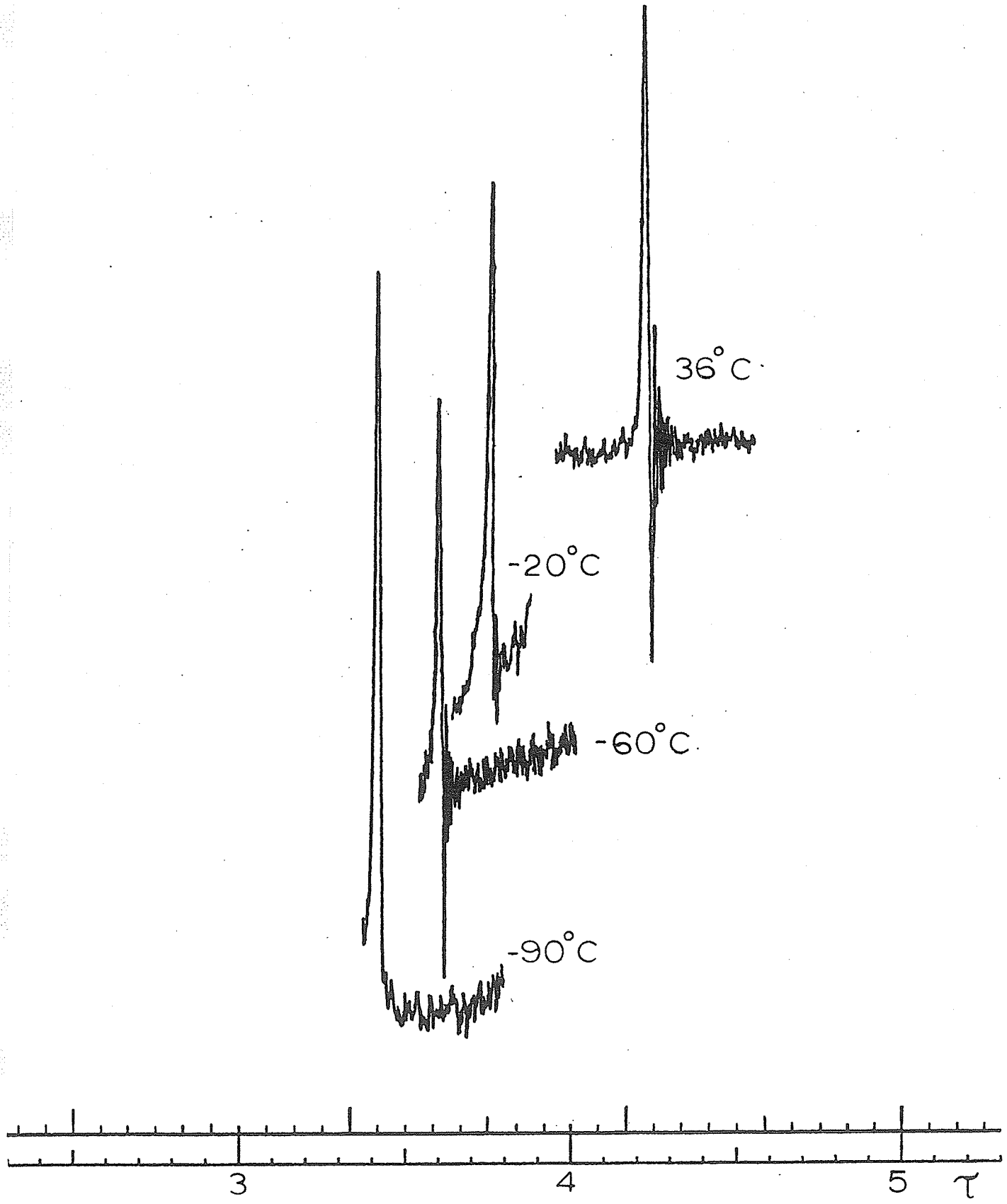

Fig. 24 Low temperature nuclear magnetic resonance spectra of $C_5H_5CuP(C_2H_5)_3$ in toluene solution.

upon cooling to -100°C (Fig. 23). In toluene solution (Fig. 24), the single peak due to the ring protons of the compound was still sharp at -90°C. These latter results in hydrocarbon solvents are consistent with that expected for the protons of a π-bonded cyclopentadienyl ring. In sulfur dioxide solution, some solvent effect occurs. The observed spectrum may be that of a σ-bonded C_5H_5 ring; however, the organometallic compound may not exist as such in sulfur dioxide solution. In any case, these NMR studies refer to the compound in solution, whereas in an X-ray structure determination one is dealing with the molecule in the solid state.

D. MASS SPECTRUM

The mass spectrum of π-$C_5H_5CuP(C_2H_5)_3$ obtained by the author is given in Fig. 25. Whitesides and Fleming (1967) reported a clearly defined parent ion in the mass spectrum of the compound at m/e 247 and 249. The parent ion actually occurs at m/e 246 and 248. These two peak heights are in the isotope ratio of Cu^{63} to Cu^{65}. The absence of peaks corresponding to a dimeric or other polymeric species indicates that the compound is probably monomeric in the gaseous state. The peaks corresponding to the ion $CuP(C_2H_5)_3^+$, m/e 181 and 183 are in the same ratio as the parent peaks. Whitesides and Fleming (1967) state that the absence of a strong peak corresponding to the ion $(C_5H_5)Cu^+$, m/e 128 and 130, strengthens the postulation of a σ-bonded C_5H_5 ring. Mass spectra have been obtained for

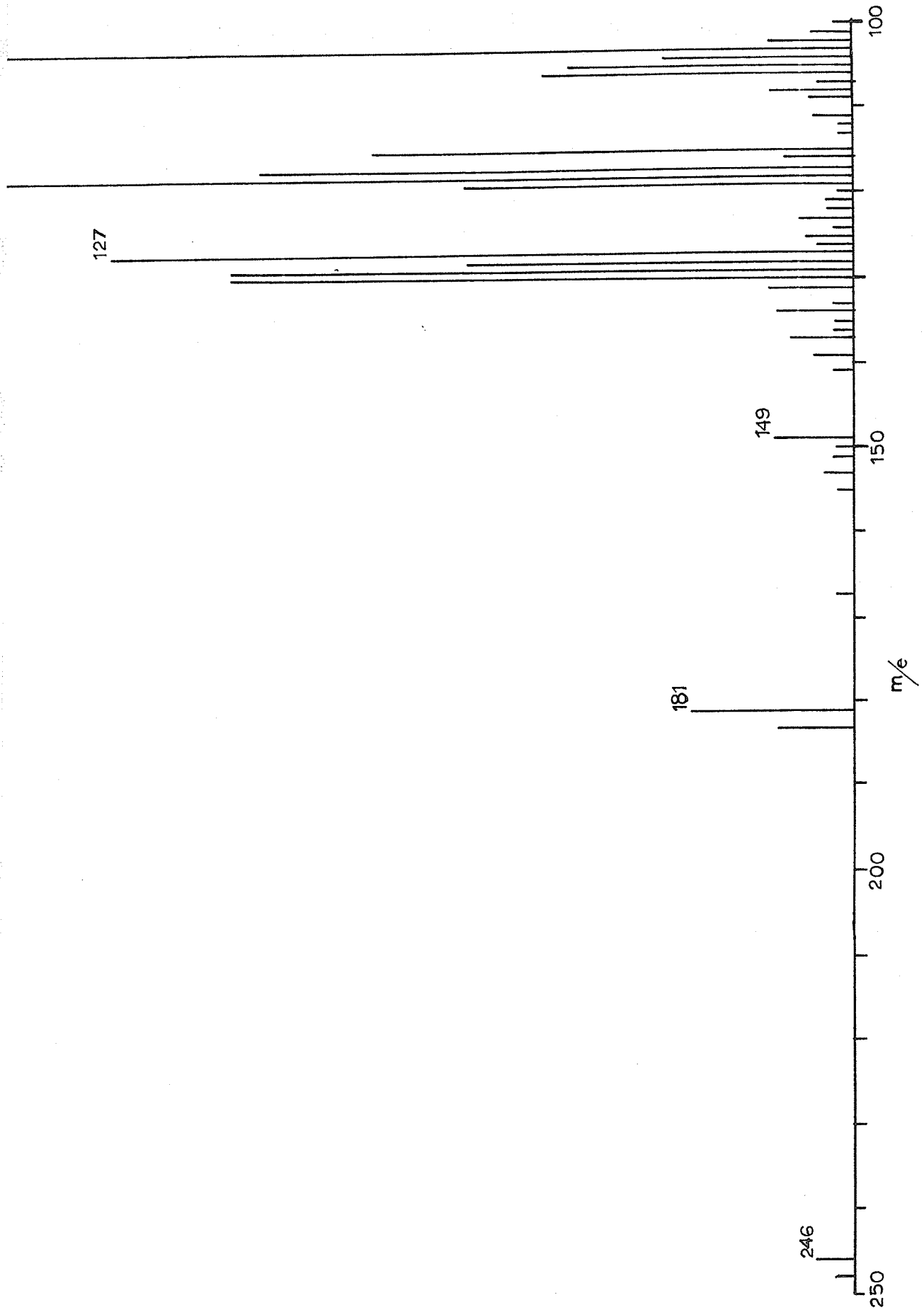

Fig. 25 Mass spectrum of $C_5H_5CuP(C_2H_5)_3$

cyclopentadienyl - containing compounds of elements of the first transition series (Friedman, Irsa and Wilkinson (1955)). Very significantly higher yields of the ion $C_5H_5M^+$ were obtained from the ionic cyclopentadienides in comparison to those obtained from the π-cyclopentadienyl compounds. The presence of a strong $C_5H_5M^+$ peak in the mass spectrum is an indication of an ionically-bonded rather than a π-bonded C_5H_5 ring. Thus, the absence of a strong peak corresponding to the $C_5H_5Cu^+$ ion suggests that the C_5H_5 ring is not ionically bonded. However, the peaks due to this ion may still contribute to the peak heights at m/e 128 and 130.

E. SUMMARY

Various methods were employed to determine the nature of the bonding of the cyclopentadienyl ring to the copper atom in cyclopentadienyl(triethylphosphine)copper(I). The infrared and chemical evidence of Wilkinson and Piper (1956) was inconclusive, nevertheless, these authors postulated a σ-bonded C_5H_5 ring for the compound (Fig. 1 (b)). The X-ray structure analysis of the compound by the author clearly shows that in the solid state the cyclopentadienyl ring is π-bonded to the copper atom as postulated in Fig. 1 (a) (see Figs. 19 and 20 and also Table 8). The presence of the parent peak at m/e 246 and 248 in the mass spectrum of the compound and the absence of a dimeric or other polymeric species, indicates that the compound is monomeric in the gaseous state. This is an indication of the weak

intermolecular forces found in the X-ray analysis. Thus, the molecule in the vapour phase is likely to be similar to that in the solid state.

The author's attempted Diels-Alder reaction of hexafluoro-2-butyne with the organometallic compound in petroleum ether solution strongly suggests the presence of a π-bonded C_5H_5 ring. The low temperature nuclear magnetic resonance studies by the author of the compound in petroleum ether and toluene solutions also suggest a π-bonded C_5H_5 ring for solutions of the compound in hydrocarbon solvents. Low temperature NMR spectra of solutions of the compound in sulfur dioxide obtained by both Whitesides and Fleming (1967) and the author indicate that a σ-bonded C_5H_5 ring may be present. However, a solvent effect occurs in the sulfur dioxide solution. Thus, the compound may not exist as such in this solvent.

PART II

THE CRYSTAL STRUCTURE OF $Fe_3As_2(CO)_9$

CHAPTER X

INTRODUCTION

Mond, Langer and Quincke (1890) discovered the first metal carbonyl compound, nickel carbonyl ($Ni(CO)_4$). Since this discovery, many more carbonyl and substituted carbonyl compounds have been prepared. The preparations, the reactions and the structures of many metal carbonyl compounds are compiled in Organic Syntheses Via Metal Carbonyls (1968). Foust, Foster and Dahl (1969) have recently published the preparation and structure determination of some new arsenic-cobalt carbonyl compounds as part of their comprehensive investigation in the field of arsenic-metal carbonyl compounds.

A new compound in the arsenic-metal carbonyl series, $Fe_3As_2(CO)_9$, was isolated as one of the products in the reaction of arsenic trifluoride with iron pentacarbonyl by L. Kruczynski (private communication). The composition of the compound was determined by mass spectrometry and by chemical analysis. The compound formed red crystals with well-developed faces upon re-crystallization from petroleum ether solution. From an analysis of the infrared spectrum of $Fe_3As_2(CO)_9$ (bands at 2035.2 s , 2005.1 m, 1994.3 mw (cm^{-1}), nujol mull), L. Kruczynski (private communication) proposed the following structure for the compound in Fig. 26.

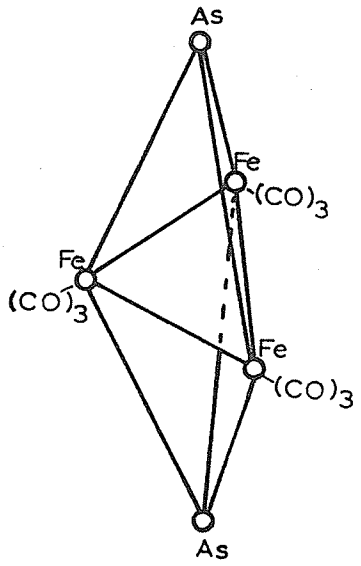

Fig. 26 Proposed structure for $Fe_3As_2(CO)_9$ by L. Kruczynski (private communication).

He also supplied crystals of the compound to the author. An X-ray analysis was then undertaken by the author to determine the actual structure of the compound.

CHAPTER XI

CRYSTAL DATA

A. DESCRIPTION OF THE CRYSTAL

The red crystals of $Fe_3As_2(CO)_9$ resembled tetragonal dipyramids (distorted octahedra). A single crystal of $Fe_3As_2(CO)_9$ was mounted about the elongated axis on the reflecting goniometer. The angle between this axis and the normal to each crystal face was approximately $60^\circ \pm 1^\circ$. Thus, this crystal did not belong to the cubic system (for octahedral crystals this angle would be $109^\circ 28'/2$). Assuming the crystal system is tetragonal or at least orthorhombic, the other two axes of the crystal are normal to this elongated axis, called the c axis. Fig. 27 (a) and (b) show the two possible sets of axes in a projection along the c axis of the crystal.

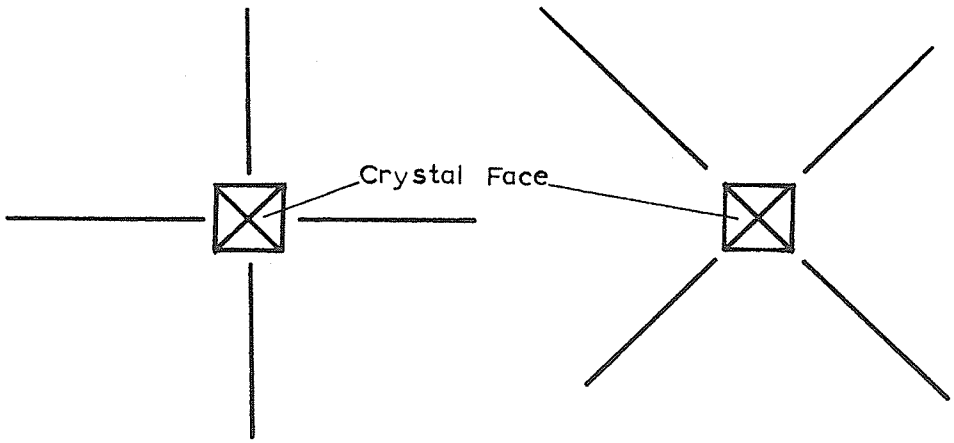

(a) (b)

Fig. 27. Possible sets of axes of a crystal of $Fe_3As_2(CO)_9$.

For either orientation, these two axes of the crystal appeared to be equal in length. Single crystal X-ray photographs were used to determine the axes, the crystal

system, the possible space groups and the unit cell dimensions of the crystal.

B. PRECESSION PHOTOGRAPHS

The form of the single crystals of $Fe_3As_2(CO)_9$ indicated that the crystal system was likely tetragonal or orthorhombic. In both of these crystal systems, the direct axes of the crystal coincide with the reciprocal axes. The crystal was mounted for rotation around the $\underline{c}$ axis by the use of a reflecting goniometer. An orientation photograph taken on the precession instrument confirmed that the $\underline{c}$ and $\underline{c}^*$ axes coincide in the crystal. The crystal was then mounted for rotation about this axis for all subsequent precession photographs.

A zero level precession photograph was taken; the precession axis was one of the two possible axes of the set in Fig. 27 (a). Another zero level photograph was recorded with the precession axis being the other axis of Fig. 27 (a). Similarly, two more zero level precession photographs were taken with the precession axes being the two possible axes in Fig. 27 (b).

One set of possible axes, either the set in Fig. 27 (a) or that in Fig. 27 (b), corresponds to the actual crystal axes and the other set corresponds to the diagonals between these axes. For the crystal to belong to the tetragonal system, the zero level photographs corresponding to the true axes must be identical to each other; similiarly, the zero level photographs corresponding

to the diagonals must also be identical to each other. However, for the crystal to belong to the orthorhombic system, only the zero level photographs corresponding to the diagonals must be identical to each other. For the single crystal of $Fe_3As_2(CO)_9$, the two zero level precession photographs corresponding to the axes in Fig. 27 (a) were identical to one another whereas the two corresponding to the axes in Fig. 27 (b) were different from each other. Therefore, the crystal belongs to the orthorhombic system and is only pseudo-tetragonal and the crystal axes correspond to those in Fig. 27 (b).

The zero level precession photographs corresponding to the axes of the crystal are given in Figs. 28 (a) and (b). A cone axis photograph of the single crystal of $Fe_3As_2(CO)_9$ was taken; the rotation axis was $\underline{c}^*$ (also $\underline{c}$ [001]) and the precession axis was $\underline{b}$ [010]. The measurement of this cone axis photograph and the subsequent calculation of the reciprocal lattice spacing d^*_{010}, established that the spacing measured along the $\underline{b}^*$ direction in Fig. 28 (b) corresponded to d^*_{010} and not some multiple of d^*_{010}. The true spacing might have been a multiple of d^*_{010} because of some systematic absences. A precession photograph of the $(h1\ell)^*$ reciprocal lattice plane was then taken. This first level photograph confirmed that the spacing along the $\underline{a}^*$ and $\underline{c}^*$ directions in Fig. 28 (a) corresponded to d^*_{100} and d^*_{001} respectively and not

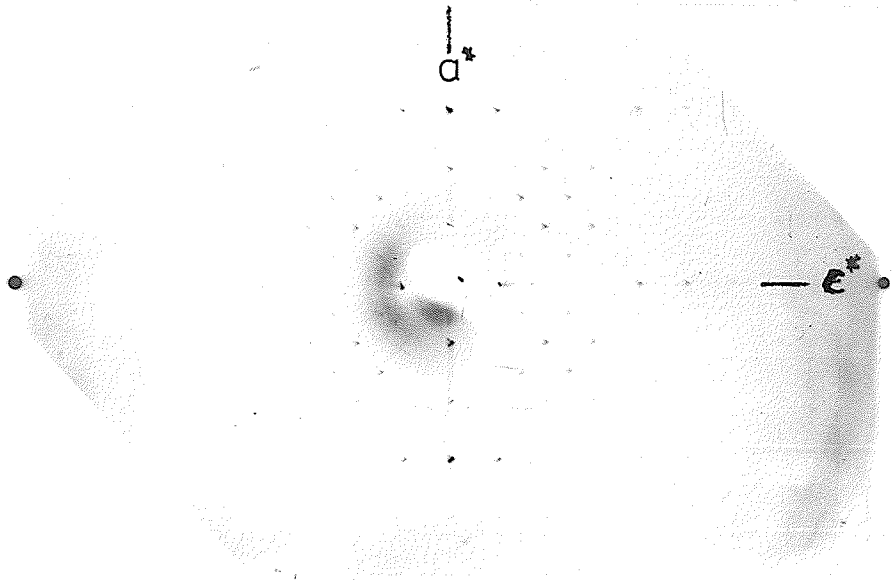

(a) h0ℓ precession photograph.

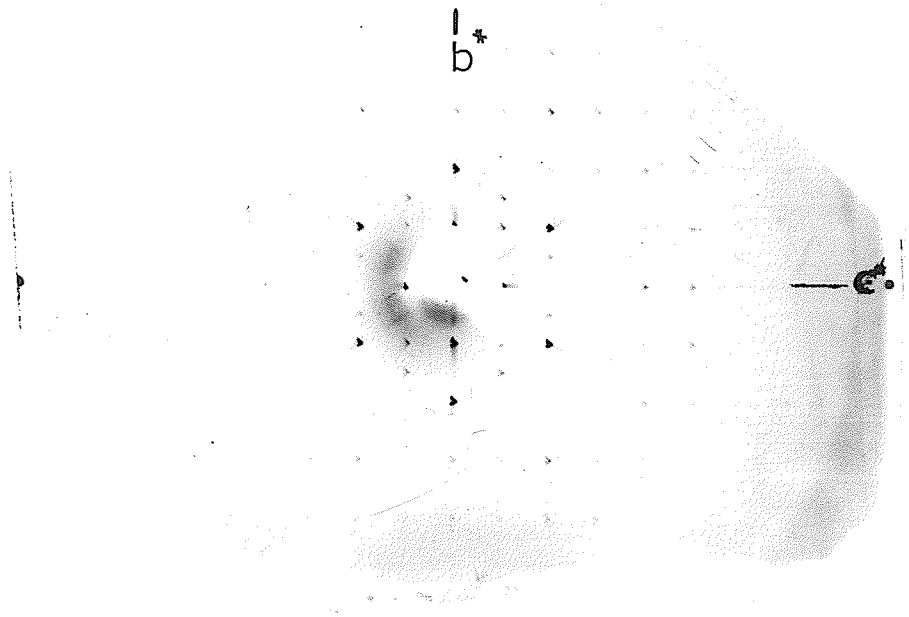

(b) 0kℓ precession photograph

Fig. 28. Contact prints of precession photographs of $Fe_3As_2(CO)_9$, Mo K_α radiation, $\bar{\mu} = 25^\circ$, F = 60 mm. .

some multiple of these spacings. The spacing measured along the $\underline{c}^*$ axis in Fig. 28 (b) actually corresponds to twice the d^*_{001} spacing due to the systematic absence, $0k\ell$ reflections present only with $\ell = 2n$ i.e. present only with ℓ even.

The $(h0\ell)^*$ and $(0k\ell)^*$ reciprocal lattice plane photographs, given in Figs. 28 (a) and (b) respectively, show that the $\underline{a}^*$ and $\underline{b}^*$ axes are normal to the $\underline{c}^*$ axis. Since both of these photographs were taken at right angles to one another, $\underline{a}^*$ is also normal to $\underline{b}^*$. The symmetry of the zero and first level photographs and the fact that α, β and γ are right angles confirm that the crystal belongs to the orthorhombic system. The reciprocal lattice spacing along the axis normal to $\underline{c}^*$ in Fig. 28 (a) is slightly larger than that along the axis normal to $\underline{c}^*$ in Fig. 28 (b). Therefore, the axis in Fig. 28 (a) is called $\underline{a}^*$ and the axis in Fig. 28 (b) is called $\underline{b}^*$ to retain the convention in direct space of $a_o < b_o$. The original assignment of the elongated axis of the crystal as the $\underline{c}$ axis is maintained to emphasize the pseudo-tetragonal symmetry of the crystal form.

An outstanding feature evident on the photograph of the $(0k\ell)^*$ reciprocal lattice plane Fig. 28 (b) is the pseudo-trigonal or pseudo-hexagonal pattern consisting of six very intense reflections ($02\bar{4}$, $02\bar{\bar{4}}$, $0\bar{4}0$, 040, $0\bar{\bar{2}}\bar{\bar{4}}$, and $0\bar{2}4$). If the structure contains a triangle of iron atoms as postulated in Fig. 26, than this pseudo-trigonal pattern strongly suggests that the iron triangle is perpendicular

to the precession axis of this photograph i.e. perpendicular to the a axis of the crystal.

C. DETERMINATION OF THE SPACE GROUP

The following systematic absences in the reflections were observed in the precession photographs:

hkℓ: present only with $h + \ell = 2n$

0kℓ: present only with $\ell = 2n$

h0ℓ: present only with $h + \ell = 2n$

hk0: present only with $h = 2n$, $k = 2n$

h00: present only with $h = 2n$

0k0: present only with $k = 2n$

00ℓ: present only with $\ell = 2n$

These systematic absences correspond to the following space groups: $Bm2_1b$, B2mb and Bmmb (Nuffield (1966), Table A3-3). By interchanging the crystal axes, the space groups corresponding to the normal orientations of the crystal are obtained. In the normal orientation, $Bm2_1b$ is equivalent to $Cmc2_1$ (No. 36), B2mb is equivalent to Ama2 (No. 40) and Bmmb is equivalent to Cmcm (No. 63). The normal orientation space groups are found in the International Tables for X-ray Crystallography (1962, Vol. I).

D. DETERMINATION OF THE UNIT CELL DIMENSIONS OF A SINGLE CRYSTAL OF $Fe_3As_2(CO)_9$

Accurate cell dimensions of a single crystal of $Fe_3As_2(CO)_9$ were obtained from zero level Weissenberg photographs by the method of C.L. Christ (1956). This method involves the calibration of each film as a

function of θ. The powder pattern of a known standard substance is recorded on both sides of a zero level Weissenberg pattern of the single crystal.

A zero level Weissenberg photograph of a single crystal of $Fe_3As_2(CO)_9$ rotating around the c axis was obtained using the method described in Chapter V. The translation of the camera was restricted to leave 1.5 cm of unexposed film on either side of the Weissenberg pattern. The goniometer head containing the crystal was removed and was replaced by another containing a thin aluminum wire (99.99% Al.). The camera drive was disconnected and the aluminum powder pattern was recorded on the film on both sides of the Weissenberg pattern. Unfiltered copper radiation ($CuK_{\alpha,\beta}$) was used in recording the Weissenberg pattern and nickel-filtered copper radiation (CuK_{α}) was employed for the aluminum powder pattern. The resulting photograph is shown in Fig. 29.

Swanson and Tatge (1953) have accurately determined the length of the cell edge for aluminum as $a_o = 4.0494$ Å. Accurate values of θ theor. were calculated for each reflection in the aluminum powder pattern using this value of a_o. The aluminum powder pattern on both sides of the film was measured with the use of a device similar to that in Fig. 7. Values of θ meas. for the reflections in the powder pattern were obtained from these measurements. The values of $k(\theta) = \frac{\theta_{theor.}}{\theta_{meas.}}$ were plotted versus θ meas.

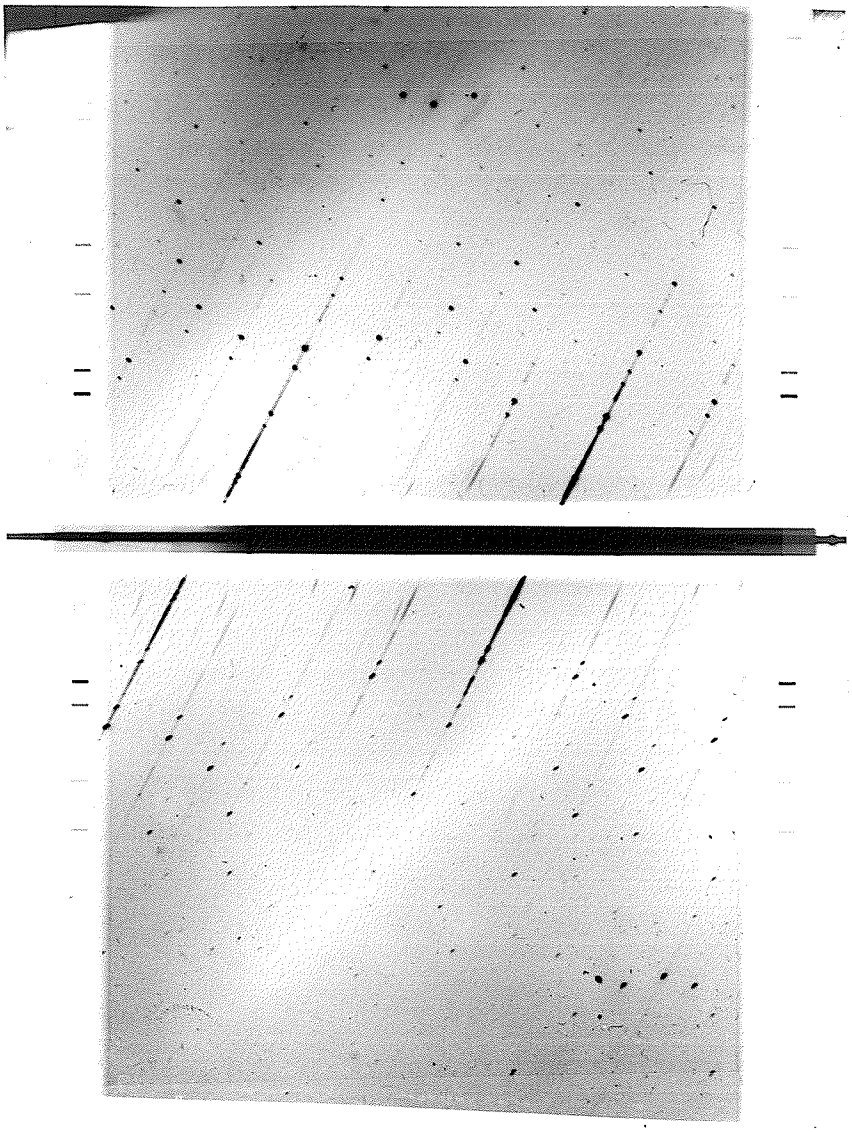

Fig. 29. hk0 Weissenberg photograph, Cu/- radiation; aluminum powder pattern, Cu/Ni radiation; camera radius 28.648 mm.

for each reflection in the aluminum pattern. This graph is given in Fig. 30. The positions of the h00 and 0k0 reflections were measured on the Weissenberg photographs and the values of θ meas. were obtained for these reflections. For each θ meas. value, the corresponding value of k (θ) is read from the graph in Fig. 30. The corrected θ value is given by $\theta_{corr.} = k(\theta)\ \theta_{meas.}$ Accurate cell dimensions are obtained from the $\theta_{corr.}$ values. These calculations and the accurate cell dimensions of $Fe_3As_2(CO)_9$ are given in Table 9. Table 9 also shows that the cell content Z = 4 i.e. there are four molecules of $Fe_3As_2(CO)_9$ per unit cell.

E. INTENSITY COLLECTION

An intensity scale was made using the method described in Chapter VII. An oscillation photograph taken of another crystal of $Fe_3As_2(CO)_9$ rotating around the a [100] axis showed very few reflections for levels higher than 10 kℓ. Thus, levels higher than this were not recorded for the intensity collection.

Equi-inclination Weissenberg photographs of the 0kℓ to 10kℓ levels of a single crystal of $Fe_3As_2(CO)_9$ (.2x.2x.3mm.) rotating around the a axis were recorded by the triple film pack technique using zirconium-filtered molybdenum (K_α) radiation. The intensities of the observed reflections on these photographs were estimated by visual comparison with the intensity scale.

The Lorentz and polorization factors were applied

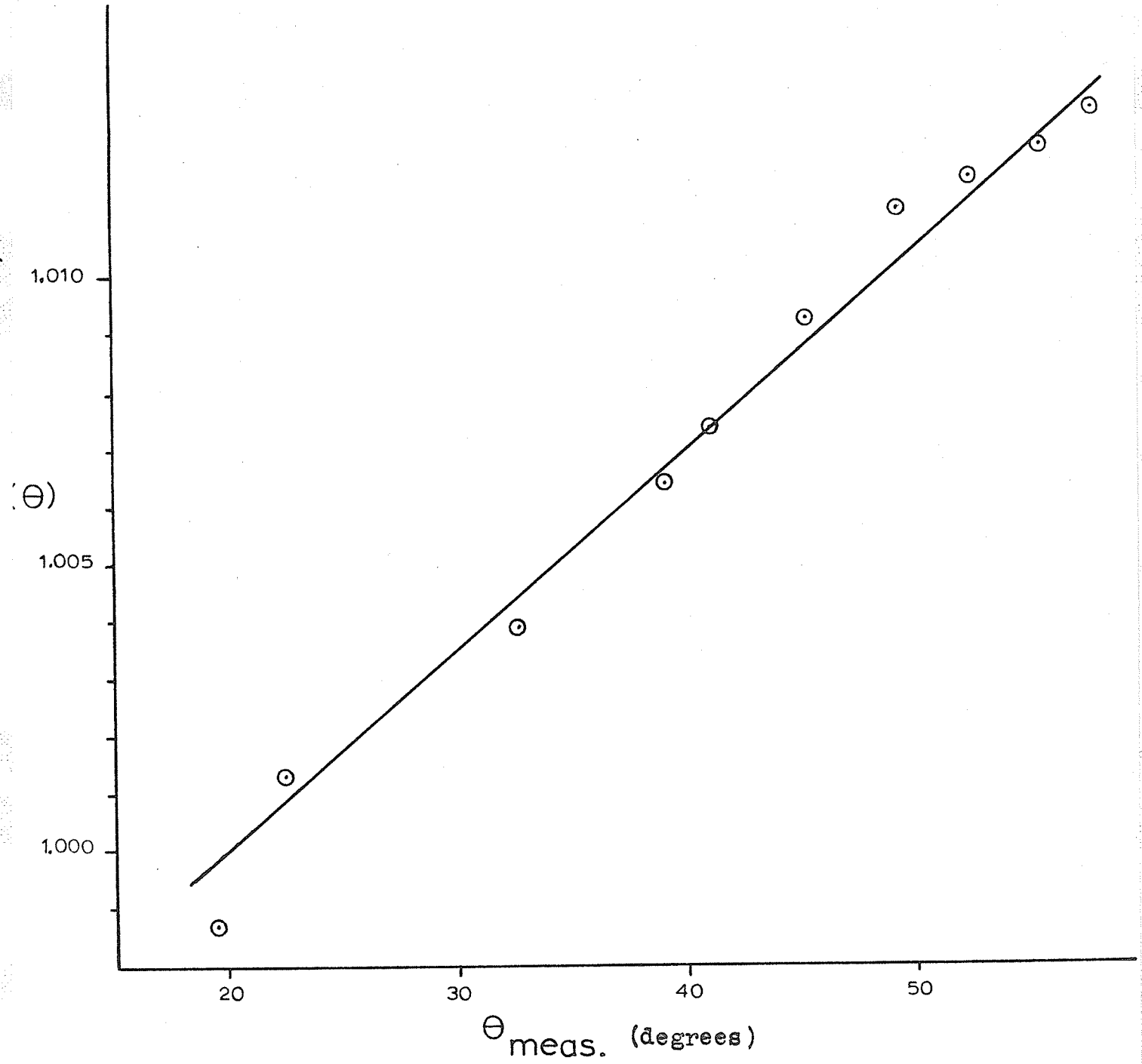

Fig. 30. Graph of k (θ) versus $\theta_{meas.}$ for the aluminum powder pattern.

TABLE 9. A. Accurate cell dimensions of a single crystal of $Fe_2As_2(CO)_9$

The hk0 Weissenberg photograph of Fig. 29 was measured.

a_o

Index	Reflection	R (mm.)	L (mm.)	2θ (°)	$\theta_{meas.}$ (°)	$\theta_{corr.}$ (°)	$d_{corr.}$ (Å)	d_{100} (Å)
600	β	104.40	59.20	45.80	22.90	22.92	1.787	10.72
	α	107.00	56.60	50.40	25.20	25.25	1.807	10.84
1000	β	121.45	42.00	79.45	39.72	40.00	1.083	10.83
	α	126.75	36.70	90.05	45.02	45.42	1.082	10.82
1200	β	131.70	31.65	100.15	50.07	50.61	0.9007	10.81
	α	139.50	23.75	115.75	57.87	58.65	0.9027	10.81

Since the x and x^* axes of the crystal coincide,

$a_o = d_{100} = 10.82 \pm .01$ Å (average of the last four results).

b_o

Index	Reflection	R (mm.)	L (mm.)	2θ (°)	$\theta_{meas.}$ (°)	$\theta_{corr.}$ (°)	$d_{corr.}$ (Å)	d_{010} (Å)
060	β	105.05	59.55	45.50	22.75	22.77	1.797	10.78
	α	106.60	56.95	49.65	24.82	24.87	1.833	11.00
080	β	112.15	51.45	60.70	30.35	30.46	1.370	10.96
	α	115.80	47.80	68.00	34.00	34.17	1.373	10.98
0100	β	120.85	42.55	78.30	39.15	39.41	1.096	10.96
	α	126.00	37.25	88.75	44.37	44.76	1.095	10.95

Since the y and y^* axes coincide in the crystal,

$b_o = d_{010} = 10.96 \pm .02$ Å (average of the last four results).

The similar measurement of an 0kl Weissenberg photograph and then a similar calculation gave values of

$b_o = 10.96 \pm .01$ Å and $c_o = 13.29 \pm .02$ Å

continued on next page

TABLE 9. (continued)

B. Unit cell dimensions of a single crystal of $Fe_3As_2(CO)_9$

The best values obtained from the hk0 and 0kℓ Weissenberg photographs are:

$a_o = 10.82 \pm .01$ Å
$b_o = 10.96 \pm .02$ Å
$c_o = 13.29 \pm .02$ Å

Each of the unit cell dimensions is the mean of four values calculated from the Weissenberg photographs; the values used fall within the ± range quoted.

The volume of the unit cell is $V = 1576.0$ Å^3

C. The density and cell content (Z)

The density ρ of a single crystal of $Fe_3As_2(CO)_9$, obtained by flotation in an aqueous potassium mercury iodide solution was 2.33 gm/cc.

The number of molecules/unit cell $Z = \frac{V\rho N}{M}$

$$Z = \frac{1576.0 \times 10^{-24} \times 2.33 \times 6.023 \times 10^{23}}{569.48} = 3.88$$

There are four molecules/unit cell in $Fe_3As_2(CO)_9$.

D. Size of crystal, linear absorption coefficient(μ) and μR.

The crystal used for the intensity collection was approximately 0.2x.2x.3 mm. .
The linear absorption coefficient, $\mu = 72$ cm^{-1} and $\mu R = 0.7$.

to the reflections using the NRC-2 Data Reduction program producing $|F_o|^2$ and $|F_o|$ for the reflections.

The levels 0kℓ to 10kℓ were brought onto the same scale initially by length of time exposure. The hk0 and hk1 cross axis Weissenberg photographs were taken of another crystal rotating about the c axis. However, these cross axis photographs were unsatisfactory in scaling the 0kℓ to 10kℓ level photographs because of the systematically absent reflections, hkℓ present only with $h + \ell = 2n$.

Only the even h levels had reflections in common with the hk0 cross-axis picture and only the odd h levels had reflections in common with the hk1 cross-axis photograph. Therefore, near the end of refinement a rescale factor for each 0kℓ to 10kℓ level was calculated as described in Appendix II and applied to the level.

CHAPTER XII

STRUCTURE DETERMINATION

The unit cell dimensions and the possible space groups of a single crystal of $Fe_3As_2(CO)_9$ were determined in the previous chapter. The intensities of the observed reflections occurring on the Weissenberg photographs of the $0k\ell$ to $10k\ell$ levels were measured and $|F_o|^2$ and $|F_o|$ were calculated for these reflections. The next step employed in the structure determination was an application of the heavy-atom method. The positions of the eight arsenic atoms were located by means of a Patterson map but the Fe-As and Fe-Fe vectors were not strongly evident on this map. An approximate electron density map with the phase angles based only on these arsenic atoms was computed. For a molecule, this centrosymmetric map located the iron atoms in a plane mid-way between the two arsenic atoms. This plane was perpendicular to the line joining the two arsenic atoms of the molecule. Equilateral triangles of iron atoms were consistent with this map. A single equilateral triangle of iron atoms in a molecule led to neither a satisfactory electron density map nor to a low R index. Successful refinement was only achieved with a model consisting of one molecule randomly distributed in two orientations related by a crystallographic two-fold axis.

A. THE POSSIBLE SPACE GROUPS: THEIR SYMMETRY AND EQUIVALENT POSITIONS

The possible space groups for the single crystal of

$Fe_3As_2(CO)_9$ are $Bm2_1b$, B2mb and Bmmb for the orientation of the axes of the crystal. By interchanging the crystal axes, one obtains the equivalent space groups $Cmc2_1$,(No. 36) Ama2 (No. 40) and Cmcm (No. 63), respectively (Bunn (1961), Appendix 8) which are in the International Tables For X-ray Crystallography (1962, Vol. I). The symmetry elements for the possible space groups are given in a projection of the unit cell along the x-axis in Figs. 31 (a), (b) and (c).

The necessary equivalent positions for each space group (excluding those positions related by the B-centering and a centre of symmetry if present) are:

for $Bm2_1b$: $(X,Y,Z);(\bar{X},Y,Z);(\bar{X},\frac{1}{2}+Y,\bar{Z})$ and $(X,\frac{1}{2}+Y,\bar{Z})$

for B2mb: $(X,Y,Z);(X,\bar{Y},\bar{Z});(X,\frac{1}{2}-Y,Z)$ and $(X,\frac{1}{2}+Y,\bar{Z})$

for Bmmb: $(X,Y,Z);(X,\bar{Y},\bar{Z});(X,\frac{1}{2}-Y,Z)$ and $(X,\frac{1}{2}+Y,\bar{Z})$.

These equivalent positions were obtained from the normal orientation of the space groups in the International Tables for X-ray Crystallography (1962, Vol. I).

B. PATTERSON SYNTHESIS

A series of Patterson sections parallel to (100) was computed using both the NRC-8 Fourier program and the values of $\left| F_o^{\,2} \right|$ obtained from the NRC-2 Data Reduction program. The space groups $Bm2_1b$, B2mb and Bmmb in direct space correspond to the space group Bmmm in Patterson space. Thus, Bmmm was the space group used for the Patterson synthesis. The Patterson fuction used was

$$P(X,Y,Z) = \frac{8}{V} \sum_{h=0}^{\infty} \sum_{k=0}^{\infty} \sum_{\ell=0}^{\infty} \left| F_{hk\ell} \right|^2 \cos 2\pi hX \cos 2\pi kY \cos 2\pi \ell Z$$

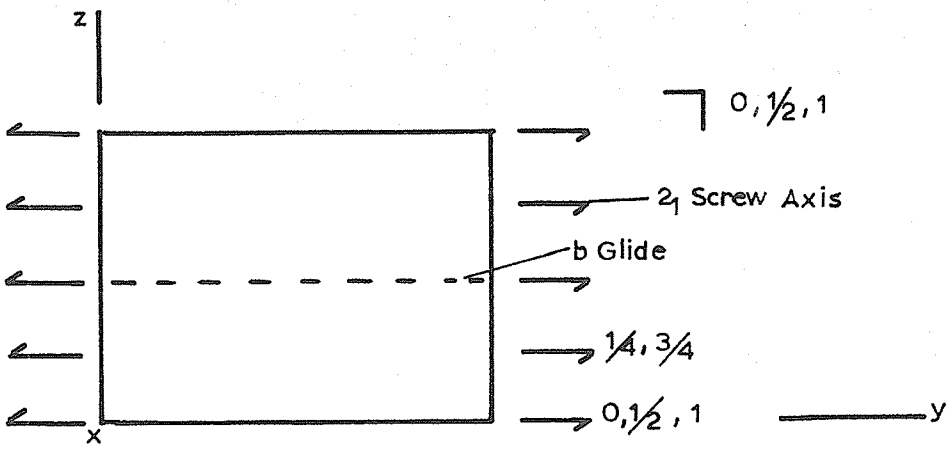

(a) Space group Bm2$_1$b with projection of the unit cell along the x-axis.

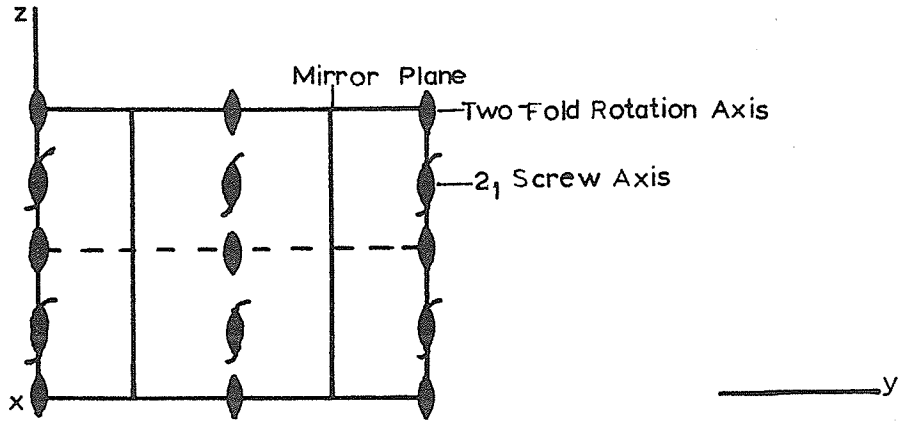

(b) Space groups B2mb with projection of the unit cell along the x-axis.

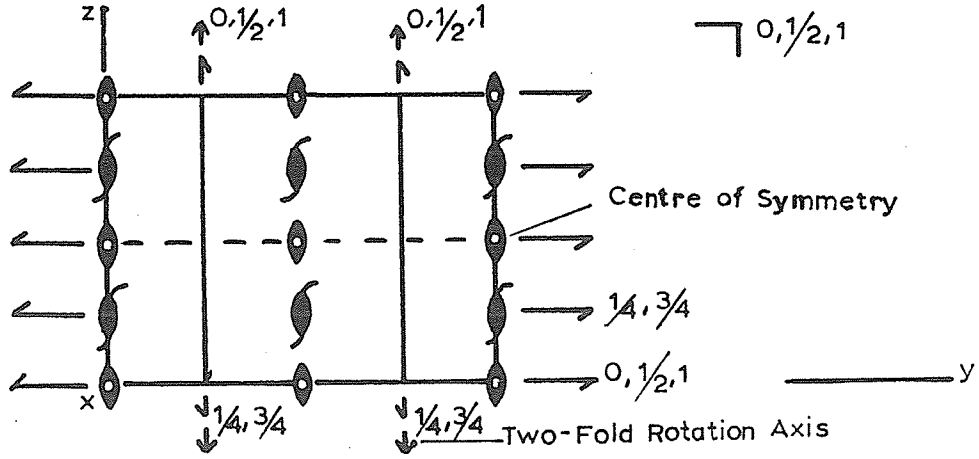

(c) Space group Bmmb with projection of the unit cell along the x-axis.

Fig. 31. Symmetry elements of possible space groups of $Fe_3As_2(CO)_9$ (Adapted from the International Tables for X-ray Crystallography (1962, Vol. I)).

where, the non-equivalent reflections are included in this expression.

Some very strong vector peaks occurred on the Patterson map. These strong peaks were assigned to the As-As vectors in the unit cell. The As-As peak, attributed to the vector occurring between the arsenic atoms of the same molecule, was along the x-axis at about X = 0.332 in fractional coordinates. The position of this intramolecular As-As vector was consistent with both the structure posulated in Fig. 26 and the strong suggestion in Fig. 28 (b) that the presumed triangle of iron atoms would be perpendicular to the x-axis. An unsuccessful attempt was made to locate the positions of all the Fe-As or Fe-Fe peaks. The arsenic atoms alone were then used to determine the phase angles of the first electron density map.

Since there are four molecules of $Fe_3As_2(CO)_9$ in the unit cell (from Table 9), there are eight arsenic atoms present. From an interpretation of the As-As vector peaks on the Patterson map, the arsenic atoms of a molecule of $Fe_3As_2(CO)_9$ were placed at (0.166, 0.25, 0.25) and (-0.166, 0.25, 0.25) (expressed in fractional coordinates) to satisfy the symmetry requirements of all three possible space groups.

The symmetry elements of the space group B2mb (equivalent to No. 40) would generate the other six arsenic atoms from this pair. Actually for space groups $Bm2_1b$ (equivalent to No. 36) and Bmmb (equivalent to No. 63),

which have a mirror plane at X = 0, Fig. 31, the position of only one of the arsenic atoms is entered in the structure factor calculation. The symmetry elements of these two space groups generate the remaining seven arsenic atoms in the unit cell. In any case, any one of these space groups would produce the same map with these arsenic atoms alone determining the phase angles.

C. ELECTRON DENSITY SYNTHESIS

The space group $Bm2_1b$ (equivalent to No. 36) was used to calculate the electron density map with only the arsenic atoms determining the phase angles. The positions of the arsenic atoms generate centres of symmetry and mirror planes (at Y = 1/4, 3/4 and Z = 1/4, 3/4) in addition to the symmetry elements of space group $Bm2_1b$. The strongest electron density peaks on this first electron density map, aside from the arsenic atom peaks, occurred on the mirror plane at X = 0. Thus, the iron atoms of the molecule are in this plane. Since the expected Fe-Fe bond distance was around 2.6 Å, the arrangement of the peaks could only be interpreted in terms of a molecule with three iron atoms at the apices of an equilateral triangle.

For a single molecule of $Fe_3As_2(CO)_9$ to conform to the symmetry requirements of space groups B2mb (equivalent to No. 40) or Bmmb (equivalent to No. 63), one iron atom must be on the mirror plane at Y = 1/4 and the other two must be related by this mirror plane (Fig. 32 (a)).

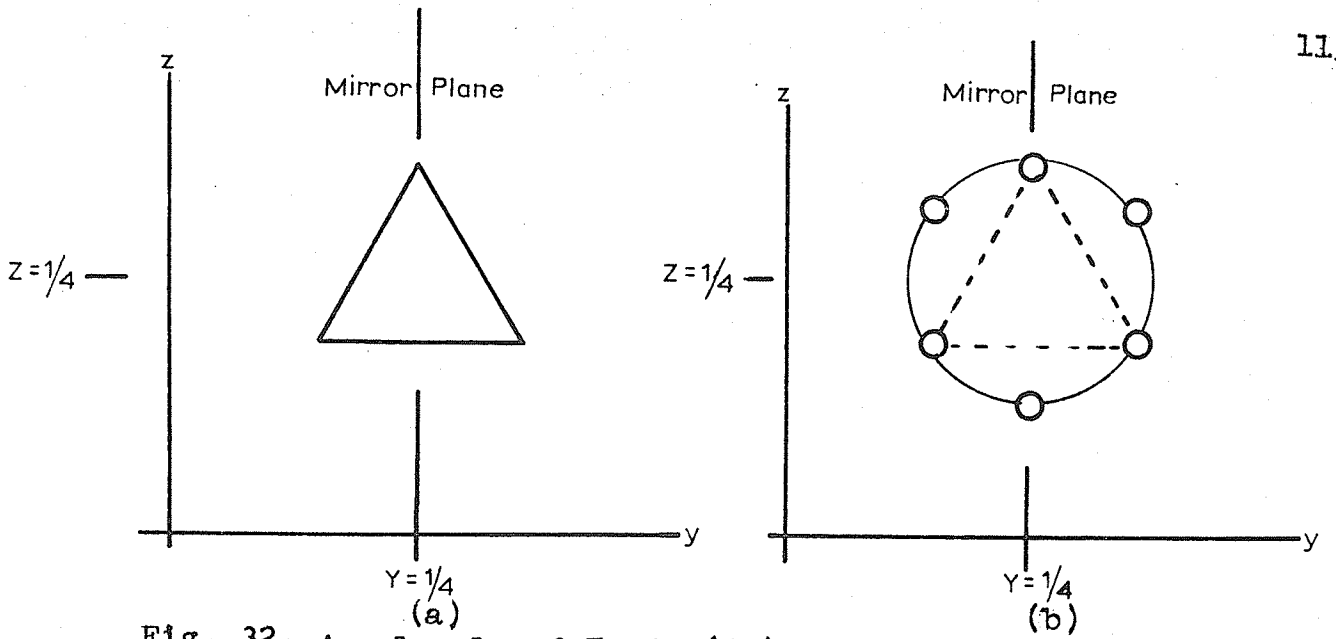

Fig. 32. A molecule of $Fe_3As_2(CO)_9$ conforming to B2mb and Bmmb. The false symmetry elements present in the first electron density map would generate additional peaks from those of this triangle of iron atoms (Fig. 32 (b)). Two of these six peaks must occur on Y = 1/4. The strong peaks which were actually observed on the mirror plane at X = 0, on this first electron density map are shown in Fig. 33.

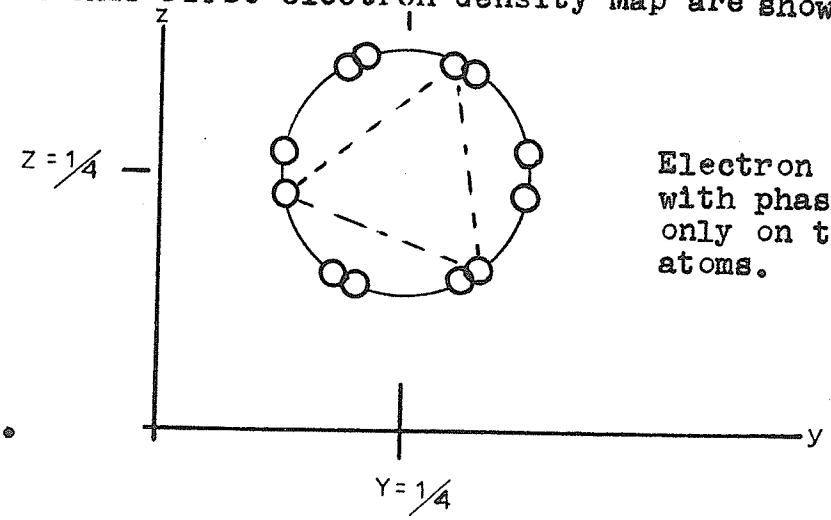

Electron density map with phase angles based only on the arsenic atoms.

Fig. 33.

However none of these strong peaks occurred on the mirror plane at Y = 1/4. Therefore, a single molecule of $Fe_3As_2(CO)_9$ could be interpreted from this map as conforming to only space group $Bm2_1b$ (equivalent to No. 36). From an examination of the positions of these peaks and from

the expected Fe-Fe distance of 2.6 $\mathring{A}$, only one choice existed for the iron atom positions.

A second electron density map was calculated with the phase angles based on both the arsenic atoms and these iron atoms. The map which was obtained showed that the electron density peaks corresponding to the iron atoms were not symmetrical. These peaks were extended in specific directions. The shape of the peaks suggested an overlap of each iron atom peak with another strong peak i.e. there was a suggestion of a statistical occurrence of two triangles of iron atoms. Leaving this latter possibility for the moment however, an attempt was made to locate the carbonyl groups for one molecule.

There are nine carbonyl groups in the molecule. Three terminal carbonyl groups were assigned to each iron atom in the molecule as postulated in Fig. 26. For the carbonyl groups in the molecule to conform to the space group $Bm2_1b$ (equivalent to No. 36), one carbonyl group bonded to each iron atom must be in the mirror plane at X = 0. The other two carbonyl groups bonded to an iron atom must be related by this mirror plane. The expected C-Fe-C angles in an $Fe(CO)_3$ group of a molecule are about ninety degrees. Possible orientations of the three carbonyl groups located in the plane at X = 0, are given in Figs. 34 (a), (b) and (c). A consideration of intermolecular steric requirements and the positions of

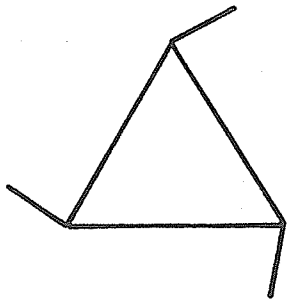

(a)

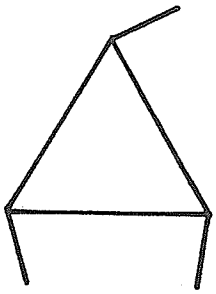

(b)

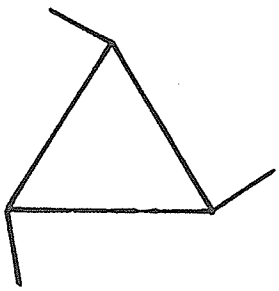

(c)

Fig. 34. Possible orientations of the carbonyl groups located in the X = 0 plane.

the peaks on this second electron density map led to only one possible set of carbonyl groups, that in Fig. 34 (a).

D. LEAST SQUARES REFINEMENT

Least squares refinement in space group $Bm2_1b$ (equivalent to No. 36) of the arsenic, iron, carbon and oxygen atom parameters obtained from the two electron density maps and using the NRC-10 Structure Factor Least Squares program gave unsatisfactory results. Some of the bond distances and angles were too far from chemically similar known bond distances and angles and R = 0.242.

The red crystals of $Fe_3As_2(CO)_9$ were pseudo - tetragonal in shape and they appeared to have a centre of symmetry as the crystal faces appeared to be equally developed. In general, if there is no centre of symmetry in the space group of the crystal, none appears in the crystal form. The faces which would be equivalent if a centre of symmetry was present, generally do not develop equally. A centrosymmetric space group is suggested for crystals of $Fe_3As_2(CO)_9$ by the fact that these crystals appear to have equally developed faces. The only centrosymmetric space group possible is Bmmb (equivalent to No. 63). However, the electron density map with phase angles based only on the arsenic atoms indicated that a single molecule of $Fe_3As_2(CO)_9$ did not conform to the centrosymmetric space group Bmmb (nor to the non-centrosymmetric space group B2mb). As a result the non-centrosymmetric space group $Bm2_1b$ (equivalent to No. 36) was initially used in

attempts to solve the crystal structure. However the attempts to refine a proposed structure in this latter space group failed. From an examination of the electron density maps and a consideration of expected bond angles and intramolecular steric requirements, this proposed structure was the only structure possible.

The crystal form suggested that the crystal belonged to a centrosymmetric space group. Also, the map of electron density, based on the phasing model of the arsenic atoms and the triangle of iron atoms using space group $Bm2_1b$ (equivalent to No. 36), showed that the electron density peaks corresponding to the iron atoms were extended in specific directions.

A third electron density map was computed using the centrosymmetric space group Bmmb (equivalent to No. 63) with the phase angles determined from the arsenic atoms and two orientations of the triangle of iron atoms. Each orientation had one-half occupancy and was related to the other orientation by the two-fold axis at X = 0, Y = 1/4 (or by the mirror plane at Y = 1/4 in Fig. 31 (c)). This arrangement of atoms and half-atoms is consistent with the strong peaks which occurred on the mirror plane at X = 0 for the first electron density map. The original triangle of iron atoms interpreted from this initial electron density map is the same triangle used in the centrosymmetric space group (with one-half occupancy). The symmetry elements generate the other orientation of

the triangle of iron atoms (the two-fold axis at X = 0, Y = 1/4 or the mirror plane at Y = 1/4). There was one-half of a molecule of $Fe_3As_2(CO)_9$ per asymmetric unit in space group $Bm2_1b$ (equivalent to No. 36). The other half of the molecule was generated by the mirror plane at X = 0. In the centrosymmetric space group Bmmb (equivalent to No. 63), there is one-half of the molecule per asymmetric unit but this one-half of the molecule has only one-half occupancy.

The electron density map based on the arsenic atoms and the two orientations of the triangle of iron atoms using space group Bmmb (equivalent to No. 63) revealed the positions of the carbonyl groups. The positions of one set of carbonyl groups corresponding to an orientation of the triangle of iron atoms are very close to the positions of the set of carbonyl groups corresponding to the other orientation (Fig. 35). Least squares refinement indicated that some carbon and oxygen atoms were best considered as coincident in the two sets of carbonyl group (e.g. C(5) and O (2) in Fig. 35). Refinement of the arsenic, the iron, the carbon and the oxygen atom positions and the thermal parameters (initially isotropic but later anisotropic) produced a final set of parameters with an R index = 0.107. These final parameters are given in Table 10.

Unit weights were initially employed in the refinement. In the last cycles of refinement, a weighting scheme was

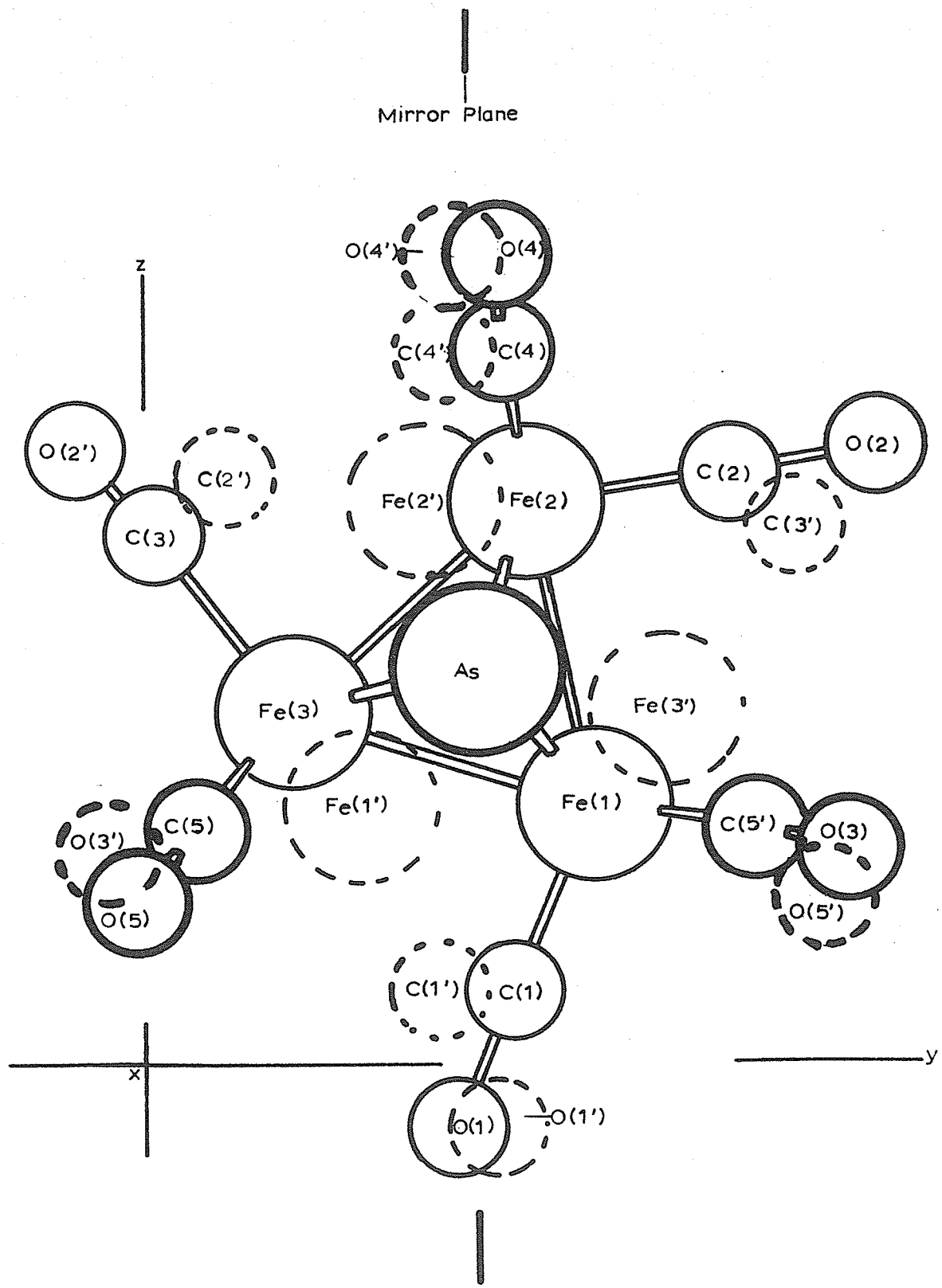

Fig. 35. The two orientations of the molecule in a projection along the x-axis of the unit cell.

TABLE 10. Atomic coordinates and their estimated standard deviations ($X10^4$) expressed in fractional coordinates.

	X		Y		Z	
As	0.1659	(2)	0.2500	(-)	0.2451	(1)
Fe(1)*	0.0000	(-)	0.3394	(4)	0.1608	(3)
Fe(2)*	0.0000	(-)	0.2869	(4)	0.3536	(3)
Fe(3)*	0.0000	(-)	0.1116	(4)	0.2186	(4)
O(1)*	0.0000	(-)	0.2349	(98)	-0.0401	(20)
O(2)	0.0000	(-)	0.5494	(18)	0.3868	(15)
O(3)*	0.1907	(37)	0.5314	(19)	0.1341	(19)
O(4)*	0.1946	(22)	0.2686	(21)	0.5058	(14)
O(5)*	0.1992	(24)	-0.0057	(18)	0.1027	(14)
C(1)*	0.0000	(-)	0.2783	(21)	0.0445	(29)
C(2)*	0.0000	(-)	0.4437	(24)	0.3715	(25)
C(3)*	0.0000	(-)	0.0092	(40)	0.3334	(27)
C(4)*	0.1212	(29)	0.2712	(14)	0.4474	(23)
C(5)	0.1187	(18)	0.0398	(16)	0.1464	(11)

* has an occupation factor of 0.5

The atomic scattering factors for C, O, Fe and As were taken from the International Tables for X-Ray Crystallography (1962, Vol. III). No correction was made for anomalous dispersion.

calculated as described in Chapter VIII and used in calculating the parameter shifts. The weighting scheme was $W = \frac{1}{(1 + 0.169\,|F_o|)^2}$.

The intensities of very strong reflections occurring at very low angles may be considerably reduced by extinction (Buerger (1960)). The reflections 024 and 040 appeared to show this effect and thus were removed from the last stages of the least squares refinement and from the calculation of the R index.

In the final least squares cycle, convergence was achieved. The largest and the average absolute values of the atomic coordinate shifts (in fractional coordinates) were the following:
3×10^{-5} and 3×10^{-5} for the arsenic atoms,
3×10^{-5} and 2×10^{-5} for the iron atoms,
329×10^{-5} and 62×10^{-5} for the oxygen atoms,
and 101×10^{-5} and 39×10^{-5} for the carbon atoms. The maximum positional parameter shift was less than one third of its estimated standard deviation (e.s.d.) and the average positional parameter shift was one-tenth of its e.s.d.

A difference Fourier synthesis was carried out for the last cycle of refinement using the NRC-8 Fourier program. The maxima and minima on this difference map were between $1e/\mathring{A}^3$ and $-1e/\mathring{A}^3$ showing the close agreement between the proposed structure and the actual structure.

CHAPTER XIII

RESULTS AND DISCUSSION

The following results of the X-ray analysis are tabulated: the final atomic coordinates (Table 10), the observed and calculated structure factors (Table 11), the bond distances and interbond angles (Table 12) and the thermal vibration tensor components, U_{ij}'s (Table 13). The X-ray analysis revealed the presence of two orientations (each with one-half occupancy) of one molecule of $Fe_3As_2(CO)_9$ distributed apparently equally and randomly throughout the crystal. A projection of the two orientations of the molecule viewed along the x-axis of the unit cell is given in Fig. 35. In Fig. 35, one orientation of the molecule is illustrated in closed circles and the second orientation is shown in dashed circles. This second orientation of the molecule is generated from the first by a rotation about the two-fold axis at X = 0, Y = 1/4 (or reflection through the mirror plane at Y = 1/4, Fig. 31 (c)). The presence of the two orientations of the molecule may be understood by an examination of the outer portion of the molecule i.e. the oxygen atoms. These nine oxygen atoms coincide either completely or at least to a great extent in both orientations. When only the external part of the molecule is viewed i.e. looking at only the oxygen atoms, both orientations are almost identical. Therefore, placing one molecule in either one or the other orientation in the unit cell

TABLE 11. The observed and calculated structure factors(x10) for $Fe_3As_2(CO)_9$.

H= 10

K	L	FOBS	FCAL
0	4	-908	-949
0	6	1001	1013
0	14	359	439
0	16	-319	-357
2	2	-603	-652
2	4	759	710
2	6	-940	-878
2	8	305	341
3	2	-457	-446
3	4	503	401
3	6	-158	-141
3	12	306	332
4	0	-622	-580
4	2	917	939
4	4	-921	-780
4	6	627	523
4	8	-162	-170
5	2	565	463
5	4	-441	-386
6	0	564	549
6	2	-585	-482

H= 9

K	L	FOBS	FCAL
0	11	211	176
1	3	-1231	-1332
1	5	1659	1581
1	7	-1315	-1207
1	9	443	429
1	11	-264	-353
1	13	628	537
1	15	-636	-542
1	17	312	307
1	19	-232	-126
2	3	-417	-357
2	11	-496	-436
2	13	265	305
3	1	-1268	-1360
3	3	1563	1534
3	5	-1239	-1235
3	7	330	997
3	9	-567	-523
3	11	436	385
3	13	-318	-348
3	15	275	275
4	1	-401	-368
4	3	709	691
4	5	-478	-431
4	7	195	221
4	11	335	337
4	13	-332	-366
4	15	230	151
5	1	1157	1141
5	3	-1377	-1184
5	5	827	775
5	7	-714	-572
5	9	503	442
5	11	-607	-533
5	13	432	438
6	1	221	244
6	3	-379	-363
7	1	-822	-741
7	3	501	479
7	5	-198	-215
7	7	528	428
7	9	-681	-555
7	11	654	540
7	13	-372	-371
9	1	527	479
9	3	-606	-538
9	5	523	457
9	7	-482	-437
9	9	428	352
10	7	-426	-346
10	9	285	320
11	1	-560	-458
11	3	469	419
11	5	-393	-375
11	7	341	331
11	9	-233	-212

H= 8

K	L	FOBS	FCAL
0	4	-1248	-1185
0	6	1092	1132
0	8	-533	-487
0	10	-275	-296
0	12	-266	-250
0	14	479	463
0	16	-370	-414
0	18	200	174
1	4	341	322
1	6	-165	-189
1	8	172	166
2	2	-691	-573
2	4	1240	1107
2	6	-696	-611
2	8	487	453
2	12	190	248
2	14	-171	-218
2	16	204	211
3	2	-887	-765
3	4	463	416
3	10	-267	-373
3	12	335	379
3	14	-179	-166
3	16	-133	-48
4	0	-1064	-962
4	2	931	848
4	4	-819	-664
4	6	555	528
4	8	-424	-386
5	2	389	448
5	4	-401	-363
5	6	177	198
6	0	444	487
6	2	-489	-449
6	4	262	281
6	8	176	175
6	10	-293	-357
6	12	480	456
6	14	-183	-168
7	2	-244	-259
7	6	222	223
7	8	-290	-332
8	0	-330	-355
8	2	97	144
8	6	200	119
8	8	-433	-360
8	10	267	233
9	2	-191	-219
9	6	192	182
10	0	189	255
10	2	-261	-312
10	4	319	385
11	8	315	326

H= 7

K	L	FOBS	FCAL
0	5	1016	987
0	7	-603	-594
0	15	-245	-245
1	3	824	776
1	7	246	285
1	9	-773	-839
1	11	687	670
1	13	-112	-114
2	3	-195	-149
2	7	138	164
2	9	-172	-205
3	1	590	537
3	3	-226	-199
3	5	346	287
3	7	-516	-476
3	9	596	614
3	11	-406	-459
3	13	228	275
3	15	-216	-227
4	1	-447	-458
4	3	938	907
5	1	-413	-368
5	3	480	410
5	5	-617	-587
5	7	600	571
5	9	-487	-508
6	3	-184	-223
6	5	-88	-94
6	7	397	379
6	9	-522	-483
7	1	489	514
7	3	-771	-701
7	5	948	877
7	7	-585	-562
8	5	200	275
8	9	159	220
9	1	-361	-357
9	3	289	319
9	5	-227	-258
9	7	157	143
9	9	-167	-155
9	11	202	157
10	1	-151	-186
10	3	200	269
10	7	-272	-285
10	9	213	191

H= 6

K	L	FOBS	FCAL
0	4	1115	995
0	6	-664	-689
0	8	1411	1329
0	10	-1209	-1198
0	12	601	641
1	4	494	465
1	6	-806	-843
1	8	526	498
1	10	-211	-204
1	12	156	171
1	14	-344	-365
1	16	266	302
1	18	-145	-124
2	2	1573	1621
2	4	-1548	-1218
2	6	632	535
2	8	-1154	-1110
2	10	1198	1275
2	12	-737	-704
2	14	198	274
2	16	-134	-167
3	2	-507	-425
3	4	440	420
3	6	113	130
4	0	1391	1221
4	2	-720	-690
4	4	942	941
4	6	-985	-1048
4	8	992	1112
4	10	-797	-753
4	12	533	515
4	14	-399	-459
4	16	319	366
4	18	-296	-315
4	20	223	151
5	2	654	655
5	4	-450	-427
5	6	-419	-365
5	8	520	479
5	10	-216	-214
6	0	-953	-1091
6	2	1028	1033
6	4	-1941	-1365
6	6	1228	1123
6	8	-965	-921
6	10	371	449
6	12	-122	-140
7	4	-154	-150
7	6	414	394
7	8	-533	-501
7	10	507	449
8	0	862	877
8	2	-956	-878
8	4	1118	1086
8	6	-902	-774
8	8	523	459
8	10	-242	-238
8	12	130	217
10	0	-530	-494
10	2	478	381
10	4	-255	-325
10	6	249	272
10	8	-261	-349
10	10	294	282
10	12	-278	-264
10	14	294	269
10	16	-155	-151
11	2	275	293
11	4	-121	-137
11	6	-217	-201
11	8	261	289
12	0	176	219
12	2	-177	-283
12	4	286	312
14	4	-316	-287
14	6	289	241

H= 5

K	L	FOBS	FCAL
0	5	560	486
0	7	-1090	-1184
0	15	-472	-381
1	3	1369	1122
1	5	146	172
1	7	381	372
1	9	-781	-791
1	11	720	709
1	13	-152	-154
2	5	-140	-133
2	7	419	415
2	9	349	318
3	1	907	766
3	5	-310	-240
3	7	-673	-643
3	9	769	773
3	11	-527	-556
3	13	170	213
4	1	-356	-405
4	3	742	819
4	5	-694	-694
4	7	-388	-387
4	13	-317	-315
5	1	69	76
5	3	810	754
5	5	-807	-771
5	7	684	702
5	9	-253	-296
6	1	373	404
6	3	-429	-372
6	5	-169	-237
6	7	754	671
6	9	-172	-197
6	11	187	208
7	1	760	759
7	3	-705	-705
7	5	687	614
7	7	-789	-699
7	9	197	221
8	1	192	244
8	3	-304	-319
8	11	-308	-250
9	1	-136	-173
9	3	543	495
9	5	-353	-322
10	3	181	187
10	5	-108	-77
10	7	-159	-234
10	9	281	340

H= 4

K	L	FOBS	FCAL
0	4	-1494	-1487
0	6	1446	1538
0	8	-326	-414
0	12	-326	-306
0	14	541	472
0	16	-593	-492
1	6	-588	-552
1	8	215	216
1	10	240	285
2	4	1480	1409
2	6	-1637	-1570
2	8	463	442
2	14	-419	-447
2	16	296	295
3	2	-643	-619
3	4	743	678
3	6	-168	-225
3	8	422	359
3	10	-512	-471
3	12	335	300
3	14	-279	-238
3	16	201	61
4	0	-1262	-1309
4	2	1331	1486
4	4	-1255	-1187
4	6	784	715
4	8	-254	-263
4	10	354	358
4	12	-242	-297
5	2	770	870
5	4	-900	-978
5	8	412	430
5	12	-372	-430
5	14	270	305
6	0	839	924
6	2	-630	-613
6	8	153	201
6	10	-551	-489
6	12	612	517
6	14	-240	-263
7	6	221	260
7	8	-160	-144
8	0	-247	-313
8	2	177	233
8	6	158	235
8	8	-237	-290
8	10	359	403
8	12	-286	-287
9	2	-190	-161
10	0	624	542
10	2	-523	-426
10	4	294	357
10	6	-352	-350
10	8	211	251
11	2	278	265
11	6	-262	-318
11	8	588	472
11	10	-204	-259
12	0	-227	-216
12	2	186	186
12	6	239	262

H= 3

K	L	FOBS	FCAL
0	5	1781	1653
0	7	-826	-691
0	9	-365	-426
0	11	357	356
0	13	-187	-125
1	3	-1825	-1813
1	5	2170	2732
1	7	-1691	-1722
1	9	684	686
1	11	-628	-499
1	13	797	690
1	15	-1014	-770
1	17	506	407
1	19	-173	-171
2	3	-353	-274
2	5	491	463
2	7	-517	-475
2	9	250	234
2	11	-574	-487
2	13	379	421
3	1	-1770	-2112
3	3	2156	2411
3	5	-2094	-2387
3	7	1348	1335
3	9	-683	-531
3	11	634	541
3	13	-550	-502
3	15	405	407
4	1	-626	-586
4	3	1937	2070
4	5	-158	-188
4	9	-455	-390
4	11	642	473
4	13	-689	-548
4	15	244	284
5	1	1804	2081
5	3	-1524	-1549
5	5	1117	1065
5	7	-884	-723
5	9	899	771
5	11	-934	-809
5	13	566	527
5	15	-218	-249
6	1	-133	-137
6	3	-799	-735
6	7	407	279
6	9	-233	-184
6	13	205	270
7	1	-1051	-1012
7	3	684	604
7	5	-563	-461
7	7	718	555
7	9	-993	-729
7	11	1036	752
7	13	-717	-487
7	15	381	319
8	1	271	263
8	13	-218	-139
9	1	904	726
9	3	-874	-718
9	5	834	676
9	7	-700	-559
9	9	658	476
9	11	-448	-413
9	13	225	237
10	7	-502	-398
10	9	605	457
11	1	-922	-668
11	3	637	540
11	5	-718	-523
11	7	671	484
11	9	-434	-306
12	1	143	180
12	3	-205	-250
12	7	486	405
12	9	-160	-202

H= 2

K	L	FOBS	FCAL
0	4	-1605	-1812
0	6	1596	1528
0	8	-912	-777
0	10	-315	-297
0	12	-422	-421
0	14	661	544
0	16	-725	-523
1	4	412	431
1	6	-403	-359
1	8	258	258
1	10	221	259
2	4	1713	1969
2	6	-984	-1183
2	8	583	636
2	10	171	144
2	12	396	340
2	14	-334	-311
2	16	327	340
3	2	-1212	-1343
3	4	665	675
3	10	-572	-564
3	12	573	447
4	0	-1803	-1827
4	2	1329	1473
4	4	-1023	-1141
4	6	878	830
4	8	-667	-597
4	12	-280	-360
4	14	154	115
5	2	598	609
5	4	-329	-769
5	6	266	291
5	8	338	361
5	12	-407	-316
5	14	222	270
6	0	672	542
6	2	-797	-629
6	4	575	515
6	8	216	173
6	10	-623	-471
6	12	710	640
6	14	-161	-187
7	2	-453	-405
7	6	503	332
7	8	-304	-374
8	0	-619	-625
8	8	-588	-530
8	10	309	324
8	12	-343	-303
8	14	240	195
9	2	-311	-344
9	6	306	250
9	8	-204	-156
10	0	329	320
10	2	-469	-447
10	4	716	555
10	6	-303	-332
11	2	144	144
11	4	-147	-130
11	6	-354	-325
11	8	711	408
12	0	-303	-338
12	2	153	190
12	4	-156	-159

H= 1

K	L	FOBS	FCAL
0	5	1054	1145
0	7	-784	-869
0	9	128	149
0	11	-250	-282
0	13	278	278
0	15	-434	-399
1	3	1065	1112
1	7	335	315
1	9	-989	-1028
1	11	960	931
2	3	-404	-388
2	5	-196	-178
2	7	608	563
2	15	282	289
3	1	714	798
3	5	264	255
3	7	-761	-781
3	9	791	714
3	11	-710	-589
3	13	299	319
3	15	-297	-277
4	1	-552	-560
4	3	836	952
4	5	-541	-466
4	13	-191	-235
5	1	-345	-304
5	3	670	668
5	5	-754	-759
5	7	643	668
5	9	-607	-589
5	11	294	374
5	15	213	197
5	17	-264	-287
6	1	415	438
6	3	-447	-505
6	5	-268	-244
6	7	798	711
6	9	-547	-474
7	1	764	733
7	3	-855	-798
7	5	1099	1132
7	7	-920	-858
8	1	164	140
8	3	-257	-301
8	7	-152	-215
8	9	381	344
8	11	-246	-237
9	1	-498	-398
9	3	549	465
9	5	-357	-277
9	9	-120	-167
9	11	314	230
10	3	320	307
10	7	-512	-378
10	9	377	321
11	3	-117	-73
12	1	123	134
12	3	-249	-230
12	7	323	230

H= 0

K	L	FOBS	FCAL
0	6	-446	-439
0	8	1812	2102
0	10	-1686	-1697
0	12	731	700
0	14	-331	-184
1	4	1067	1095
1	6	-820	-778
1	8	741	638
1	10	-286	-283
1	14	-466	-450
1	16	267	381
2	4	-1864	-1957
2	6	752	757
2	8	-1035	-991
2	10	1435	1519
2	12	-1063	-834
3	2	-1208	-1232
3	4	405	418
3	6	217	179
3	8	-317	-396
3	12	154	204
4	0	1937	1959
4	2	-453	-356
4	4	844	760
4	6	-1059	-1106
4	8	1403	1512
4	10	-1179	-1130
4	12	565	529
4	14	-496	-548
4	16	419	399
4	18	-287	-313
4	20	218	258
5	2	790	725
5	4	-249	-314
5	8	592	566
5	10	-294	-357
6	0	-1105	-1389
6	2	333	930
6	4	-1992	-2095
6	6	1479	1451
6	8	-1118	-1087
6	10	559	549
6	14	254	227
7	4	-257	-250
7	6	625	525
7	8	-967	-707
7	10	613	524
8	0	1282	1281
8	2	-1073	-962
8	4	1344	1418
8	6	-1260	-916
8	8	407	445
8	10	-285	-280
9	4	358	322
10	0	-976	-699
10	2	401	402
10	4	-381	-329
10	6	228	314
10	8	-536	-482
10	10	474	376
10	12	-269	-241
10	14	292	253
11	2	427	358
11	6	-241	-282
11	8	436	360
12	0	170	199
12	4	427	406
12	6	-254	-229
12	10	-276	-191

TABLE 12. Interatomic distances and angles and their estimated standard deviations.

A. Bond distances

			σ	
As-Fe(1)	2.331	Å	0.003	Å
As-Fe(2)	2.338		0.003	
As-Fe(3)	2.376		0.003	
Average As-Fe	2.348		0.003	
Fe(1)-Fe(2)	2.626		0.006	
Fe(1)-Fe(3)	2.612		0.007	
Fe(2)-Fe(3)	2.630		0.007	
Average Fe-Fe	2.623		0.007	
Fe(1)-C(1)	1.685		0.036	
Fe(1)-C(5')	1.855		0.019	
Fe(2)-C(2)	1.735		0.027	
Fe(2)-C(4)	1.817		0.031	
Fe(3)-C(3)	1.894		0.040	
Fe(3)-C(5)	1.786		0.018	
Average Fe-C	1.803		0.028	
C(1)-O(1)	1.221		0.060	
C(2)-O(2)	1.176		0.033	
C(3)-O(2')	0.958		0.045	
C(4)-O(4)	1.111		0.037	
C(5)-O(5)	1.159		0.030	
C(5')-O(3)	1.115		0.037	
Average C-O	1.125		0.040	
Fe(1)-O(1)	2.906		0.049	
Fe(1)-O(3)	2.969		0.032	
Fe(2)-O(2)	2.911		0.020	
Fe(2)-O(4)	2.926		0.022	
Fe(3)-O(2')	2.849		0.021	
Fe(3)-O(5)	2.944		0.023	
Average Fe-O	2.927		0.030	

TABLE 12. (continuted)

B. Bond angles

Fe(1)-As-Fe(2)	68.4°	0.1°
Fe(1)-As-Fe(3)	67.4	0.1
Fe(2)-As-Fe(3)	67.8	0.1
Average Fe-As-Fe	67.9	0.1
Fe(1)-Fe(2)-Fe(3)	59.6	0.1
Fe(1)-Fe(3)-Fe(2)	60.1	0.1
Fe(2)-Fe(1)-Fe(3)	60.3	0.1
C(1)-Fe(1)-C(5')	100.8	1.0
C(5')-Fe(1)-C(5''')	87.6	0.8
C(2)-Fe(2)-C(4)	90.00	1.2
C(4)-Fe(2)-C(4'')	92.4	1.2
C(3)-Fe(3)-C(5)	99.9	1.2
C(5)-Fe(3)-C(5'')	91.9	0.8
Average C-Fe-C	94.8	1.2
O(1)-Fe(1)-O(3)	99.8	1.4
O(3)-Fe(1)-O(3'')	88.0	0.8
O(2)-Fe(2)-O(4)	87.9	0.5
O(4)-Fe(2)-O(4'')	92.0	0.6
O(2')-Fe(3)-O(5)	98.1	0.5
O(5)-Fe(3)-O(5'')	93.0	0.7
Average O-Fe-O	93.8	0.9
Fe(1)-C(1)-O(1)	179.6	3.6
Fe(1)-C(5')-O(3)	177.4	2.1
Fe(2)-C(2)-O(2)	177.9	2.2
Fe(2)-C(4)-O(4)	176.0	2.5
Fe(3)-C(3)-O(2')	174.2	3.1
Fe(3)-C(5)-O(5)	177.1	1.8
Average Fe-C-O	177.0	2.5

' refers to the equivalent atom from the one in Table 10 reflected across the mirror plane at Y = 1/4.

'' refers to the equivalent atom from the one in the parameters list (Table 10) reflected across the mirror plane at X = 0.

''' refers to the equivalent atoms from the one in the parameters list reflected across both the mirror planes at Y = 1/4 and X = 0.

TABLE 13. Thermal vibration tensor components U_{ij} ($\AA^2$)

	U_{11}	U_{22}	U_{33}	U_{23}	U_{13}	U_{12}
As	0.010	0.050	0.037	0.000	0.000	0.000
Fe(1)	0.016	0.033	0.030	0.000	0.000	0.000
Fe(2)	0.012	0.042	0.032	-0.006	0.000	0.000
Fe(3)	0.015	0.035	0.038	-0.009	0.000	0.000
O(1)	0.164	0.075	0.029	0.033	0.000	0.000
O(2)	0.151	0.061	0.065	-0.043	0.000	0.000
O(3)	0.181	0.037	0.069	-0.042	0.098	-0.054
O(4)	0.030	0.044	0.065	-0.023	-0.025	0.012
O(5)	0.048	0.050	0.029	0.023	0.023	0.019
C(1)	0.108	0.000	0.041	0.011	0.000	0.000
C(2)	0.056	0.016	0.037	0.006	0.000	0.000
C(3)	0.023	0.056	0.036	-0.005	0.000	0.000
C(4)	0.037	0.000	0.075	0.003	0.020	0.003
C(5)	0.049	0.069	0.047	-0.025	0.000	0.016

makes little difference sterically to the placing of the next molecule. As a result, the packing of the molecules is random throughout the crystal.

The statistically disordered structure of $Fe_3As_2(CO)_9$ is similar in some respects to that of $Fe_3(CO)_{12}$ whose crystal structure was determined by Wei and Dahl (1969). In the crystal structure of $Fe_3(CO)_{12}$ there is a random distribution of an $Fe_3(CO)_{12}$ molecule in two orientations. The two orientations are related by a crystallographic centre of symmetry with each orientation having one-half occupancy. The crystal packing in $Fe_3(CO)_{12}$ was also random due to the near coincidence of the carbonyl groups in both orientations of the molecule. The smallest intermolecular distance in the crystal structure of $Fe_3As_2(CO)_9$ is 3.1 Å (between oxygen atoms). The smallest intermolecular distance in the crystal structure of $Fe_3(CO)_{12}$ is 3.0 Å and this distance also occurs between oxygen atoms. Fig. 36 is a projection of the unit cell of $Fe_3As_2(CO)_9$ along the x-axis with the arsenic and iron atoms of the two orientations of the molecule shown.

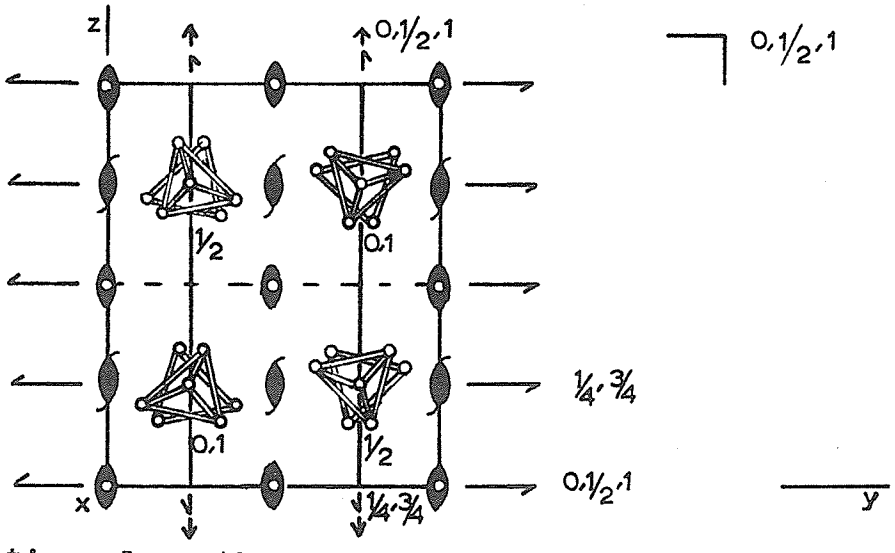

Fig. 36. Projection along the x-axis of the unit cell of $Fe_3As_2(CO)_9$.

A projection of the molecule along the x-axis of the unit cell is given in Fig. 37. Another projection of the molecule (along the line in common with the plane through As,Fe(1) and As'' and the plane at X=0)is given in Fig. 38. Figs. 37 and 38 show that the molecular structure of $Fe_3As_2(CO)_9$ is identical to that proposed by L. Kruczynski (private communication) in Fig. 26.

Table 12 contains the bond distances and angles. The As-Fe distances average 2.35 Å. The Fe-Fe distances average 2.62 Å and are equivalent within their estimated standard deviations. Thus, the $Fe_3As_2(CO)_9$ molecule contains an equilateral triangle of iron atoms. The iron atoms in $Fe_3As_2(CO)_9$ are chemically equivalent in contrast to the iron atoms in the structures of $Fe_3(CO)_{12}$ (Wei and Dahl (1969)), $HFe_3(CO)_{11}$ (Dahl and Blount (1965)) and $Fe_3(CO)_{11}P(C_6H_5)_3$ (Dahm and Jacobson (1968)). In the latter molecules there were isosceles triangles of iron atoms. The Fe-Fe distances determined in each of these crystal structures are:

for $Fe_3(CO)_{12}$: 2.67, 2.68 and 2.56 Å

for $HFe_3(CO)_{11}^-$: 2.68, 2.70 and 2.58 Å

for $Fe_3(CO)_{11}P(C_6H_5)_3$ (two isomers per asymmetric unit): 2.70, 2.67 and 2.57 Å for one isomer and 2.70, 2.71 and 2.56 Å for the other isomer.

The average Fe-C and C-O bond distances in Table 12 average 1.80 and 1.12 Å respectively. These Fe-C and C-O bond distances may be compared with the average Fe-C and

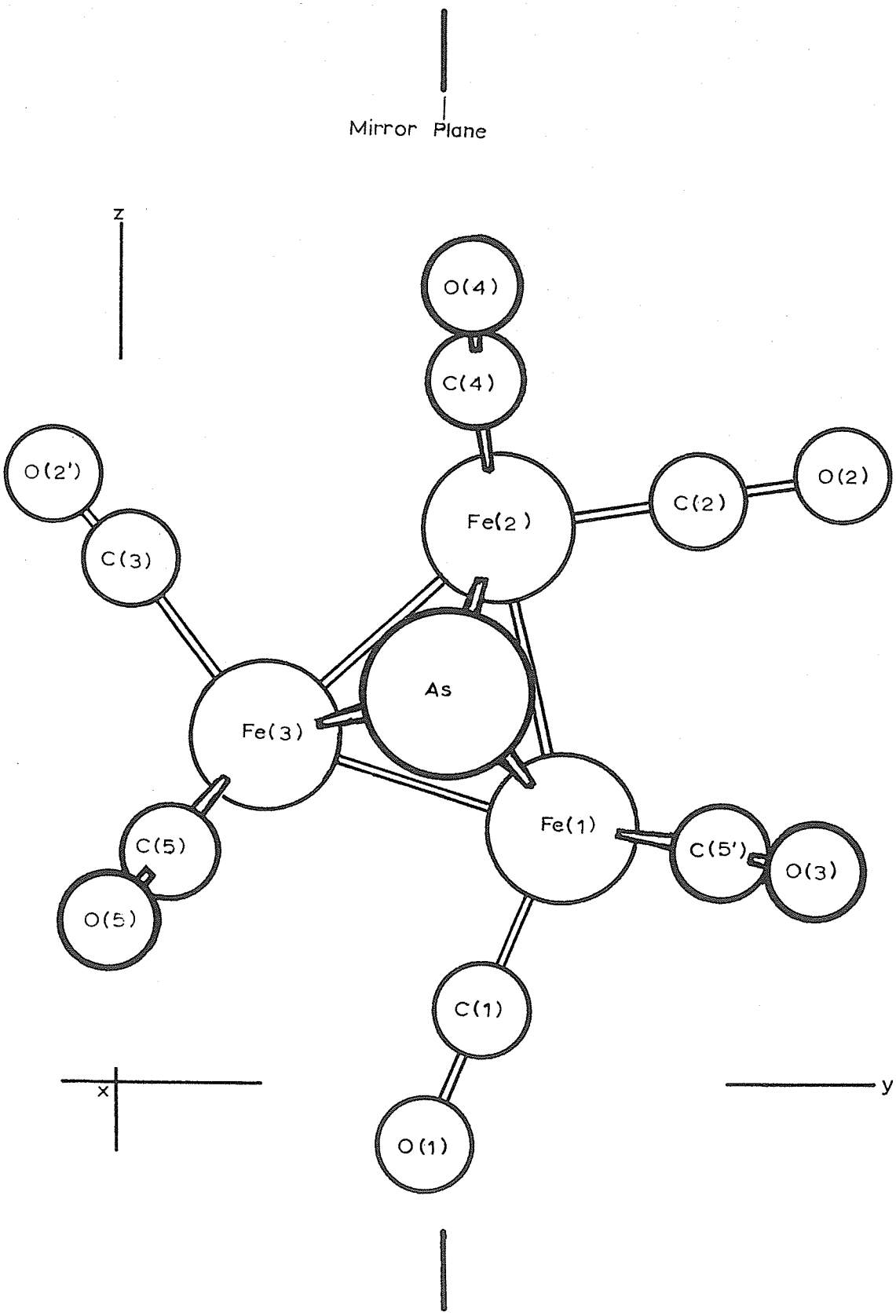

Fig. 37. Projection of the molecule along the x-axis of the unit cell.

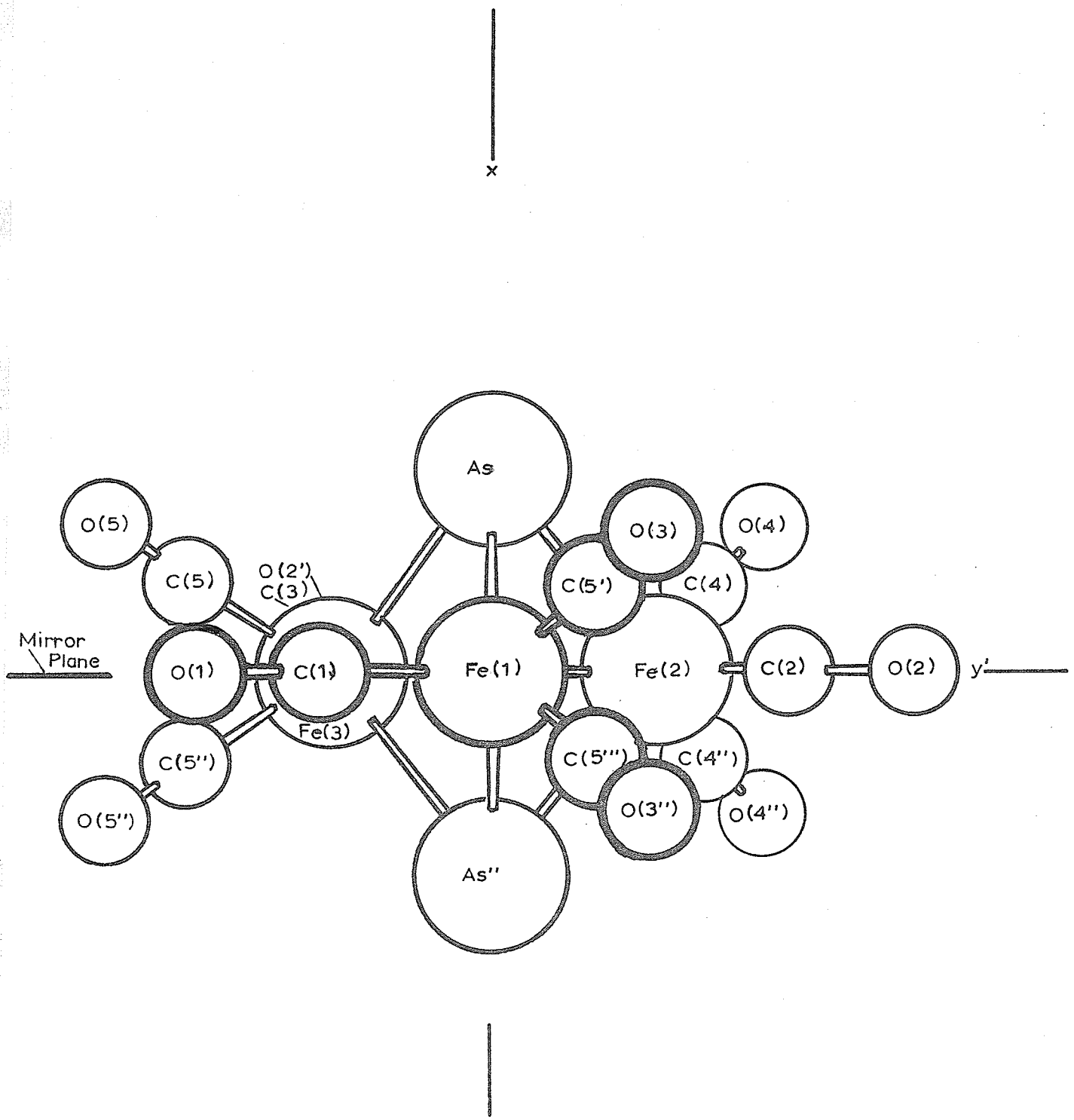

Fig. 38. Projection of the molecule along the line in common with the plane through As, Fe(1) and As'' and also the plane at X = 0 .

C-O bond distances of 1.79 and 1.12 Å respectively obtained in the crystal structure determination of $Fe(CO)_5$ by Donohue and Caron (1964). These values may also be compared with the average Fe-C bond distance of 1.82 Å and the average C-O bond distance of 1.14 Å obtained in the structure of $Fe(CO)_5$ by Beagley et al. (1969) by electron diffraction.

The C-Fe-C bond angles in $Fe_3As_2(CO)_9$ average 94.8° and the Fe-C-O bond angles average 177.0° (Table 12). These values may be compared with the average C-Fe-C and Fe-C-O bond angles of 99.0° and 178.3° respectively, in the crystal structure determination of $Fe(CO)_3C_4H_6$ by Mills and Robinson (1963).

The idealized molecular symmetry of $Fe_3As_2(CO)_9$ can be seen to be $3/m(C_{3h})$ by an examination of Fig. 37. A few individual bond distances and angles in Table 12 vary somewhat from the average values. However, a more accurate value of these bond distances would probably be an average over the idealized $3/m(C_{3h})$ symmetry.

The π-cyclopentadienyl(triethylphosphine)copper(I) crystal structure may be compared with that of $Fe_3As_2(CO)_9$. Crystals of the latter are much more stable than those of the former. The crystal of $Fe_3As_2(CO)_9$ which was used for the intensity collection, remained intact after the X-ray photographs were taken. However, the crystal of $\pi\text{-}C_5H_5CuP(C_2H_5)_3$ which was used for the intensity

collection, decomposed soon after all the photographs were taken. In the crystal structure of $Fe_3As_2(CO)_9$, the disorder is due to this large molecule assuming a random distribution in one of two orientations which are related to one another by a two-fold axis (or a mirror plane). In the crystal structure of π-$C_5H_5CuP(C_2H_5)_3$, the disorder is due to the few non-identical carbon atoms of two enantiomers which are distributed randomly throughout the crystal. The $Fe_3As_2(CO)_9$ molecule has oxygen atoms at its outer portions and is more rigid than the π-$C_5H_5CuP(C_2H_5)_3$ molecule which has hydrogen atoms at its outer regions.

APPENDIX I

Calculation of the U_{ij}'s and the eigenvalues and the eigenvectors of the thermal ellipsoid of vibration from the B_{ij} anisotropic thermal parameters of an atom.

The following statements are added to the NRC-12 Bond Scan Program after the numbered computer cards (numbered in columns 77-80).

The statements following computer card 110 are:

```
      DIMENSION  BIJ(20,6),U(20,6),TENS(6),VECT(9),AD(3,3),UADT(3,3)
      DIMENSION  NM(20)
```

The statement following computer card 870 is:

```
      SINB=SINA(2)
```

The statements following computer card 1210 are:

```
      READ(READR,9008) SYMNO(I),SYMBOL(I),ATOMNO(I),(XO(I,J),J=1,3),
     1NM(I)
      NM(I)=NM(I)-1
      NN=NM(I)
```

where the computer cards 1220, 1230, 1260 and 1270 are removed.

The statements following computer card 1250 are:

```
      IF(NUM) 18,19,18
   18 READ(READR,9009) (SYGX(I,J),J=1,3)
   19 IF(NM(I)) 21,21,20
   20 READ(READR,9010) (BIJ(I,L),L=1,6)
 9010 FORMAT(20X,6F10.5)
      U(I,1)=(BIJ(I,1)*A*A*SINB*SINB)/(2.*9.8696)
      U(I,2)=(BIJ(I,2)*B*B)/(2.*9.8696)
      U(I,3)=(BIJ(I,3)*C*C*SINB*SINB)/(2.*9.8696)
      U(I,4)=(BIJ(I,4)*B*C*SINB)/(4.*9.8696)
      U(I,5)=(BIJ(I,5)*A*C*SINB*SINB)/(4.*9.8696)
      U(I,6)=(BIJ(I,6)*A*B*SINB)/(4.*9.8696)
```

The statements following computer card 1840 are:

```
      WRITE(PRINTR,9012)
 9012 FORMAT(' ATOM NO.          B11        B22        B33        B23
     1B13        B12')
      DO 91 I=1,NATOMS
      IF(NM(I)) 91,91,94
   94 WRITE(PRINTR,9011) SYMBOL(I),ATOMNO(I),(BIJ(I,J),J=1,6)
```

```
 9011 FORMAT(' ',A4,I4,4X,6F10.5)
   91 CONTINUE
      WRITE(PRINTR,9013)
 9013 FORMAT(' ATOM NO.          U11        U22        U33        U23
     1U13        U12')
      DO 92 I=1,NATOMS
      IF(NM(I)) 92,92,95
   95 WRITE(PRINTR,9011) SYMBOL(I),ATOMNO(I),(U(I,K),K=1,6)
   92 CONTINUE
      AD(1,1)=1./SINA(2)
      AD(1,2)=0.0
      AD(1,3)=COSA(2)/SINA(2)
      AD(2,1)=0.0
      AD(2,2)=1.
      AD(2,3)=0.0
      AD(3,1)=0.0
      AD(3,2)=0.0
      AD(3,3)=1.
      DO 93  I=1,NATOMS
      IF(NM(I)) 93,93,96
   96 UADT(1,1)=U(I,1)*AD(1,1)+U(I,6)*AD(1,2)+U(I,5)*AD(1,3)
      UADT(1,2)=U(I,1)*AD(2,1)+U(I,6)*AD(2,2)+U(I,5)*AD(2,3)
      UADT(1,3)=U(I,1)*AD(3,1)+U(I,6)*AD(3,2)+U(I,5)*AD(3,3)
      UADT(2,1)=U(I,6)*AD(1,1)+U(I,2)*AD(1,2)+U(I,4)*AD(1,3)
      UADT(2,2)=U(I,6)*AD(2,1)+U(I,2)*AD(2,2)+U(I,4)*AD(2,3)
      UADT(2,3)=U(I,6)*AD(3,1)+U(I,2)*AD(3,2)+U(I,4)*AD(3,3)
      UADT(3,1)=U(I,5)*AD(1,1)+U(I,4)*AD(1,2)+U(I,3)*AD(1,3)
      UADT(3,2)=U(I,5)*AD(2,1)+U(I,4)*AD(2,2)+U(I,3)*AD(2,3)
      UADT(3,3)=U(I,5)*AD(3,1)+U(I,4)*AD(3,2)+U(I,3)*AD(3,3)
      TENS(1)=AD(1,1)*UADT(1,1)+AD(1,2)*UADT(2,1)+AD(1,3)*UADT(3,1)
      TENS(2)=AD(1,1)*UADT(1,2)+AD(1,2)*UADT(2,2)+AD(1,3)*UADT(3,2)
      TENS(3)=AD(2,1)*UADT(1,2)+AD(2,2)*UADT(2,2)+AD(2,3)*UADT(3,2)
      TENS(4)=AD(1,1)*UADT(1,3)+AD(1,2)*UADT(2,3)+AD(1,3)*UADT(3,3)
      TENS(5)=AD(2,1)*UADT(1,3)+AD(2,2)*UADT(2,3)+AD(2,3)*UADT(3,3)
      TENS(6)=AD(3,1)*UADT(1,3)+AD(3,2)*UADT(2,3)+AD(3,3)*UADT(3,3)
      MO=3
      MV=0
      CALL EIGEN(TENS,VECT,MO,MV)
      WRITE(PRINTR,9014) SYMBOL(I),ATOMNO(I),(TENS(J),J=1,6),
     1(VECT(K),K=1,9)
 9014 FORMAT(' ',A4,I4,/' '6F10.5,/' '9F10.5)
   93 CONTINUE
```

The preceeding statements are the modifications made by the author to the NRC-12 Bond Scan program. These modifications employ the EIGEN subroutine of the I.B.M. Scientific Subroutine Package.

APPENDIX II

Calculation of the rescale factors for the levels and the re-cycling of the NRC-10 Structure Factor Least Squares program.

The following calculations apply to the h0ℓ to h9ℓ levels of a crystal. Slight alterations are necessary to apply the method to levels of a crystal axis other than the b axis.

The quantity minimized in the calculation of the rescale factors is $S = \sum_k \sum_{h,\ell} (P_k |F_o|_{hk\ell} - |F_c|_{hk\ell})^2$, where P_k is the scale factor that the k^{th} level is multiplied by to bring it onto the same scale as the other k levels.

For a minimum,

$$\frac{\partial S}{\partial P_k} = 0 = \sum_{h,\ell} \left[2(P_k |F_o|_{hk\ell} - |F_c|_{hk\ell}) |F_o| \right],$$

where k = 0,1,2...9

$$P_k \sum_{h,\ell} |F_o|^2_{hk\ell} = \sum_{h,\ell} |Fc|_{hk\ell} \, |F_o|_{hk\ell}$$

$$P_k = \frac{\sum_{h,\ell} |F_c|_{hk\ell} |F_o|_{hk\ell}}{\sum_{h,\ell} |F_o|^2_{hk\ell}}$$

for each k level.

The computer cards containing the indices of reflection which are read into the NRC-2 Data Reduction program must be arranged so that the levels are in descending order i.e. from levels 9,8,.....to 0.

The following statements are added to the NRC-10 Structure Factor Least Squares program to re-cycle the program, to calculate the rescale factors and to apply these factors only after the first cycle.

The statements following computer card 30 are:

```
      DIMENSION TOP(20),DEN(20),P(20)
      INTEGER  VL
```

In the statements following computer card 960, NTYM is the number of consecutive cycles of least squares desired and NLVL is the number of levels (10).

The first data card must contain the values of NTYM AND NLVL:

```
      KTYM = 1
      READ(READR,9) NTYM,NLVL
  777 WRITE(PRINTR, 1) NPAGE
      LV=0
      VL=0
      DO 949 M=1,NLVL
      TOP(M)=0.0
  949 DEN(M)=0.0
      LMAX=NLVL
      MLAX=NLVL
```

The statements following computer card 1280 are:

```
      IF(KTYM - 1) 778,778,779
  779 SCALE = SCALEP
  778 XFTH = XFTH*XFTH
```

The statements following computer card 5080 are:

```
      IF(QRS) 810,810,811
  810 QRS=0.0
      IQ=0
      GO TO 249
  811 CONTINUE
```

The statements following computer card 5930 are:

```
  950 IF(LMAX-IK) 951,300,951
  951 LMAX=LMAX-1
      LV=LV + 1
      GO TO 950
  300 IF(IEXCL) 952,952,303
  952 TOP(LV)=TOP(LV) + ABS(AMPL(4))*ABS(AMPL(1))
      DEN(LV)=DEN(LV) + AMPL(1)*AMPL(1)
      GO TO 261
```

The statements following computer card 6280 are:

```
    DO 953 M=1,NLVL
953 P(M)=TOP(M)/DEN(M)
    WRITE(PRINTR,954) (P(M),M=1,NLVL)
954 FORMAT(' LEVEL SCALES ARE',10F10.3)
```

The statements following computer card 6760 are:

```
    IF(KTYM - 1)  970,971,970
971 AMPL(1) = AMPL(1)*P(VL)
970 CONTINUE
```

The statements following computer card 6970 are:

```
    IF(KTYM - NTYM) 781, 780, 780
781 KTYM = KTYM + 1
    GO TO 777
780 WRITE(PRINTR, 29)
```

The statements following computer card 8290 are:

```
    IF(BISO(IR)) 900,900,901
900 BISO(IR)=0.0
901 CONTINUE
```

The statements following computer card 8350 are:

```
    IF(B11(IR)) 800,800,801
800 B11(IR)=0.0
801 CONTINUE
```

The statements following computer card 8360 are:

```
    IF(B22(IR)) 802,802,803
802 B22(IR)=0.0
803 CONTINUE
```

The statements following computer card 8370 are:

```
    IF(B33(IR)) 804,804,805
804 B33(IR)=0.0
805 CONTINUE
```

The preceeding statements are modifications, to the NRC-10 S.F.L.S. program, made by the author.

APPENDIX III

Full matrix revision of NRC-10 by the author.

```
C     CRYSTALLOGRAPHIC PROGRAM NO.10. STRUCTURE FACTOR LEAST SQUARES
C     BLOCK DIAGONAL. FIRST VERSION.   (AHMED, APRIL 1966)
C     FULL MATRIX REVISION.       ( DELBAERE,MCBRIDE    1968 )
C
      DIMENSION  F(10),FD(10),AF(10),AFD(10),NREF(10)
      DIMENSION  DFM(125),VECT(125),SUM(8000)
      DIMENSION TOP(20),DEN(20),P(20)
      INTEGER  VL
      INTEGER  READR,PRINTR,TYPEWR,TAPEA,TAPEB,TAPEC,FST,PUNCH
      INTEGER  TITLE(20), LISTA(12),SERA(12),LISTB(12),SERB(12)
      INTEGER  SERLA,SERLB,CENTRE,SYSTEM,R(3,3,24),CENT(16),NPOS(16)
      INTEGER  MATCES(24,16),W(32),SERL
      INTEGER  SYMN(35),SYMB(35),ATOMN(35),VIB(35),INDTRS(35),CRV(35)
      INTEGER  SYMBOL(10),ORDIND,PARITY,ICODEP( 9),ICOM(10)
      INTEGER  PHI,ANOMLS,CS(1280),SYM,SSYMB(20),SATOM(20),SIND(200)
      REAL     LAMBDA,GQT(9), T(3,24),EXPL(201),HS(9,24),JRS
      REAL     X(35),Y(35),Z(35),SX(35),SY(35),SZ(35),BISO(35)
      REAL     B11(35),B22(35),B33(35),B23(35),B13(35),B12(35),OCCFR(35)
      REAL     CONST(90),A(300),C(300),B(300),D(300),TPHS(3,24)
      REAL     AMPL(10),FF(10),TS(24),SHIFT(10),SYGMA(10),DF(10)
      EQUIVALENCE (AMPL(9),BC),(FO,AMPL(1)),(XNET,AMPL(5))
      EQUIVALENCE (AMPL(4),FC),(AMPL(6),AO),(AMPL(7),BO),(AMPL(8),AC)
    1 FORMAT('1PROGRAM NO.10, STRUCTURE FACTOR LEAST SQUARES',78X,
     1'PAGE',I4)
    2 FORMAT(20A4)
    3 FORMAT('0',20A4)
    4 FORMAT(6X,2I2,3(I3,I7),2I5)
    5 FORMAT('0IDENTIFICATION OF RESULTS TAPE IS',I11)
    6 FORMAT('0MOUNT INPUT TAPE(S)')
    7 FORMAT('0IDENTIFICATION OF INPUT TAPE IS',I13)
    8 FORMAT('0WRONG TAPE MOUNTED, TRY AGAIN AND CONTINUE')
    9 FORMAT(3I2,12X,I2,12(1X,I2,I2))
   10 FORMAT('0JOB NO.=',I3,/'0DIRECTORY OF RESULTS TAPE. SERIAL NO.',
     1I4,/'0',5X,'LIST NO.',3X,'SERIAL NO.'/)
   11 FORMAT(3I2,14X,2I5)
   12 FORMAT('0IDENTIFICATION OF DUMP TAPE IS',I14)
   14 FORMAT(6X,I4,2X,A4,I4,3F10.5,F10.3,2I5,F5.3)
   15 FORMAT(12X,A4,I4,6F10.5)
   16 FORMAT('0DIRECTORY CARD IS OUT OF ORDER')
   17 FORMAT('0JOB TERMINATED BY PROGRAM NO.10, SAVE INPUT AND OUTPUT TA
     1PES')
   18 FORMAT(10X,I2,I3,1X,9I1,2F5.2,F5.0,F5.3,I5,3F5.2,I5,F10.4)
   19 FORMAT(9X,I2,9X,I2)
   20 FORMAT('0PARAMETERS LIST IS OUT OF ORDER')
   21 FORMAT('0LIST NO.',I4,' ON TAPE IS OUT OF ORDER')
   22 FORMAT('0SYMBOL FOR ATOM NO.',I4,'  IS INCORRECT')
   23 FORMAT(6X,3I4,    I2,7X,F8.2,40X,F5.3)
   24 FORMAT(1X,4I5,F10.4,2F10.2)
   25 FORMAT(1X,4I5,F10.4,6F10.2)
   26 FORMAT('+',22X,'*')
   27 FORMAT('1',20A4,42X,'PAGE',I4,/'0     H     K     L    INDR  SIN SQ
```

```
     1  F OBS     F CALC      A OBS      B OBS     A CALC     B CALC      DEL
     2F    100(DEL F)/FO'/)
    28 FORMAT('0SUM F OBS =',F12.2,9X,' SUM F CALC=',F12.2,9X,'SUM DELTA
     1F=',F12.2,/'0R-INDEX=',F8.4,9X,'VALUE OF SCALE K EMPLOYED=',F8.4)
    29 FORMAT('0END OF JOB. DISMOUNT AND SAVE INPUT AND OUTPUT TAPES')
    30 FORMAT(10X,F5.3,13I5)
    31 FORMAT(12X,A4,I4,10I1)
    40 FORMAT('0NEW SCALE=',F9.4,9X,'SUM (W.DF)SQ=',F15.4,/'0NO. OF REFLE
     1CTIONS INCLUDED IN L.S. SUMS=',I6)
    41 FORMAT('1',20A4,14X,'SHIFTS',22X,'PAGE',I4)
    42 FORMAT('1',20A4,7X,'STARTING PAR.S. SERIAL NO.=',I3,5X,'PAGE',I4)
    43 FORMAT('1',20A4,7X,'NEW PARAMETERS. SERIAL NO.=',I3,5X,'PAGE',I4)
    44 FORMAT('0SYM.  SYMBOL NO.    X/A        Y/B        Z/C        B ISO.
     1  OCC.FR.    B11        B22        B33        B23        B13        B12'
     2/)
    45 FORMAT(' ',I3,5X,A4,I4,11F10.5)
    46 FORMAT(17X,11F10.5)
    47 FORMAT(3I2,' PARAMETERS    ',2I5)
    48 FORMAT(2(3I2,I4,2X,A4,I4,3F10.5,F10.3,2I5,F5.3,/))
    49 FORMAT(3I2,I4,2X,A4,I4,6F10.5)
    51 FORMAT('0PLEASE MAKE THE TAPE ON UNIT',I4,' AVAILABLE FOR OUTPUT')
    52 FORMAT('0RESULTS ARE DUMPED ON TAPE. DUMP NO.=',I4,4X,' SFO,SFC,SD
     1ELF,R=',3F10.2,F8.4,/)
    53 FORMAT('+',90X,F10.2,F10.1)
    54 FORMAT('0NO. OF AMPLITUDES MUST BE 5 OR 9')
    55 FORMAT('0NO. OF ATOMS, ATOMIC PARAMETERS, A(I,J) ELEMENTS TO BE CO
     1MPUTED =',3I10)
    56 FORMAT('0ATOMS IN SPECIAL POSITIONS ARE',/'0ATOM   NO.   INDICATOR
     1S',/)
    57 FORMAT(' ',A4,I6,2X,10I2)
    60 FORMAT('0LIST, SERIAL, RECORDS, WORDS/RECORD =',4I5)
    61 FORMAT('+',65X,'DUMP NO.',I3,'  IS SKIPPED')
    62 FORMAT('0A11,A12,A22,B1,B2 =',5F16.4)
C                    ******************************************
      READR=5
      PRINTR=6
      TYPEWR=6
      PUNCH=7
      NPAGE=1
C     GENERATE EXPONENTIAL TABLE
      DO 100 I=1,201
  100 EXPL(I)=EXP(-0.05*(I-1))
C     READ TITLE AND DIRECTORY AND CHECK IDENTIFICATIONS
      KTYM = 1
      READ(READR,9) NTYM,NLVL
  777 WRITE(PRINTR, 1) NPAGE
      DO 838 I = 1,7
      F(I) = 0.0
      FD(I) = 0.0
      NREF(I) = 0.0
  838 CONTINUE
      LV=0
      VL=0
      DO 949 M=1,NLVL
```

```
      TOP(M)=0.0
  949 DEN(M)=0.0
      LMAX=NLVL
      MLAX=NLVL
      NPAGE=2
      READ(READR,2) TITLE
      WRITE(PRINTR,3) TITLE
      READ(READR,4) NTAPES,NMOUNT,TAPEA,IDA,TAPEC,IDC,TAPEB,IDB,FST,LAST
      IF(FST) 103,103,101
  101 WRITE(TYPEWR,6)
      WRITE(PRINTR,6)
  102 CONTINUE
  103 READ(TAPEA) IDT
      WRITE(PRINTR,7) IDT
      IF(IDA-IDT)  104,105,104
  104 WRITE(PRINTR,8)
      WRITE(TYPEWR,8)
      GO TO 780
  105 IF(NTAPES-1) 112,112,106
  106 READ(TAPEB) IDT
      WRITE(PRINTR,12) IDT
      IF(IDC-IDT) 104,113,104
  112 WRITE(PRINTR,12) IDC
  113 WRITE(PRINTR,5) IDB
      READ(READR,9) JOBB,LSTB,SERLB,NLISTB,(LISTB(I),SERB(I),I=1,12)
      IF(LSTB) 107,114,107
  114 WRITE(PRINTR,10) JOBB,SERLB
      WRITE(PRINTR,19) (LISTB(I),SERB(I),I=1,NLISTB)
C     READ SFLS DIRECTIVE CARDS
C     FIRST CARD
      READ(READR,18) ISER,JSER,IPAR,ILS,ILHS,IPRINT,ITAPE,IOBS,IUNOBS,
     1ISINSQ,IPLANE,XFO,XFTH,THRESH,SINSQM,NW,P1,P2,P3,NSPECL,SCALE
      IF(KTYM - 1)778,778,779
  779 SCALE = SCALEP
  778 XFTH = XFTH*XFTH
      ILS=ILS-1
      IPRINT=IPRINT-1
      IOBS=IOBS-1
      IUNOBS=IUNOBS-1
      ISINSQ=ISINSQ-1
      P1 = P1/SCALE
      P2 = P2/SCALE
      P3 = P3/SCALE
C     SECOND CARD
      READ(READR,30) FUDGE,NPESD,NDUMP,NRFLD,NAMPLP,(ICODEP(I),I=1,9)
      IF(NAMPLP-5) 115,117,116
  116 IF(NAMPLP-9) 115,117,115
  115 WRITE(PRINTR,54)
      GO TO 108
  117 IF(NSPECL) 400,400,118
C     READ SFLS 3 DIRECTIVE CARDS
  118 WRITE(PRINTR,56)
      DO 128 I=1,NSPECL
      K=10*I
```

```
      J=K-9
      READ(READR,31) SSYMB(I),SATOM(I),(SIND(L),L=J,K)
  128 WRITE(PRINTR,57) SSYMB(I),SATOM(I),(SIND(L),L=J,K)
      GO TO 400
C     ENTER WHEN ERRORS ARE DETECTED
  107 WRITE(PRINTR,16)
  108 REWIND TAPEA
      REWIND TAPEB
      REWIND TAPEC
      WRITE(PRINTR,17)
      CALL EXIT
  109 WRITE(PRINTR,21) LST
      GO TO 108
  110 WRITE(PRINTR,22) I
      GO TO 108
  400 WRITE(TAPEC) IDC
C
C     READ THE LISTS FROM INPUT TAPE
  119 READ(TAPEA) JOBA,LSTA,SERLA,NLISTA,(LISTA(I),SERA(I),I=1,12)
      IA=0
      IB=0
      WRITE(TAPEB) IDB
      WRITE(TAPEB) JOBB,LSTB,SERLB,NLISTB,(LISTB(I),SERB(I),I=1,12)
  120 IB=IB+1
  121 IA=IA+1
  125 READ(TAPEA) LST,SERL,NRCRD,NWORD
      IF (LST-4) 122,134,160
  122 WRITE(TAPEB) LST,SERB(IB),NRCRD,NWORD
      IF(LST-2) 127,129,132
C     TO SKIP A LIST
  123 DO 124 I=1,NRCRD
  124 READ(TAPEA)
      GO TO 121
C     UNITCELL (LIST 1)
  127 READ (TAPEA)  (W(I),I=1,6),LAMBDA,W(7),W(8)
      WRITE(TAPEB)  (W(I),I=1,6),LAMBDA,W(7),W(8)
      READ(TAPEA)  (W(I),I=1,NWORD)
      WRITE(TAPEB) (W(I),I=1,NWORD)
      READ (TAPEA)  (GQT(I),I=1,NWORD)
      WRITE(TAPEB)  (GQT(I),I=1,NWORD)
      READ (TAPEA)  (W(I),I=1,NWORD)
      WRITE(TAPEB)  (W(I),I=1,NWORD)
      GO TO 120
C     SYMMETRY (LIST 2)
  129 READ (TAPEA)  NMATX,NSYM,CENTRE,LAT,SYSTEM
      WRITE(TAPEB)  NMATX,NSYM,CENTRE,LAT,SYSTEM,I,I,I,I,I,I,I,I
      DO 130 K=1,NMATX
      READ(TAPEA)  MATNO,((R(I,J,K),I=1,3),J=1,3),(T(I,K),I=1,3)
  130 WRITE(TAPEB) MATNO,((R(I,J,K),I=1,3),J=1,3),(T(I,K),I=1,3)
      DO 131 K=1,NSYM
      READ (TAPEA)  CENT(K),NPOS(K),(MATCES(M,K),M=1,11)
      WRITE(TAPEB)  CENT(K),NPOS(K),(MATCES(M,K),M=1,11)
      READ (TAPEA)  (MATCES(M,K),M=12,24)
  131 WRITE(TAPEB)  (MATCES(M,K),M=12,24)
```

```
      GO TO 120
C     FORMFACTORS (LIST 3)
  132 DO 133 K=1,NRCRD
      READ (TAPEA)  (W(I),I=1,NWORD)
  133 WRITE(TAPEB)  (W(I),I=1,NWORD)
      IF(IPAR)  120,120,141
C     PARAMETERS  (LIST 4)
  134 IF(SERL-ISER)  123,136,123
  136 WRITE(TAPEB)  LST,SERL,NRCRD,NWORD
      DO 137 K=1,NRCRD
      READ (TAPEA)  SYMN(K),SYMB(K),ATOMN(K),X(K),Y(K),Z(K),SX(K),SY(K),
     1 SZ(K),   BISO(K),VIB(K),INDTRS(K),B11(K),B22(K),B33(K),
     2B23(K),B13(K),B12(K),OCCFR(K)
  137 WRITE(TAPEB)  SYMN(K),SYMB(K),ATOMN(K),X(K),Y(K),Z(K),SX(K),SY(K),
     1 SZ(K),   BISO(K),VIB(K),INDTRS(K),B11(K),B22(K),B33(K),
     2B23(K),B13(K),B12(K),OCCFR(K)
      NATOM=NRCRD
      GO TO 120
C     TO READ LIST 4 FROM CARDS
  141 READ (READR,11)  JOB,LST,SERL,NATOM,ISYGMA
      IF(LST-4)  142,144,142
  142 WRITE (PRINTR,20)
      GO TO 108
  144 NRCRD=NATOM
      NWORD=19
      WRITE(TAPEB)  LST,SERL,NRCRD,NWORD
      DO 150 K=1,NATOM
      READ(READR,14)  SYMN(K),SYMB(K),ATOMN(K),X(K),Y(K),Z(K),BISO(K),
     1VIB(K),INDTRS(K),OCCFR(K)
      IF(OCCFR(K)) 139,138,139
  138 OCCFR(K)=1.0
  139 IF(ISYGMA)  146,146,145
  145 READ (READR,14)  W(1),W(2),W(3),SX(K),SY(K),SZ(K)
      IF(ATOMN(K)-W(3)) 142,147,142
  146 SX(K)=0.
      SY(K)=0.
      SZ(K)=0.
  147 IF(VIB(K)-1) 148,148,149
  148 B11(K)=0.
      B22(K)=0.
      B33(K)=0.
      B23(K)=0.
      B13(K)=0.
      B12(K)=0.
      GO TO 150
  149 READ(READR,15) W(1),W(2),B11(K),B22(K),B33(K),B23(K),B13(K),B12(K)
      IF(ATOMN(K)-W(2)) 142,150,142
  150 WRITE(TAPEB) SYMN(K),SYMB(K),ATOMN(K),X(K),Y(K),Z(K),SX(K),SY(K),
     1 SZ(K),   BISO(K),VIB(K),INDTRS(K),B11(K),B22(K),B33(K),
     2B23(K),B13(K),B12(K),OCCFR(K)
      IB=IB+1
      ISER=-ISER
      GO TO 120
C     COS AND SIN TABLE (LIST 5)
```

```
  160 N=1
      DO 161 K=1,NRCRD
      M=N+31
      READ(TAPEA)    (CS(L),L=N,M)
  161 N=M+1
      IA=IA+1
C     DERIVE LATTICE FACTOR AND SCALE
      GO TO(171,172,173,174,172,172,172,173),LAT
  171 TEMP=1.0
      GO TO 175
  172 TEMP=2.0
      GO TO 175
  173 TEMP=3.0
      GO TO 175
  174 TEMP=4.0
  175 GM=TEMP/SCALE
C     RESET INDICATORS AND SUMS
      SYSTEM=SYSTEM-4
      ONE=1.0
      RLSQ=1./(LAMBDA*LAMBDA)
      NCTRE=1
      BHKL=0.
      DHKL=0.
  170 NINCL=0
      SFO=0.
      SFC=0.
      SDF=0.
      SWDFSQ=0.
C     PLANES LIST (LIST 6)
  162 READ (TAPEA)  LST,SERL,NRCRD,NWORD
      IF(LST-6)  109,163,109
  163 READ(TAPEA) FOOO,NPLNS,I1,I2,I3,NAMPL,NCRVES,C1,C2,C3,(W(L),
     1L=1,NAMPL),(SYMBOL(N),N=1,NCRVES)
      NVEC = 125
      NSUM = NVEC*(NVEC+1)/2
      WRITE(PRINTR,520) NVEC,NSUM
  520 FORMAT(' NVEC',I10,' NSUM',I10)
      DO 517 J=1,NVEC
  517 VECT(J) = 0.0
      DO 518 I=1,NSUM
  518 SUM(I) = 0.0
  155 NREFL=NPLNS
  156 NELMNT=0
      MPAR=0
      LINES=0
      ISER=IABS(ISER)
      NWORD=11+NAMPLP+NCRVES
  159 NP=NREFL
  151 WRITE(TAPEC) LST,SERL,NP,NWORD
C     DERIVE CONSTANTS FOR THE ATOMS
      DO 181 I=1,NATOM
      IF(ATOMN(I)) 140,143,143
  140 NCTRE=0
  143 IF(LINES) 157,157,158
```

```
157 WRITE(PRINTR,42) TITLE,ISER,NPAGE
    NPAGE=NPAGE+1
    WRITE(PRINTR,44)
    LINES=50
158 J=1
    ISYMB=SYMB(I)
164 IF(ISYMB-SYMBOL(J)) 165,166,165
165 J=J+1
    IF(J-NCRVES) 164,164,110
166 CRV(I)=J
    K=SYMN(I)
    IF(CENT(K)) 167,167,168
167 CONST(I)=GM*OCCFR(I)
    GO TO 169
168 CONST(I)=GM*OCCFR(I)*2.
169 MPAR=MPAR+INDTRS(I)
    IF(INDTRS(I)-9+ILS) 176,177,176
176 NELMNT=NELMNT+INDTRS(I)*(INDTRS(I)+1)/2
    GO TO 178
177 NELMNT=NELMNT+27
178 IF(VIB(I)-1) 181,180,181
180 VIB(I)=2
    BP=BISO(I)*RLSQ
    B11(I)=BP*GQT(1)
    B22(I)=BP*GQT(5)
    B33(I)=BP*GQT(9)
    B23(I)=BP*GQT(6)*2.0
    B13(I)=BP*GQT(3)*2.0
    B12(I)=BP*GQT(2)*2.0
    LINES=LINES-1
181 WRITE(PRINTR,45) SYMN(I),ISYMB,ATOMN(I),X(I),Y(I),Z(I),BISO(I),
   1OCCFR(I),B11(I),B22(I),B33(I),B23(I),B13(I),B12(I)
    WRITE(PRINTR,55) NATOM,MPAR,NELMNT
    WRITE(PRINTR,27) TITLE,NPAGE
    LINES=50
    NPAGE=NPAGE+1
    IF(IPLANE) 200,200,182
182 READ(READR,23)  NIH,NIK,NIL,INDRP,FOPP,WHKLP
    GO TO 200
183 IF(IH-NIH) 201,184,201
184 IF(IK-NIK) 201,185,201
185 IF(IL-NIL) 201,186,201
186 IF(INDRP-1) 193,193,192
192 IEXCL=1
    GO TO 195
193 INDR=INDRP
195 IF(FOPP) 196,197,196
196 FO=FOPP
197 IF(WHKLP) 198,194,198
198 WHKL=WHKLP
194 READ(READR,23) NIH,NIK,NIL,INDRP,FOPP,WHKLP
    IF(NIH-99) 201,188,188
188 IPLANE=0
    GO TO 201
```

```
C       TO EXCLUDE THE UNOBSERVED REFLECTIONS
  190 IF(INDR) 215,215,191
  191 AMPL(4)=0.
      IEXCL=1
      GO TO 299
C       READ THE RECORD FOR ONE PLANE
  200 READ (TAPEA)  IH,IK,IL,INDR,JSIGN,ORDIND,PARITY,MULT,SINSQ,WHKL,
     1(AMPL(M),M=1,NAMPL),(FF(M),M=1,NCRVES)
      IEXCL=0
      AMPL(2)=AMPL(3)
      AMPL(3)=AMPL(4)
      IF(IPLANE)  183,201,183
  201 IF(ISINSQ) 206,206,207
  207 IF(SINSQ-SINSQM) 191,206,206
  206 IF(IUNOBS) 190,215,215
C       COMPUTE THE EQUIVALENT INDICES
  215 DO 209 K=1,NMATX
  202 IF(SYSTEM) 205,203,203
  203 DO 204 J=1,3
  204 HS(J,K)=IH*R(1,J,K)+IK*R(2,J,K)+IL*R(3,J,K)
      GO TO 208
  205 HS(1,K)=IH*R(1,1,K)
      HS(2,K)=IK*R(2,2,K)
      HS(3,K)=IL*R(3,3,K)
  208 TS(K)=IH*T(1,K)+IK*T(2,K)+IL*T(3,K)
      HS(4,K)=HS(1,K)*HS(1,K)
      HS(5,K)=HS(2,K)*HS(2,K)
      HS(6,K)=HS(3,K)*HS(3,K)
      HS(7,K)=HS(2,K)*HS(3,K)
      HS(8,K)=HS(1,K)*HS(3,K)
      HS(9,K)=HS(1,K)*HS(2,K)
      TPHS(1,K)=HS(1,K)*6.283185
      TPHS(2,K)=HS(2,K)*6.283185
  209 TPHS(3,K)=HS(3,K)*6.283185
      SINSQP=SINSQ*RLSQ
      AHKL=0.
      CHKL=0.
      INDX=1
      IF(CENTRE) 211,210,211
  210 BHKL=0.
      DHKL=0.
C
C       CALCULATE CONTRIBUTIONS TO THE STRUCTURE FACTORS
  211 DO 260 IR=1,NATOM
      IF(ATOMN(IR)) 212,213,213
  212 ANOMLS=1
      GO TO 214
  213 ANOMLS=0
  214 IF(VIB(IR)) 221,221,224
  221 QRS=BISO(IR)*SINSQP
      IQ=QRS*20.0
      IF(IQ-200) 223,223,222
  222 IQ=200
  223 XQ=QRS-IQ*0.05
```

```
      TX=EXPL(IQ+1)*(1.-XQ*(1.-0.5*XQ))
  224 I=CRV(IR)
      FFR=FF(I)*CONST(IR)
      IF(ANOMLS) 226,226,225
  225 FFI=FF(I+1)*CONST(IR)
  226 SYM=SYMN(IR)
      N=NPOS(SYM)
      DO 254 MTX=1,N
      IS=MATCES(MTX,SYM)
      ANGLE=HS(1,IS)*X(IR)+HS(2,IS)*Y(IR)+HS(3,IS)*Z(IR)+TS(IS)
C     COS AND SIN ROUTINE
  231 PHI=ANGLE
      IF(ANGLE) 232,235,233
  232 PHI=10000.*(ANGLE+1.00005-PHI)
      GO TO 234
  233 PHI=10000.*(ANGLE+0.00005-PHI)
  234 NN=(PHI+1250)/1250
      GO TO(237,238,239,240,241,242,243,244),NN
  235 FCOS=1.0
      FSIN=0.0
      GO TO 246
  237 K=PHI+1
      ICOS=CS(K)/10000
      ISIN=CS(K)-10000*ICOS
      GO TO 245
  238 K=2501-PHI
      ISIN=CS(K)/10000
      ICOS=CS(K)-10000*ISIN
      GO TO 245
  239 K=PHI-2499
      ISIN=CS(K)/10000
      ICOS=10000*ISIN-CS(K)
      GO TO 245
  240 K=5001-PHI
      ICOS=CS(K)/(-10000)
      ISIN=CS(K)+10000*ICOS
      GO TO 245
  241 K=PHI-4999
      ICOS=CS(K)/(-10000)
      ISIN=(-10000)*ICOS-CS(K)
      GO TO 245
  242 K=7501-PHI
      ISIN=CS(K)/(-10000)
      ICOS=(-10000)*ISIN-CS(K)
      GO TO 245
  243 K=PHI-7499
      ISIN=CS(K)/(-10000)
      ICOS=CS(K)+10000*ISIN
      GO TO 245
  244 K=10001-PHI
      ICOS=CS(K)/10000
      ISIN=10000*ICOS-CS(K)
  245 FCOS=FLOAT(ICOS)*0.0001
      FSIN=FLOAT(ISIN)*0.0001
```

```
  246 IF(VIB(IR)) 250,250,247
  247 QRS=HS(4,IS)*B11(IR)+HS(5,IS)*B22(IR)+HS(6,IS)*B33(IR)+HS(7,IS)*
     1B23(IR)+HS(8,IS)*B13(IR)+HS(9,IS)*B12(IR)
      IF(QRS) 810,810,811
  810 QRS=0.0
      IQ=0
      GO TO 249
  811 CONTINUE
      IQ=QRS*20.0
      IF(IQ-200) 249,249,248
  248 IQ=200
  249 XQ=QRS-IQ*0.05
      TX=EXPL(IQ+1)*(1.-XQ*(1.-0.5*XQ))
  250 FFT=FFR*TX
      A(INDX) =FFT*FCOS
      B(INDX)=FFT*FSIN
      IF(ANOMLS)  252,252,251
  251 FFT=FFI*TX
      C(INDX)=FFT*FCOS
      D(INDX)=FFT*FSIN
      CHKL=CHKL+C(INDX)
      IF(CENTRE) 252,230,252
  230 DHKL=DHKL+D(INDX)
  252 AHKL=AHKL+A(INDX)
      IF(CENTRE)  253,253,254
  253 BHKL=BHKL+B(INDX)
  254 INDX=INDX+1
  260 CONTINUE
      AFO=ABS(FO)
C     PHASE ANGLE
      IF(CENTRE) 256,256,255
  255 IF(NCTRE)  256,256,259
  256 AC=AHKL-DHKL
      BC=BHKL+CHKL
      FC=SQRT(AC*AC+BC*BC)
      AFC=FC
      CALPH=AC/FC
      SALPH=BC/FC
      IF(CENTRE)257,257,258
  257 AO=FO*CALPH
      BO=FO*SALPH
      GO TO 271
  258 FO=SIGN(FO,AHKL)
      FC=SIGN(FC,AHKL)
      GO TO 271
  259 FC=AHKL
      CALPH=SIGN(ONE,FC)
      SALPH=0.
      FO=SIGN(FO,FC)
      AFC=ABS(FC)
C     DELTA F ANALYSIS
  271 DELF=AFO-AFC
      ADELF=ABS(DELF)
      IF(ISINSQ) 278,277,277
```

```
  277 IF(SINSQ-SINSQM) 286,278,278
  278 IF (INDR) 281,281,272
C     UNOBSERVED REFLECTIONS
  272 IF(IUNOBS) 286,286,273
  273 IF(DELF) 274,286,286
  274 IF(ADELF-AFO-AFO) 290,290,286
C     OBSERVED REFLECTIONS
  281 IF(IOBS) 290,282,282
  282 IF(ADELF-XFO*AFO) 290,290,284
  284 IF(IOBS) 290,286,285
  285 FTHSQ=AFO*AFO*THRESH/XNET
      IF(DELF*DELF-XFTH*FTHSQ) 290,290,286
  286 IEXCL=1
C     OUTPUT OF THE STRUCTURE FACTORS ON THE PRINTER
  290 IF(IPRINT) 299,291,291
  291 FOP=SCALE*FO
      FCP=SCALE*FC
      ADELFP=SCALE*ADELF
  822 IF(ABS(FOP)- 20.) 823,823,824
  823 I = 1
      GO TO 829
  824 IF(ABS(FOP)- 40.) 825,825,826
  825 I = 2
      GO TO 829
  826 IF(ABS(FOP)- 70.) 827,827,828
  827 I = 3
      GO TO 829
  828 IF(ABS(FOP)- 100.) 830,830,831
  830 I = 4
      GO TO 829
  831 IF(ABS(FOP)- 140.) 832,832,833
  832 I = 5
      GO TO 829
  833 IF(ABS(FOP)- 190.) 834,834,835
  834 I = 6
      GO TO 829
  835 I = 7
  829 F(I) = ABS(FOP)+ F(I)
      FD(I) = ADELFP + FD(I)
      NREF(I) = NREF(I) + 1
      IF(AFO) 1292,1291,1292
 1291 RINDX=0.0
      GO TO 1293
 1292 RINDX=ADELF*100./AFO
 1293 IF(CENTRE) 293,293,292
  292 WRITE(PRINTR,24)  IH,IK,IL,INDR,SINSQ,FOP,FCP
      GO TO 294
  293 AOP=SCALE*AO
      BOP=SCALE*BO
      ACP=SCALE*AC
      BCP=SCALE*BC
      WRITE (PRINTR,25) IH,IK,IL,INDR,SINSQ,FOP,FCP,AOP,BOP,ACP,BCP
  294 IF(IEXCL) 298,298,295
```

```
  295 WRITE(PRINTR,26)
      GO TO 296
  298 WRITE(PRINTR,53) ADELFP,RINDX
  296 LINES=LINES-1
      IF(LINES) 297,297,299
  297 WRITE(PRINTR,27) TITLE,NPAGE
      NPAGE=NPAGE+1
      LINES=50
C     OUTPUT ON TAPE
  299 WRITE(TAPEC) IEXCL,IH,IK,IL,INDR,JSIGN,ORDIND,PARITY,MULT,SINSQ,
     1WHKL,(AMPL(M),M=1,NAMPLP),(FF(M),M=1,NCRVES)
  950 IF(LMAX-IH) 951,300,951
  951 LMAX=LMAX-1
      LV=LV + 1
      GO TO 950
  300 IF(IEXCL) 952,952,303
  952 TOP(LV)=TOP(LV) + ABS(AMPL(4))*ABS(AMPL(1))
      DEN(LV)=DEN(LV) + AMPL(1)*AMPL(1)
      GO TO 261
C     ACCUMULATE TOTALS FOR THE RESIDUALS
  301 SWDFSQ=WDELF*WDELF+SWDFSQ
      SFO=SFO+AFO
      SFC=SFC+AFC
      SDF=SDF+ADELF
      NINCL=NINCL+1
  303 NREFL=NREFL-1
  414 IF(NREFL) 305,305,200
  305 END FILE TAPEC
      DO 953 M=1,LV
  953 P(M)=TOP(M)/DEN(M)
      WRITE(PRINTR,954) (P(M),M=1,LV)
  954 FORMAT(' LEVEL SCALES ARE',10F10.3)
  304 REWIND TAPEA
      REWIND TAPEC
      SDSQ=SWDFSQ/(NINCL-NPESD)
      RINDX=SDF/SFO
      SFO=SCALE*SFO
      SFC=SCALE*SFC
      SDF=SCALE*SDF
      SWDSQ= SCALE*SCALE*SWDFSQ
      WRITE(PRINTR,28) SFO,SFC,SDF,RINDX,SCALE
      DO 837 I = 1,7
      AF(I) = F(I)/NREF(I)
      AFD(I) =  FD(I)/NREF(I)
      WRITE(PRINTR,836) I,AF(I),AFD(I),NREF(I)
  836 FORMAT(I2,' MEAN FO IS',F10.5,' MEAN DELTA F IS',F10.5,
     1' NO OF REFLECTIONS',I5)
  837 CONTINUE
      IF(ILS) 353,370,370
C     STORE COS AND SIN TABLE
  353 IF(ITAPE) 359,359,358
  358 NRCRD=40
      NWORD=32
      LST=5
```

```
      WRITE(TAPEB) LST,SERB(IB),NRCRD,NWORD
      N=1
      DO 354 I=1,40
      M=N+31
      WRITE(TAPEB) (CS(L),L=N,M)
  354 N=M+1
      IB=IB+1
C     STORE LIST 6
      SFO=0.
      SFC=0.
      SDF=0.
      NRC=NPLNS+1
      NWD=10+NAMPLP+NCRVES
      LST=6
      WRITE(TAPEB) LST,SERB(IB),NRC,NWD
      NREFL=NPLNS
      WRITE(TAPEB) FOOO,NPLNS,I1,I2,I3,NAMPLP,NCRVES,C2,C3,SCALE,
     1(ICODEP(I),I=1,NAMPLP),(SYMBOL(N),N=1,NCRVES)
      READ(TAPEC)
  341 READ(TAPEC) LST,SERL,NRCRD,NWORD
      WRITE(PRINTR, 60) LST,SERL,NRCRD,NWORD
      IF(LST-8) 355,342,342
  342 READ(TAPEC)
      GO TO 341
  355 DO 357 I=1,NRCRD
      READ(TAPEC) IEXCL,IH,IK,IL,INDR,JSIGN,ORDIND,PARITY,MULT,SINSQ,
     1WHKL,(AMPL(M),M=1,NAMPLP),(FF(M),M=1,NCRVES)
  958 IF(MLAX-IH) 955,956,955
  955 WRITE(PRINTR,71) IH
   71 FORMAT(' ',85X,'H=',I3/' ',83X,'K  L FOBS FCAL')
      MLAX=MLAX-1
      VL=VL+1
      GO TO 958
  956 IF(FO) 998,999,999
  998 IFO=(IFIX(SCALE*FO*20.-1.))/2
      IFC=(IFIX(SCALE*FC*20.-1.))/2
      GO TO 997
  999 IFO=(IFIX(SCALE*FO*20.+1.))/2
      IFC=(IFIX(SCALE*FC*20.+1.))/2
  997 CONTINUE
      IF(IEXCL) 967,356,967
  356 AFO=ABS(FO)*SCALEP
      WRITE(PRINTR,73) IK,IL,IFO,IFC
   73 FORMAT(' ',80X,I4,I3,2I5)
  348 AFC=ABS(FC)*SCALE
      SFO=SFO+AFO
      SFC=SFC+AFC
      SDF=SDF+ABS(AFO-AFC)
      GO TO 357
  967 WRITE(PRINTR,74) IK,IL,IFO,IFC
   74 FORMAT(' ',79X,'*',I4,I3,2I5)
  357 WRITE(TAPEB) IH,IK,IL,INDR,JSIGN,ORDIND,PARITY,MULT,SINSQ,
     1WHKL,(AMPL(M),M=1,NAMPLP),(FF(M),M=1,NCRVES)
```

```
      NREFL=NREFL-NRCRD
      IF(NREFL) 343,343,341
  343 RINDX=SDF/SFO
      WRITE(PRINTR,28) SFO,SFC,SDF,RINDX,SCALEP
  359 CONTINUE
      REWIND TAPEB
      REWIND TAPEC
      IF(KTYM - NTYM) 781, 780, 780
  781 KTYM = KTYM + 1
      GO TO 777
  780 WRITE(PRINTR, 29)
        CONTINUE
      CALL EXIT
C     WEIGHTING SCHEMES. ENTER IF REFLECTION IS INCLUDED IN LS SUMS
  261 GO TO (262,265,267,268,269),NW
  262 IF(AFO-P1) 263,263,264
  263 RTW=AFO/P1
      GO TO 270
  264 RTW=P1/AFO
      GO TO 270
  265 IF(AFO-P1) 266,266,264
  266 RTW=1.
      GO TO 270
  267 RTW=(AFO-P2)/P1
      RTW=1./SQRT(1.+RTW*RTW)
      GO TO 270
  268 RTW=1./SQRT(P1+AFO*(1.+AFO*(P2+AFO*P3)))
      GO TO 270
  269 RTW = 1./(1. + 0.169*ABS(FOP))
  270 WDELF=RTW*DELF
      IF(ILS) 301,311,311
C     PARTIAL DERIVATIVES WRT THE PARAMETERS
  311 IM=1
      IV=1
      INDX=1
      KT=1
      DFM(KT)= RTW*FCP
      ISPCL = 1
      ISIND = 1
      DO 334 IR=1,NATOM
      SYM=SYMN(IR)
      N=NPOS(SYM)
      IF(INDTRS(IR)) 310,310,312
  310 INDX=INDX+N
      GO TO 334
  312 NPAR=INDTRS(IR)
      DO 313 K=1,NPAR
  313 DF(K)=0.
      DO 327 MTX=1,N
      IS=MATCES(MTX,SYM)
      IF(ATOMN(IR)) 314,317,317
  314 IF(CENTRE) 315,315,316
C     ANOMALOUS AND NONCENTROSYMMETRIC
  315 GRS=(A(INDX)-D(INDX))*CALPH+(B(INDX)+C(INDX))*SALPH
```

```
      JRS=(B(INDX)+C(INDX))*CALPH-(A(INDX)-D(INDX))*SALPH
      GO TO 320
C     ANOMALOUS AND CENTROSYMMETRIC
  316 GRS=A(INDX)*CALPH+C(INDX)*SALPH
      JRS=B(INDX)*CALPH+D(INDX)*SALPH
      GO TO 320
  317 IF(CENTRE) 318,318,319
C     NON-ANOMALOUS AND NONCENTROSYMMETRIC
  318 GRS=A(INDX)*CALPH+B(INDX)*SALPH
      JRS=B(INDX)*CALPH-A(INDX)*SALPH
      GO TO 320
C     NON-ANOMALOUS AND CENTROSYMMETRIC
  319 GRS=A(INDX)*CALPH
      JRS=B(INDX)*CALPH
  320 DF(1)=DF(1)-TPHS(1,IS)*JRS
      DF(2)=DF(2)-TPHS(2,IS)*JRS
      DF(3)=DF(3)-TPHS(3,IS)*JRS
      IF(NPAR-9) 324,326,325
  324 DF(4)=DF(4)+GRS
      GO TO 327
  325 DF(10)=DF(10)+GRS
  326 DF(4)=DF(4)-HS(4,IS)*GRS
      DF(5)=DF(5)-HS(5,IS)*GRS
      DF(6)=DF(6)-HS(6,IS)*GRS
      DF(7)=DF(7)-HS(7,IS)*GRS
      DF(8)=DF(8)-HS(8,IS)*GRS
      DF(9)=DF(9)-HS(9,IS)*GRS
  327 INDX=INDX+1
      IF(NPAR-5) 329,328,330
  328 DF(5)=DF(4)/OCCFR(IR)
  329 DF(4)=-DF(4)*SINSQP
      GO TO 332
  330 IF(NPAR-9) 332,332,331
  331 DF(10)=DF(10)/OCCFR(IR)
  332 NU = NPAR
      NC = 1
      IF(NSPECL) 376,376,379
  379 IF(SYMB(IR)- SSYMB(ISPCL)) 376,380,376
  380 IF(ATOMN(IR) - SATOM(ISPCL)) 376,383,376
  383 DO 389 I=1,10
      ICOM(I) = SIND(ISIND)
  389 ISIND = ISIND + 1
      ISPCL = ISPCL + 1
      DO 500 I=1,NPAR
      IF(ICOM(I)) 501,502,501
  501 NC = NC + 1
      GO TO 500
  502 DO 504 K=NC,NPAR
  504 DF(K) = DF(K+1)
      NU = NU -1
  500 CONTINUE
  376 DO 333 J=1,NU
  333 DF(J) = DF(J)*RTW
      DO 335 I =1,NU
```

```
      KT = KT +1
  335 DFM(KT) = DF(I)
  334 CONTINUE
      IJ = 1
      DO 505 J=1,KT
      DO 506 I=1,J
      SUM(IJ) = SUM(IJ) + DFM(I)*DFM(J)
  506 IJ = IJ + 1
  505 VECT(J) = VECT(J) + DFM(J)*WDELF
      GO TO 301
  370 NT = 1
      EPS = 0.001
      CALL GELS(VECT,SUM,KT,NT,EPS,IER,DFM)
      WRITE(PRINTR,516) IER
  516 FORMAT(' IER =',I10)
      WRITE(PRINTR,515) VECT(1)
  515 FORMAT('0SCALE G CHANGE IS',F10.5)
      SCALEP = SCALE/(1. + VECT(1)*SCALE)
      WRITE(PRINTR,40) SCALEP, SWDSQ,NINCL
      ISIND = 1
      ISPCL=1
      IL = 1
      IK = 1
      LINES=0
      DO 390 IR = 1,NATOM
      IF(LINES) 377,377,378
  377 WRITE(PRINTR,41) TITLE,NPAGE
      NPAGE=NPAGE+1
      WRITE(PRINTR,44)
      LINES=50
  378 JSPCL=0
      NPAR = INDTRS(IR)
      IF(NSPECL) 507,507,508
  508 IF(SYMB(IR)-SSYMB(ISPCL)) 507,509,507
  509 IF(ATOMN(IR)- SATOM(ISPCL))507,510,507
  510 DO 511 I=1,10
      ICOM(I) =SIND(ISIND)
  511 ISIND = ISIND + 1
      ISPCL = ISPCL +1
      DO 512 I=1,NPAR
      IF(ICOM(I)) 513,514,513
  514 SHIFT(I) = 0.0
      SYGMA(I) = 0.0
      GO TO 512
  513 IL=IL+1
      SHIFT(I)=VECT(IL)
      IK = IK + IL
      SYGMA(I) =  SQRT(SDSQ/SUM(IK))
  512 CONTINUE
      GO TO 537
  507 DO 537 I=1,NPAR
      IL=IL+1
      SHIFT(I)=VECT(IL)
      IK = IK + IL
```

```
      SYGMA(I) =  SQRT(SDSQ/SUM(IK))
  537 CONTINUE
C     OUTPUT OF PARAMETERS, SHIFTS AND ESD'S
      TEMP=0.
      SHIFT(10)=0.0
      SYGMA(10)=0.0
      X(IR)=X(IR)+SHIFT(1)
      SX(IR)=SYGMA(1)
      Y(IR)=Y(IR)+SHIFT(2)
      SY(IR)=SYGMA(2)
      Z(IR)=Z(IR)+SHIFT(3)
      SZ(IR)=SYGMA(3)
      IF(NPAR-5) 382,381,384
  381 OCCFR(IR)=OCCFR(IR)+SHIFT(5)
  382 BISO(IR)=BISO(IR)+SHIFT(4)
      IF(BISO(IR)) 900,900,901
  900 BISO(IR)=0.0
  901 CONTINUE
      WRITE(PRINTR,45) SYMN(IR), SYMB(IR),ATOMN(IR),(SHIFT(I),I=1,NPAR)
      WRITE(PRINTR,46) (SYGMA(I),I=1,NPAR)
      GO TO 388
  384 IF(NPAR-9) 386,386,385
  385 OCCFR(IR)=OCCFR(IR)+SHIFT(10)
  386 B11(IR)=B11(IR)+SHIFT(4)
      IF(B11(IR)) 800,800,801
  800 B11(IR)=0.0
  801 CONTINUE
      B22(IR)=B22(IR)+SHIFT(5)
      IF(B22(IR)) 802,802,803
  802 B22(IR)=0.0
  803 CONTINUE
      B33(IR)=B33(IR)+SHIFT(6)
      IF(B33(IR)) 804,804,805
  804 B33(IR)=0.0
  805 CONTINUE
      B23(IR)=B23(IR)+SHIFT(7)
      B13(IR)=B13(IR)+SHIFT(8)
      B12(IR)=B12(IR)+SHIFT(9)
  387 WRITE(PRINTR,45) SYMN(IR), SYMB(IR),ATOMN(IR),SHIFT(1),SHIFT(2),
     1SHIFT(3),TEMP,SHIFT(10),(SHIFT(I),I=4,9)
      WRITE(PRINTR,46) SYGMA(1),SYGMA(2),SYGMA(3),TEMP,SYGMA(10),
     1(SYGMA(I),I=4,9)
  388 LINES=LINES-2
  390 CONTINUE
C     OUTPUT OF THE NEW PARAMETERS ON CARDS, PRINTER AND TAPE
      LST=4
      ISYGMA=1
      NWORD=19
      WRITE(PUNCH,47) JOBB,LST,JSER,NATOM,ISYGMA
      LINES=0
      WRITE(TAPEB) LST,JSER,NATOM,NWORD
      DO 396 I=1,NATOM
      IF (LINES) 393,393,394
  393 WRITE(PRINTR,43) TITLE,JSER,NPAGE
```

```
      WRITE(PRINTR,44)
      LINES=50
      NPAGE=NPAGE+1
  394 WRITE(PRINTR,45) SYMN(I), SYMB(I), ATOMN(I),X(I),Y(I),Z(I),
     1BISO(I),OCCFR(I),B11(I),B22(I),B33(I),B23(I),B13(I),B12(I)
      LINES=LINES-1
      WRITE(TAPEB) SYMN(I),  SYMB(I),ATOMN(I),X(I),Y(I),Z(I),SX(I),
     1SY(I),SZ(I),BISO(I),VIB(I),INDTRS(I),B11(I),B22(I),B33(I),B23(I),
     2B13(I),B12(I),OCCFR(I)
      WRITE(PUNCH,48)  JOBB,LST,JSER,SYMN(I),  SYMB(I),ATOMN(I),X(I),
     1Y(I),Z(I),BISO(I),VIB(I),INDTRS(I),OCCFR(I),JOBB,LST,JSER,SYMN(I),
     2  SYMB(I),ATOMN(I),SX(I),SY(I),SZ(I)
      IF(VIB(I)) 396,396,395
  395 WRITE(PUNCH,49) JOBB,LST,JSER,SYMN(I),  SYMB(I),ATOMN(I),B11(I),
     1B22(I),B33(I),B23(I),B13(I),B12(I)
  396 CONTINUE
      IB=IB+1
      GO TO 353
      END
```

This program employs the GELS subroutine of the I.B.M. Scientific Subroutine Package in calculating the parameters' shifts. This revision uses the Gaussian elimination method for the solution of the normal equations. The inverse matrix of A is not calculated.

APPENDIX IV

Weighting scheme additions to the NRC-10 Structure Factor Least Squares program by the author.

The statement following computer card 30 is:

```
      DIMENSION  F(10),FD(10),AF(10),AFD(10),NREF(10)
```

The statements following computer card 960 are:

```
      DO 838 I = 1,7
      F(I) = 0.0
      FD(I) = 0.0
      NREF(I) = 0.0
  838 CONTINUE
```

The statements following computer card 5720 are:

```
  822 IF(ABS(FOP)- 20.) 823,823,824
  823 I = 1
      GO TO 829
  824 IF(ABS(FOP)- 40.) 825,825,826
  825 I = 2
      GO TO 829
  826 IF(ABS(FOP)- 70.) 827,827,828
  827 I = 3
      GO TO 829
  828 IF(ABS(FOP)- 100.) 830,830,831
  830 I = 4
      GO TO 829
  831 IF(ABS(FOP)- 140.) 832,832,833
  832 I = 5
      GO TO 829
  833 IF(ABS(FOP)- 190.) 834,834,835
  834 I = 6
      GO TO 829
  835 I = 7
  829 F(I) = ABS(FOP)+ F(I)
      FD(I) = ADELFP + FD(I)
      NREF(I) = NREF(I) + 1
```

The statements following computer card 6440 are:

```
      DO 837 I = 1,7
      AF(I) = F(I)/NREF(I)
      AFD(I) =  FD(I)/NREF(I)
      WRITE(PRINTR,836) I,AF(I),AFD(I),NREF(I)
  836 FORMAT(I2,' MEAN FO IS',F10.5,' MEAN DELTA F IS',F10.5,
     1' NO OF REFLECTIONS',I5)
  837 CONTINUE
```

The statement replacing computer card 7160 is:

```
  269 RTW = 1./(1. + 0.169*ABS(FOP))
```

REFERENCES

AHMED, F.R., HALL, S.R., PIPPY, M.E. and SAUNDERSON, C.P. (1966): The N.R.C. Crystallographic Programs, The National Research Council of Canada, Ottawa.

BEAGLEY, D.W.J., CRUICKSHANK, D.W.J., PINDER, P.M., ROBIETTE, A.G.E. and SHELDRICK, G.M. (1969): Acta. Cryst. 25, 737.

BENNETT, M.J. Jr., COTTON, F.A., DAVIDSON A., FALLER, J.W., LIPPARD, S.J. and MOREHOUSE, S.M. (1966): J. Am. Chem. Soc. 88, 4371.

BRAGG, W.L. (1913): Proc. Camb. Phil. Soc. 17, 43.

BRAUER, G. (1954): Handbuch der Praparativen Organischen Chemie, p. 755.

BUERGER, M.J. (1942): X-ray Crystallography. New York: Wiley and Sons, Inc.

BUERGER, M.J. (1960): Crystal Structure Analysis. New York: Wiley and Sons, Inc.

BUERGER, M.J. (1964): The Precession Method. New York: Wiley and Sons, Inc.

BUNN, C.W. (1961): Chemical Crystallography. 2nd Ed. Oxford University Press.

CHRIST, C.L. (1956): Am. Minerologist 41, 569.

CORFIELD, P.W.R. and SHEARER, H.M.M. (1966): Acta. Cryst. 21, 957.

COSTA, G., PELLIZER, G. and RUBESSA, F. (1964): J. Inorg. and Nucl. Chem. 26, 961.

COX, A.P., THOMAS, L.F., and SHERIDAN, J. (1958): Nature 181 1157.

DAHL, L.F. and BLOUNT, J.F. (1965): Inorg. Chem. 4, 1373.

DAHM, D.J. and JACOBSON, R.A. (1968): J. Am. Chem. Soc. 90, 5106.

DONOHUE, J. and CARON, A. (1964): Acta. Cryst. 17, 663.

DUNITZ, J.D., ORGEL, L.E., RICH, A. (1956): Acta. Cryst. 9, 373.

EWALD, P.P. (1921): Z Krist. 56, 129.

FOUST, A.S., FOSTER, M.S. and DAHL, L.F. (1969): J. Am. Chem. Soc. 91, 5631.

FRIEDMAN, L., IRSA, A.P. and WILKINSON, G. (1955): J. Am. Chem. Soc. 77, 3689.

HENNE, A.L. and FINNEGAN, W.G. (1949): J. Am. Chem. Soc. 71, 298.

HOUSE, H.O., RESPESS, W.L. and WHITESIDES, G.M. (1966): J. Org. Chem. 31, 3128.

I.B.M. MANUAL H-20-0205-3. SCIENTIFIC SUBROUTINE PACKAGE, VERSION II.

INTERNATIONAL TABLES FOR X-RAY CRYSTALLOGRAPHY (1962): Vols. I and III, (C.H. Macgillavry and G.D. Rieck, eds.) Kynoch Press, Birmingham, England.

KRESPAN, C.G., McKUSICK, B.C. and CAIRNS, T.L. (1960): J. Am. Chem. Soc. 82, 1515.

KRUCZYNSKI, L. (PRIVATE COMMUNICATION)

LIPSON, H. and COCHRAN, W. (1966): The Determination of Crystal Structures, p. 301. London: Bell and Sons.

McBRIDE, D.W., DUDEK, E. and STONE, F.G.A. (1964): J. Chem. Soc., p. 1752.

MILLS, O.S. and ROBINSON, G. (1963): Acta. Cryst. 16, 758.

MOND, L. LANGER, C. and QUINCKE, J. (1890): J. Chem. Soc., p. 749.

NUFFIELD, E.W. (1966): X-ray Diffraction Methods p. 273. New York: Wiley and Sons, Inc.

ORGANIC SYNTHESES VIA METAL CARBONYLS (1968): (Irving Wender and Piero Pino, eds.) New York: Interscience Publishers, Inc.

PATTERSON, A.L. (1934): Phys. Rev. 46, 372.

PATTERSON, A.L. (1935): Z. Krist. 90, 517.

PAULING, L. (1967): The Chemical Bond, p. 148. Ithaca, New York: Cornell University Press .

PIPER, T.S. and WILKINSON, G. (1956): J. Inorg. and Nucl. Chem. 3, 104.

SMITH, D.C., ALPERT, M., SAUNDERS, R.A., BROWN, G.M. and MORAN, N.B. (1952): Infrared Spectra of Fluorinated Hydrocarbons, p. 75. N.R.L. Report 3924, Office of Naval Research, Naval Research Laboratory, Washington, D.C.

STOUT, G.H. and JENSEN, L.H. (1968): X-ray Structure Determination - A Practical Guide, p. 455. New York: The Macmillan Company.

SWANSON, H.E. and TATGE, E. (1953): Standard X-ray Diffraction Powder Patterns. National Bureau of Standards Circular 539, Vol I.

WEI, C.H. and DAHL, L.F. (1969): J. Am. Chem. Soc. 91, 1351.

WHITESIDES, G.W. and FLEMING, J.S. (1956): J. Inorg. and Nucl. Chem. 2, 32.

WILKINSON, G., COTTON, F.A., BIRMINGHAM, J.M. (1956): J. Inorg. and Nucl. Chem. 2, 95.

WILKINSON, G., COTTON, F.A. (1959): Progress in Inorganic Chemistry (F.A. Cotton, ed.), New York: Interscience Publishers, Inc.

WILKINSON, G. and PIPER, T.S. (1956): J. Inorg. and Nucl. Chem. 2, 32.